GEOLOGICAL SURVEY OF CANADA
OPEN FILE 3731

in collaboration with
THE CANADIAN GEOMORPHOLOGICAL RESEARCH GROUP

A HANDBOOK OF GEOPHYSICAL TECHNIQUES FOR GEOMORPHIC AND ENVIRONMENTAL RESEARCH

Robert Gilbert, compiler

with contributions by
M. Douma, L. Dyke, R. Gilbert, R. L. Good, J. A. Hunter,
C. Hyde, Y. Michaud, S. E. Pullan, and S. D. Robinson

1999

Ressources naturelles Canada
Natural Resources Canada

Canada

GEOLOGICAL SURVEY OF CANADA
OPEN FILE 3731

in collaboration with
THE CANADIAN GEOMORPHOLOGICAL RESEARCH GROUP

A HANDBOOK OF GEOPHYSICAL TECHNIQUES FOR GEOMORPHIC AND ENVIRONMENTAL RESEARCH

Robert Gilbert
compiler

with contributions by

Martin Douma, Larry Dyke, Robert Gilbert, Ron L. Good
James A. Hunter, Christophe Hyde, Yves Michaud,
Susan E. Pullan, and Stephen D. Robinson

1999

Cover photograph: Participants in the Canadian Geomorphology Research Group Workshop at Queen's University, September 1997 conducting a ground penetrating radar survey (see Chapter 5) at the Cataraqui Conservation Area. In the foreground is a 200 kHz antenna which is placed on the ground at 2-m intervals along a measured line. In the background is the operator with the control unit carried on a back pack. Photograph by R. Gilbert.

Authors' addresses

Robert Gilbert
Department of Geography
Queen's University
Kingston ON K7L 3N6

Martin Douma
Larry Dyke
Ron L. Good
James A. Hunter
Christophe Hyde[1]
Susan E. Pullan
Geological Survey of Canada
601 Booth Street
Ottawa ON K1A OE8

Yves Michaud
Québec Geoscience Centre
Geological Survey of Canada
2535 Boulevard Laurier
Case Postal 7500
Sainte-Foy Québec G1V 4C7

Stephen D. Robinson[2]
Department of Geography
McGill University
805 Sherbrooke Street West
Montreal Québec H3A 2K6

[1] *Current address:*
Dept. of Earth and Ocean Sciences
University of British Columbia
Vancouver BC V6T 1Z4

[2] *Current address:*
Geological Survey of Canada, Ottawa

CONTENTS

CHAPTER 1 Introduction

Robert Gilbert

On September 20 and 21, 1997 the Canadian Geomorphology Research Group, with the support of then President, Dr. Chris Burn, sponsored a workshop at Queen's University on geophysical techniques in geomorphic research. It was led by members of the geoscience community, most of whom are contributors to this volume, and was attended by about 30 academics, scientists and graduate students. The impetus for the present volume was the consensus at the workshop and since, that the subject matter would be of interest to a wider audience of geomorphologists, physical geographers, and environmental earth scientists. Dr. John J. Clague, in his capacity as current President of the C.G.R.G., enthusiastically supported this view, and facilitated publication by the Geological Survey of Canada of this expanded version of the document provided to participants at the workshop.

This volume is designed to provide geomorphologists and others conducting research on earth-surface processes and landforms with an introduction to selected geophysical techniques which can provide useful information for these studies. This is based on the premise that some earth scientists may not have received formal training in geophysics and so may not be familiar with the techniques and instrumentation that may be available to address the questions of their research. For this reason, the presentations here focus on first principles, and provide illustrations and examples from geomorphic study of the surface and subsurface of land and water that may be very useful in assessing geomorphic processes, landforms, and environmental and paleoenvironmental change. Information is provided on how to conduct surveys using the techniques described, and how to interpret the results, including, in both cases the pitfalls to avoid. Each technique is relatively easy to learn and inexpensive to apply; in most cases, each is suited to small field parties operating with limited logistical support.

The material is presented in five chapters, each dealing with a different technique. Electromagnetic survey maps changes in conductivity and magnetic properties of the earth to depths in the range of 1 km, and so documents the character of the ground and materials contained in it. Shallow seismic survey offers the opportunity to record from reflected or refracted sound energy the structure of the subsurface and its properties. Where boreholes are available, logging techniques provide detailed information on the properties of materials down the hole that may be compared with the materials recovered from the holes, and used to map in three dimensions the nature of the subsurface. Ground-penetrating radar provides high resolution data on the shallow subsurface of land and has limited but important applications to studies of lakes and their sediments. Acoustical techniques are used in lacustrine and marine surveys, especially mapping of bathymetry and the character of sediment accumulation on the bottom.

CHAPTER 2 Electromagnetic techniques

Christophe Hyde and Larry Dyke

Introduction

Electromagnetic (EM) techniques are used to detect either lateral or vertical changes in electrical conductivity of the ground which may delineate geomorphic features. Conductivity variation may reflect changes in the solid matrix and/or the interstitial fluid of the sediment under investigation. Detection of geomorphic features such as eskers, karst cavities and permafrost and delineation of subsurface stratigraphy such as clay or sand-layer thickness, depth to water table and salt-water contamination are all examples of EM applied to geomorphology.

Unlike two other methods, acoustic and GPR, discussed in this volume, EM techniques operate in the diffusion regime of wave behaviour, not the propagation regime. Reduced resolution and loss of accuracy particularly in depth and thickness estimation are the principal disadvantages of operating in the diffusion range of the EM wave spectrum. However, these methods offer much greater depth penetration than these other methods, particularly below the water table and in conductive material such as clays and saline groundwater.

Selection of an EM instrument depends on the depth penetration required and the range of ground conductivities expected in the area under investigation. Depth penetration is a function of ground conductivity, several instrument variables such as transmitter-receiver geometry, operating instrument frequency and output power, and natural or cultural ambient noise levels. Several techniques can be used to minimize or to evaluate noise levels and to distinguish cultural from geomorphic anomalies.

Historical background and applications

The EM ground method was developed during the 1920s in Scandinavia, the United States and Canada, regions where the detection of electrically conductive base-metal deposits was facilitated by their large contrast with electrically resistive host rock and generally thin overburden. The airborne version was introduced some 30 years later (Telford et al., 1990). Until the early 1960s, practically all EM equipment transmitted and received continuously on one frequency at a time. Such a continuous wave system is said to be operating in the frequency domain (FEM or FDEM). The first successful attempts to transmit transient pulses and to measure the response of the earth during off-time did not appear until the early 1960s. Since the early 1970s, there has been a dramatic increase in the development of such time-domain systems (TEM or TDEM) (Telford et al., 1990).

Although the initial development of the EM method was and continues to be driven by the mineral exploration industry, environmental applications now form an important portion of EM applications. A partial list of proven EM applications is highlighted in Table 2.1.

Table 2.1. *Proven applications of EM.*

1. Groundwater contamination delineation
2. Groundwater exploration
3. Sand and gravel exploration
4. General geological mapping
5. Diamond exploration
6. Cathodic protection system design
7. Base metal exploration
8. Water leakage into potash mines delineation
9. Archeology
10. Permafrost delineation
11. Saline intrusion delineation
12. Sea-ice thickness measurements
13. Soil salinity
14. Dike and canal leak detection
15. Cavity detection
16. Tank and pipe detection
17. Power transmission line grounding design
18. Sensitive clay delineation
19. Geomorphology

Electromagnetic methods

Electromagnetic techniques are usually defined as sub-surface investigation techniques which utilize time-varying - typically with 1 Hz to 100 KHz bandwidth - electric and/or magnetic fields. Passive geophysical methods such as magnetic field methods where local variation of the earth's DC magnetic field is measured and spontaneous polarization (SP) methods where local DC electric fields are measured are not classified as EM methods. In addition, techniques which operate with frequencies above 100 KHz, such as the GPR method with typical operating range spanning 1 MHz to 1 GHz, and which also transmit and emit time-varying electric fields are not classified as EM methods. The distinction between the two frequency ranges is important because it divides the diffusion regime (below 100 KHz) from the wave propagation regime (above 1 MHz). In the diffusion regime, depth of investigation is typically less than one skin depth and is defined as:

$$\delta = \sqrt{\frac{2}{\omega \mu \sigma}}$$

where ω is the angular frequency (rad/s), μ is magnetic permeability (H/m) and σ is conductivity (S/m). Depending on instrument operating frequency and ground conductivity the skin depth can range from under one metre to over one kilometre. In comparison, GPR systems which operate in the wave propagation regime have a maximum depth of investigation over several tens of metres in ideal conditions. In the propagation regime, the EM fields travel as a wave with amplitude varying both in time and space. Typically as the frequency of the wave increases resulting in shorter wavelength, resolution of the system increases and depth of investigation decreases. In contrast, in the diffusion regime, EM fields are operating within one wavelength of the EM wave. Typically, diffusion systems have lower resolution but greater depth of investigation. Table 2.2 highlights the main differences between diffusion and propagation.

Table 2.2. *Diffusion and propagation*

Wave equation

$$\frac{\partial^2 \boldsymbol{H}}{\partial z^2} + (\mu\epsilon\omega^2 - i\mu\sigma\omega)\boldsymbol{H} = 0$$

where **H** is magnetic field strength (A/m)
μ magnetic permeability (H/m)
ϵ dielectric permittivity (F/m)
ω angular frequency (Hz)
σ conductivity (S/m)
z distance (m)

where $\mu\epsilon\omega^2 << \mu\sigma\omega$

diffusion

dominates, and the wave equation reduces to:

$$\frac{\partial^2 \boldsymbol{H}}{\partial z^2} - i\mu\sigma\omega\boldsymbol{H} = 0$$

- Given conductivity of most earth materials:
  10^{-2} mS/m < σ < 10^4 mS/m
- Given frequency range: **f < 10^5 Hz**
- Example of physical process explained by diffusion:
  Heat conduction
- Depth of investigation is usually less than skin depth, defined as:

$$\delta = \sqrt{\frac{2}{\omega\mu\sigma}}$$

where $\mu\sigma\omega << \mu\epsilon\omega^2$

propagation

dominates, and the wave equation reduces to:

$$\frac{\partial^2 \boldsymbol{H}}{\partial z^2} + \mu\epsilon\omega^2\boldsymbol{H} = 0$$

- Given conductivity of most earth materials,
  10^{-2} mS/m < σ < 10^4 mS/m
- Given frequency range: **f > 10^6 Hz**
- Examples of physical processes explained by wave propagation:
  Seismic wave transmission
  GPR wave transmission
- Depth of investigation is usually over several wavelengths, defined as:

$$\lambda = \frac{2\pi}{\omega\sqrt{\mu\epsilon}}$$

Classification is useful to further describe the EM group of methods (Fig. 2.1). The main categories include:

1. Mode of transportation, e.g. airborne, ground, borehole and sea-floor methods.

2. Waveform characteristics. EM transmitters can either output single harmonic waveforms (frequency domain) or wide-bandwidth waveforms (time domain) such as the pulse, ramp or half-sine. Conversely, frequency-domain receivers can measure amplitude and phase of a single harmonic waveform (or real and imaginary components), and time-domain receivers typically measure channels, time-windows that are usually logarithmically spaced, of the received waveform.

3. Nature of the source. The source can be naturally emitted as is the case in magnetotelluric methods where the source of the fields is located outside the earth - mostly a product of solar activity - and audio-magnetotelluric methods where the source of the fields is related to lightning activity. However, the most commonly used EM methods employ artificial transmitters, usually located close to the receiver, or far away (100s to 1000s of km) as with VLF transmitters.

4. Measured physical parameter. Magnetic field, electric field and potential difference (voltage). Although this type of classification is mostly based on type of receiver and resulting type of field measured, the transmitter type usually emits fields using a physical process similar to the one used by the receiver, but this is not always the case. For example, with Inductive Source Resistivity (ISR) methods the transmitter couples with the ground by induction whereas the receiver couples with the ground by capacitive-coupling or direct coupling.

Grounded electrical methods employ an artificial source of current which is introduced into the ground through point electrodes (Telford et al., 1990). The resulting electrical potential is measured with two potential electrodes. Data can then be transformed to apparent resistivity of the ground, a function of the current introduced in the earth, the measured voltage and the electrode array geometry (Fig. 2.2). The practical difficulty involved in dragging several electrodes and long wires through rough terrain and the problems involved in planting electrodes in outcrop or permafrost terrain have made the EM method more popular than grounded methods in mineral exploration and in other applications.

Capacitive-coupled techniques are relatively new, and have been in use mostly in prototype form since the 1980s (Fig. 2.3). Both terminology and array configurations are similar to those used by the grounded electrical methods. Current antennae emit an electric field and potential antennae measure the electric field in the vicinity of the current flow. As with the grounded electrical method, depth penetration depends on ground conductivity and antennae array geometry. However, the capacitive-coupled method does not have the disadvantages, slow survey speed and difficulty in coupling electrodes to the ground, associated with the grounded electrical method. Unlike EM techniques which do not measure resistive terrain accurately, the capacitive-coupled method is accurate to conductivities well below 1 mS/m, the EM instrument limit. Although not yet widely

used, the ability of this technique to be both rapid and able to map wide ranges of conductivities, seems promising and should ensure its growing popularity.

Classification according to:

1. Transportation mode
   a. airborne
   b. ground
   c. borehole
   d. sea-floor
2. Waveform type
   a. frequency-domain (FEM or FDEM)
   b. time-domain (TEM or TDEM)
3. Nature of source
   a. natural sources
      (i.e. magnetotelluric)
   b. artificial transmitters
      most commonly used
4. Type of coupling with the earth
   a. inductive
      associated with magnetic fields
   b. capacitive
      associated with electric fields
   c. direct (grounded methods)
      associated with current

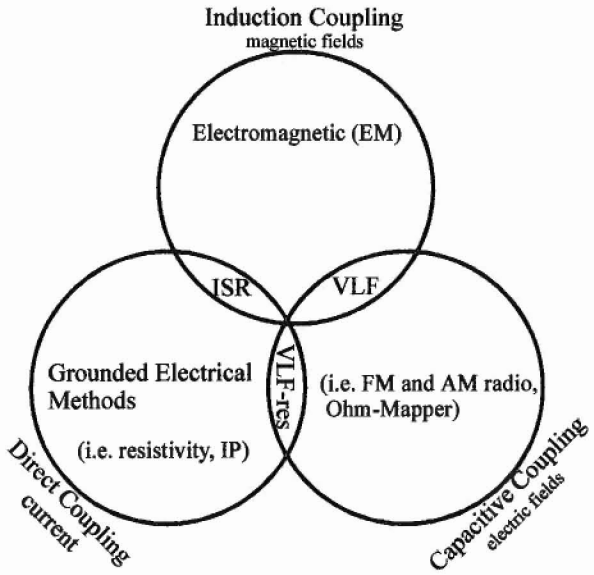

Figure 2.1. *Time-varying electrical and magnetic geophysical methods.*

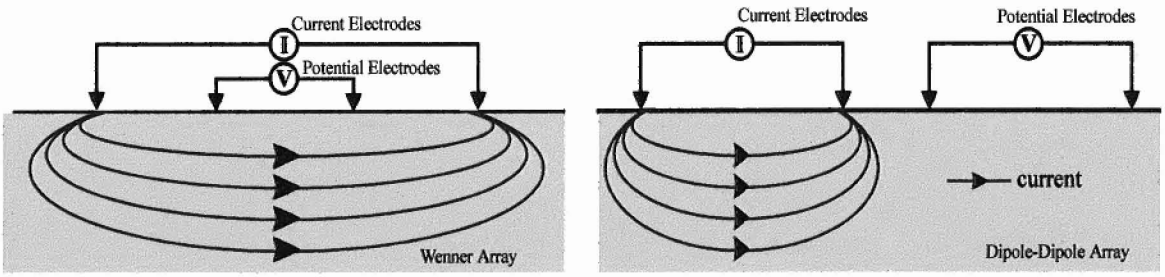

Figure 2.2. *Grounded electrical methods - two examples of direct coupling.*

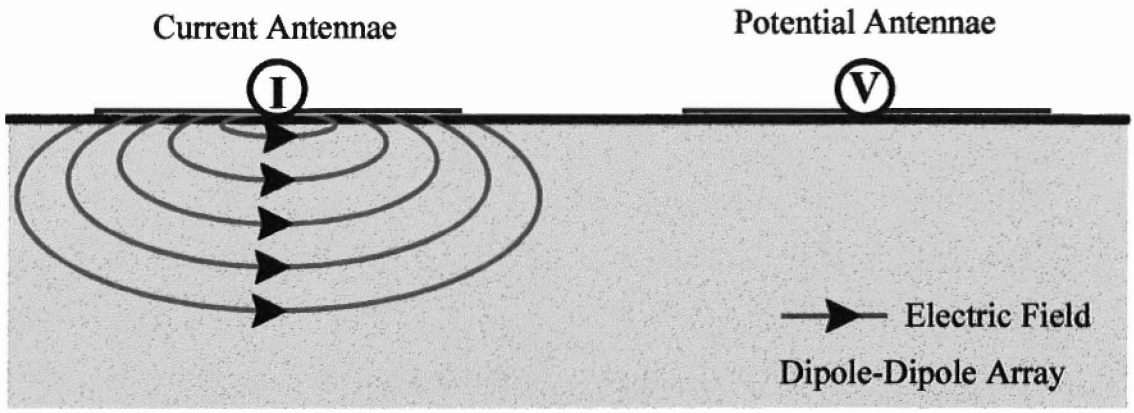

- Electric field measured and emitted
- Faster profiling than grounded electrical method
- Ground conductivity and array geometry, length of antennae and separation distance determine penetration depth

Figure 2.3. *Capacitive-coupled methods.*

EM techniques typically employ induction coils, either small multi-turn coils or large single-turn loops as transmitters with an induction coil receiver (Fig. 2.4). The time-varying current generated in the transmitter produces, as described by Ampère's Law, a time-varying magnetic field. The magnetic field induces currents in the earth, proportional in part to its conductivity. These secondary currents in the earth produce a secondary magnetic field. As described by Faraday's Law, the receiver coil measures a voltage proportional to the time-derivative of the magnetic field, a combination of the primary magnetic field generated by the transmitter and the secondary magnetic field generated by the earth. As with the capacitive-coupled techniques, the relative speed required to complete EM surveys have made this technique popular in the mining and environmental industry. However, its inability to map resistive terrain restricts its use.

Waveform types fall under two categories, either frequency domain or time domain. In the frequency domain method the transmitter emits a sinusoidally varying current at a specific frequency (Fig. 2.5). The receiver, usually an induction coil, measures the time-derivative of both the primary field (Tx) and secondary field (earth). The data are usually displayed in one of the following three formats.

- Amplitude and phase: Amplitude of the secondary field is measured usually as a percentage of the theoretical free-space (a zero conductivity assumption) primary field. Phase shift, the time delay of the secondary field with respect to the primary field, is measured as a fraction of the waveform period.
- In-phase and quadrature: The received or total field is separated into two components, in-phase which is in-phase with the primary field and quadrature which lags the primary field by 90°. The in-phase component is also called "real", while the quadrature component is

also called "imaginary". The EM31 instrument used in the case study in this chapter displays both apparent conductivity, a direct function of the quadrature component and the in-phase component.

- Tilt-angle: Several simpler systems such as the VLF method measure the total field amplitude, defined as the vector sum of the primary field emitted by transmitter and the secondary field generated by the earth. In addition, the receiver coil is tilted to find the minimum and/or maximum direction of the total field amplitude. With tilt-angle systems, the objective is to measure deviations from the primary field direction and to interpret these in terms of buried conductors (Klein and Lajoie, 1980).

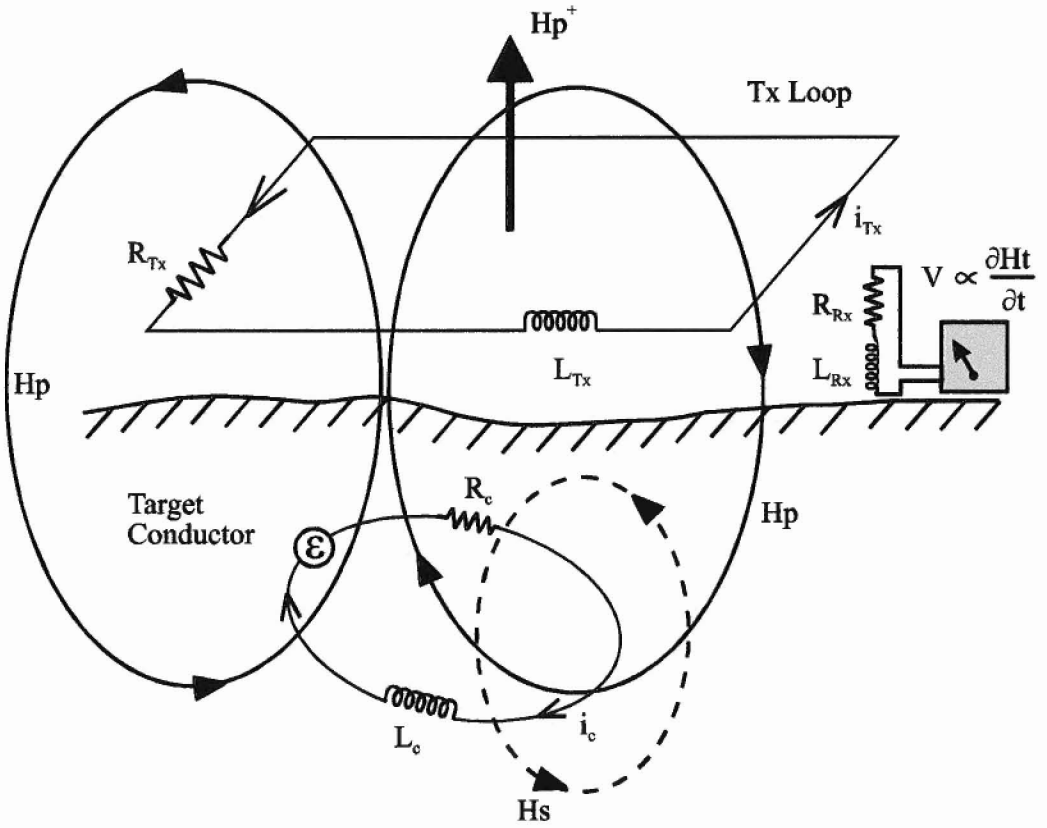

Hp, Hs, Ht	Primary, Secondary, Total Magnetic Field
Tx	Transmitter
Rx	Receiver
C	Conductor
ε	EMF (electro-motive force)
i	Current
V	Voltage
R	Resistance
L	Inductance

Figure 2.4. *Electromagnetic (EM) methods - induction schematic (Marchand, 1990).*

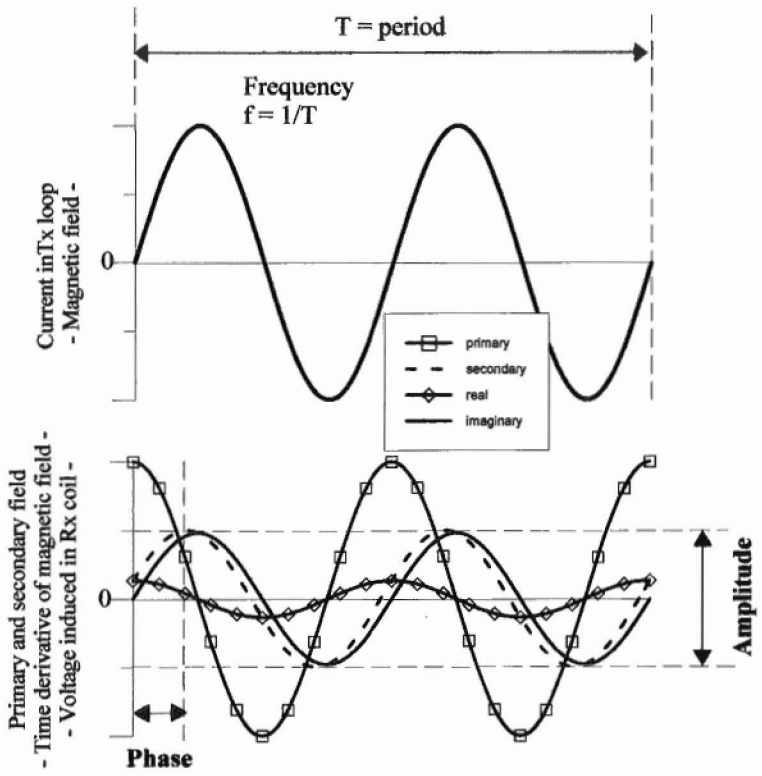

- Primary field - emitted by transmitter
- Secondary field - "emitted" by earth
- Total field is the vector sum of primary & secondary fields
- Secondary field can be described by either amplitude and phase or real and imaginary components (the latter are synonymous with in-phase and quadrature)
- In-phase component is in phase with transmitted primary field
- Quadrature component is 90° out-of-phase with transmitted primary field
- Secondary = secondary amplitude * $\cos(\omega t - \phi)$
  where ω is the angular frequency, ϕ is the phase shift
- Secondary amplitude = $\text{Real}^2 + \text{Imaginary}^2$
  usually expressed as percentage of primary field
- Phase shift, the lag of the secondary field behind the primary field,
  may be expressed as a fraction of a period ($(2\pi)/\omega$)

Figure 2.5. *Frequency-domain waveforms.*

In the time-domain method the transmitter emits an alternating wide-band waveform, a common type is the alternating "square" waveform or "pulse" system used by many ground TEM systems. As with the FEM method, the receiver is usually an induction coil and measures the time-derivative of the total magnetic field (Fig. 2.6). In "pulse" systems, the time-derivative of the primary field is a pulse, while the time-derivative of the secondary field, measured in the "off-time" (while the transmitter is off) is a decay function with short decay characteristics for resistive ground

and long decay characteristics for conductive ground. Ground-based TEM methods, although generally requiring larger survey teams and longer data acquisition times are extremely powerful because they can essentially duplicate multi-frequency data with single readings. Multiple frequency data or the time-domain equivalent, multiple time-windows acquired in a single reading are used to provide sounding information, conductivity and therefore structure, as a function of depth.

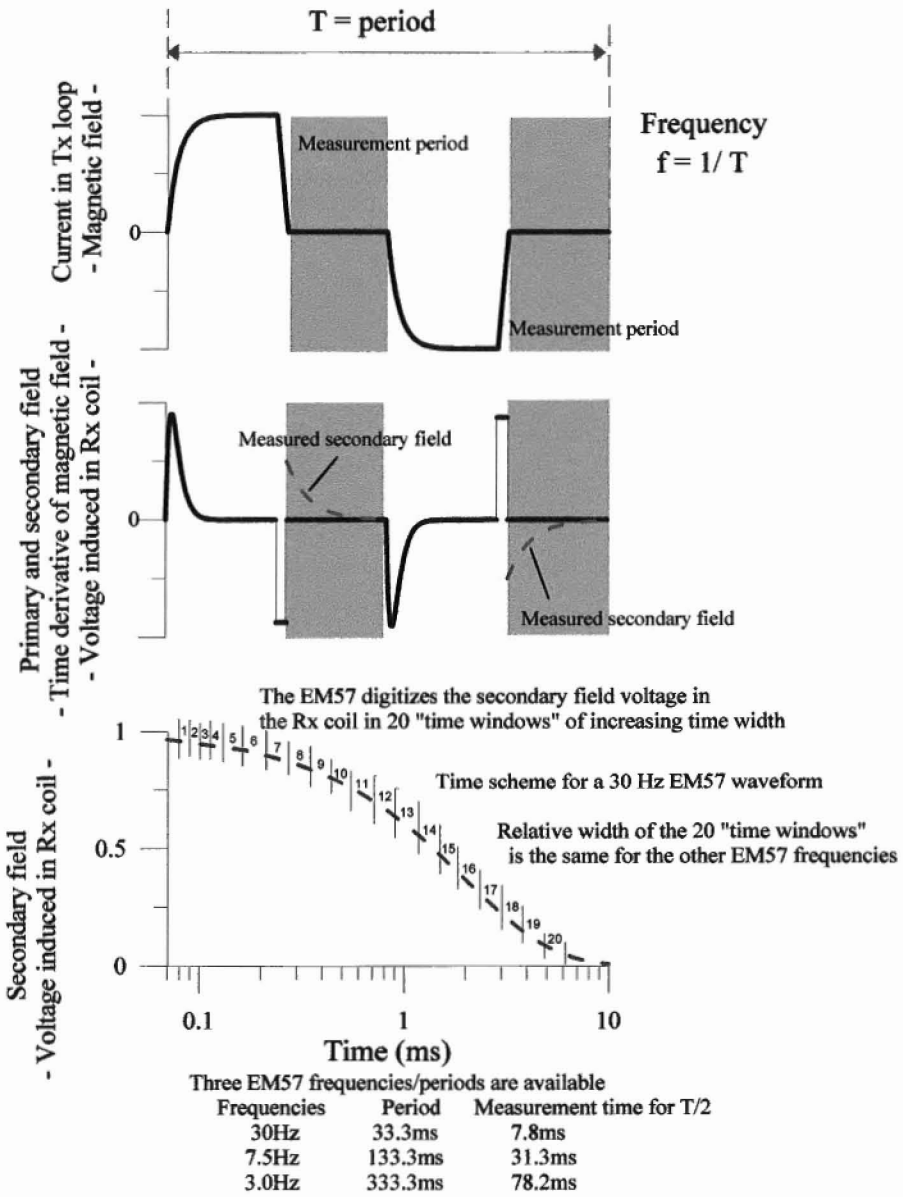

Figure 2.6. *Time-domain waveforms in an example from the EM57 "pulse" system.*

Factors affecting terrain conductivity

In many groundwater studies the soil and rock matrix are assumed to be an electrical insulator and therefore electric current flows through the soil water (Fig 2.7). Under this condition, major factors affecting the electric conductivity of the bulk soil or rock are (McNeill, 1990):

1. porosity,
2. conductivity of included soil moisture,
3. shape of soil/rock pore spaces,
4. degree of saturation (fraction of pore space actually filled with moisture),
5. temperature, and
6. presence of clays with moderate to high cation exchange capacity.

For a completely saturated soil the influence of the first three factors is described by Archie's Law, an empirically based relationship which is sufficiently accurate for unconsolidated as well as lithified materials (Jackson et al., 1978).

$$\sigma_a = \sigma_w \times n^m + \sigma_{clay}$$

where σ_a = bulk conductivity(S/m), σ_w = water conductivity (S/m), n = fractional porosity (0 to 1), m = grain geometry factor varying from 1.3 for spheres to 2.0 for plates, σ_{clay} = clay conductivity (or grain conductivity) (S/m).

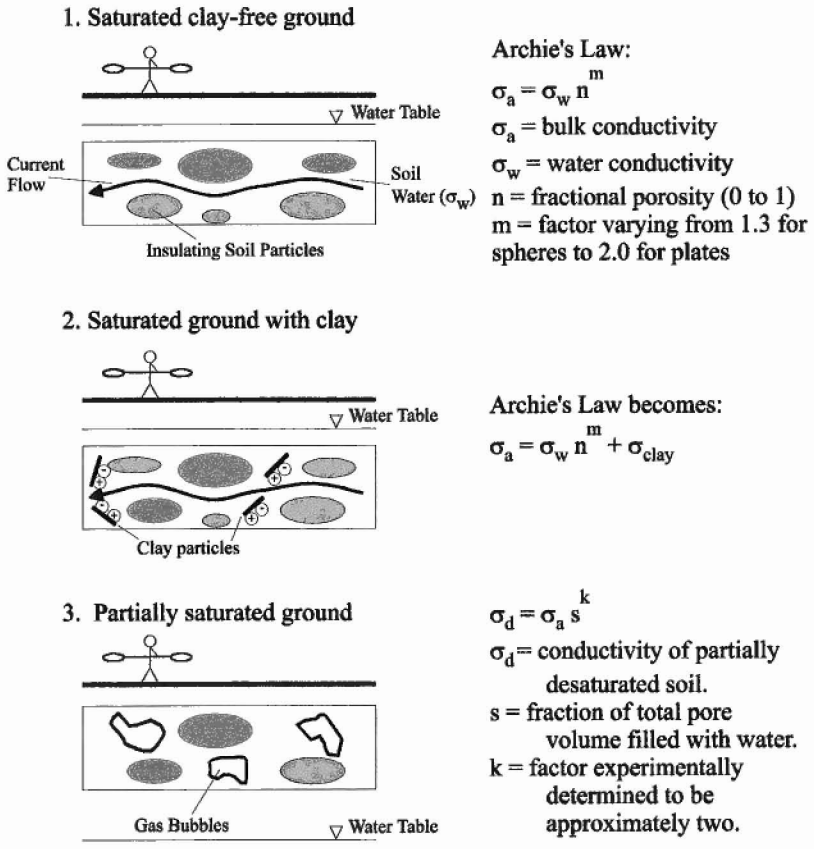

Figure 2.7. *Factors affecting terrain conductivity.*

Typical porosities and conductivities are shown in Table 2.3 and Figure 2.8 respectively.

Table 2.3. *Representative porosity ranges for sedimentary materials (after Todd, 1964).*

Material	Porosity (%)
Soils	50-60
Clay	45-55
Silt	40-50
Medium to coarse mixed sand	35-45
Uniform sand	30-40
Fine to medium mixed sand	30-35
Gravel	30-40
Gravel and sand	20-35
Sandstone	10-20
Shale	1-10
Limestone	1-10

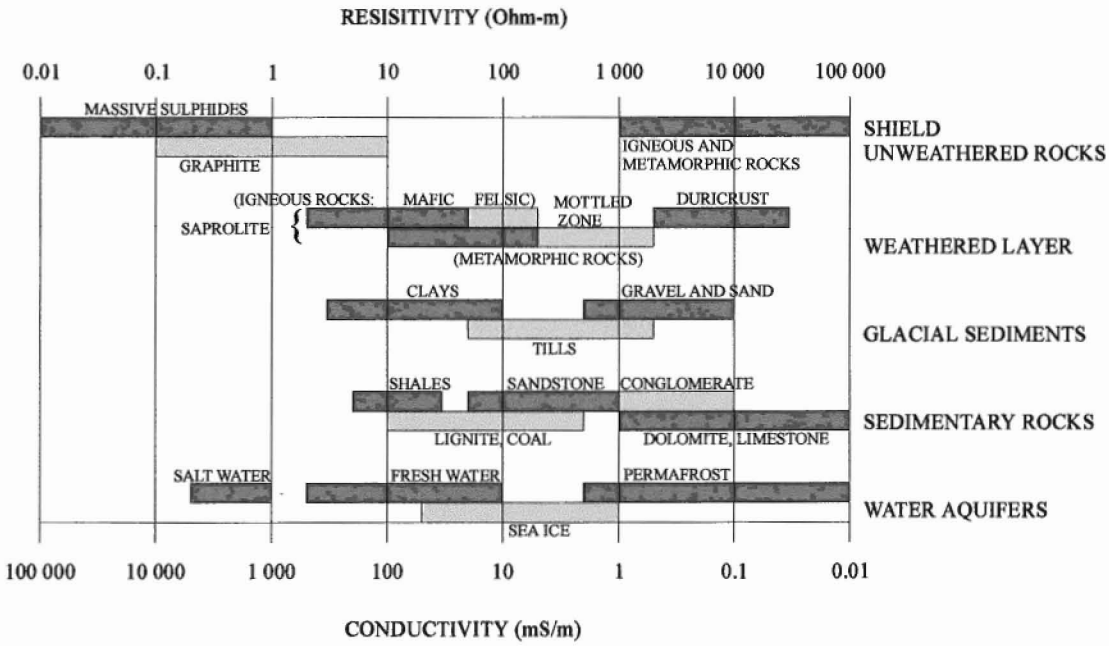

Figure 2.8. *Typical ranges of conductivities of earth materials (Palacky, 1988).*

An approximate relation is often needed between bulk soil conductivity and ionic concentration. Referring to Archie's equation for saturated clay-free ground,

$$\sigma_a = \sigma_w \times n^m$$

and assuming typical soil porosity of 40% and average particle shape factor of 1.5, n^m is approximately equal to 0.25 (Table 2.4). In addition, because water conductivity (σ_w) is a function of the product of ion concentration and ionic mobility, it is possible to derive standard factors relating water conductivity to total dissolved solids (TDS). Examples of this relation are

for sodium chloride, $\sigma_w = TDS / 4.5$
for sulphuric acid, $\sigma_w = TDS / 1.25$
for TDS in "most" natural waters, $\sigma_w = TDS / 6.25$.

In summary, ground conductivity in soils varies with:

1. Soil structure (coarser structure and/or smaller porosity produces lower conductivity).
2. Clay content (increasing clay fraction, produces higher conductivity).
3. Soil moisture content (increasing moisture produces higher conductivity).
4. Increasing conductivity of the soil water.

Typical conductivity anomalies in environmental and geomorphic applications are a function of one or more of the variables listed in the paragraph above. In addition, where bedrock is under the influence of the applied EM field, conductivity of the rock matrix may influence the EM response. Archie's Law still applies in these cases and clay conductivity (σ_{clay}) can be substituted and generalized by rock matrix conductivity ($\sigma_{rock\ matrix}$) such that:

$$\sigma_a = \sigma_w \times n^m + \sigma_{rock\ matrix}$$

The rock types that generally produce conductivity anomalies are shales, weathered rocks, massive sulphides, and graphite (Fig. 2.8). In the first example, shown in Figure 2.9, a resistive till overlies a conductive shale bedrock. Bedrock highs produce conductivity highs and bedrock valleys produce conductivity lows. If the situation were reversed, conductive clay overburden over a resistive limestone, bedrock highs would produce conductivity lows and bedrock valleys would produce conductivity highs. In the second example, soil moisture content or distance to the more conductive water table controls the EM response. Conductivity highs are recorded in the valleys, conductivity lows over the hills. Clay content controls the EM response in the third example. A conductivity anomaly is recorded over the conductive clay surrounded by resistive till. All three scenarios listed under water quality change, exhibit a conductivity anomaly caused by varying soil water conductivity. In the first of these three scenarios, coastal salt water intrusion increases freshwater conductivity. In the second example, the salinized soil above the water table produces a strong conductivity anomaly. Because salt is hygroscopic, those areas which are highly salinized seem to retain enough soil moisture to keep the conductivity at measurable levels, even when the soil is relatively dry (McNeill, 1990). In the last example, electrically conductive contaminants (e.g. electrolytic solution) leaking from barrels increases conductivity in both the unsaturated and saturated ground.

Table 2.4. *Factors affecting terrain conductivity*

Archie's Law for saturated ground with clay:

$$\sigma_a \cong \sigma_w n^m + \sigma_{clay}$$

(1) for typical soils (sandy soil, sandy loam)

$$n^m \cong \frac{1}{4}$$

(2) for typical soil water, σ_w is determined by product of concentration of ions and ionic mobility

$$\sigma_w(mS/m) \cong \frac{TDS}{6}\ (ppm\ or\ mg/l) \qquad TDS = Total\,Dissolved\,Solids$$

$$\sigma_a(mS/m) \cong \frac{TDS}{6}\ (ppm)\ x\ \frac{1}{4} + \sigma_{clay}$$

$$\cong \frac{TDS}{25}\ (ppm) + \sigma_{clay}$$

(3) for acid mine drainage (sulphuric acid)

$$\sigma_a(mS/m) \cong \frac{TDS}{1.25}\ (ppm) \times \frac{1}{4} + \sigma_{clay}$$

$$\cong \frac{TDS}{5}\ (ppm) + \sigma_{clay}$$

(4) temperature dependence ≅ 2% per degree C
conductivity increases as a function of temperature.

Description of an EM instrument - the Geonics EM31

The EM31 is a typical EM instrument in that both transmitter and receiver are induction coils. The transmitter of this frequency domain system emits a 9.8 kHz magnetic field. As described by Faraday's Law, the time-varying magnetic field induces electric currents in a conductive earth (or a conductive lens as shown in Figure 2.10). These currents generate a secondary magnetic field as described by Ampère's Law which in turn induce a voltage in the receiving coil. For low conductivities, this voltage measured in quadrature is proportional to the ground conductivity and

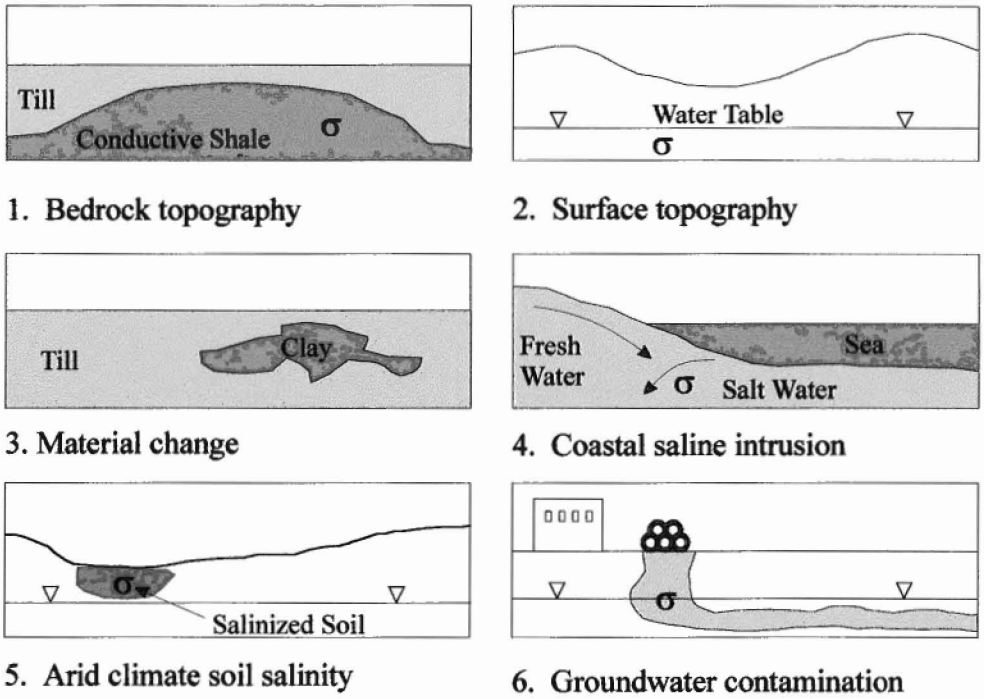

Figure 2.9. *Conductivity anomalies in environmental and geomorphic applications.*

the EM31 displays this quadrature reading as an apparent conductivity. This measurement is described as apparent because it is valid only for a halfspace - a uniform conductivity volume below the instrument.

Coil separation between the transmitter and receiver, coil orientation, operating frequency and ground conductivity are all variables which determine the effective depth of investigation of the instrument (Fig. 2.11). Two typical coil orientations, both co-planar, used with the EM31 are the vertical dipole mode where the coils are horizontal but the dipole moment is vertical and the horizontal dipole mode where the two coils are vertical but the dipole moments are horizontal. In the vertical dipole mode, effective penetration is approximately 1.5 times the coil separation, while in the horizontal dipole mode, effective penetration is approximately 0.75 times the coil separation. Taking measurements at both coil orientations is an effective tool for rapid shallow sounding. The EM34, an instrument similar to the EM31 offers variable coil separations of 10, 20 and 40 m, resulting in greater depth penetration. It is useful to remember that depth penetration estimates based solely on coil separation are only a rule of thumb and remain highly dependent on ground conductivity. For very conductive ground, depth of investigation may be restricted to the top metre, while for very resistive ground, depth of investigation may be extended to 2 or 3 times the coil separation.

It is worthwhile examining in more detail the quadrature to apparent conductivity conversion used by the EM31 (and EM34) as it is only valid at low conductivities. The graph in Figure 2.11 shows that, depending on coil orientation, apparent conductivity values above 100 mS/m are 10% to 20% below true ground conductivity and above 1000 mS/m are 35% to 70% below true ground conductivity. Below 1 mS/m, the currents induced in the ground are not strong enough to be measured by the receiver, and therefore, this family of fixed-separation loop-loop EM instruments is of limited use in discriminating resistive terrains.

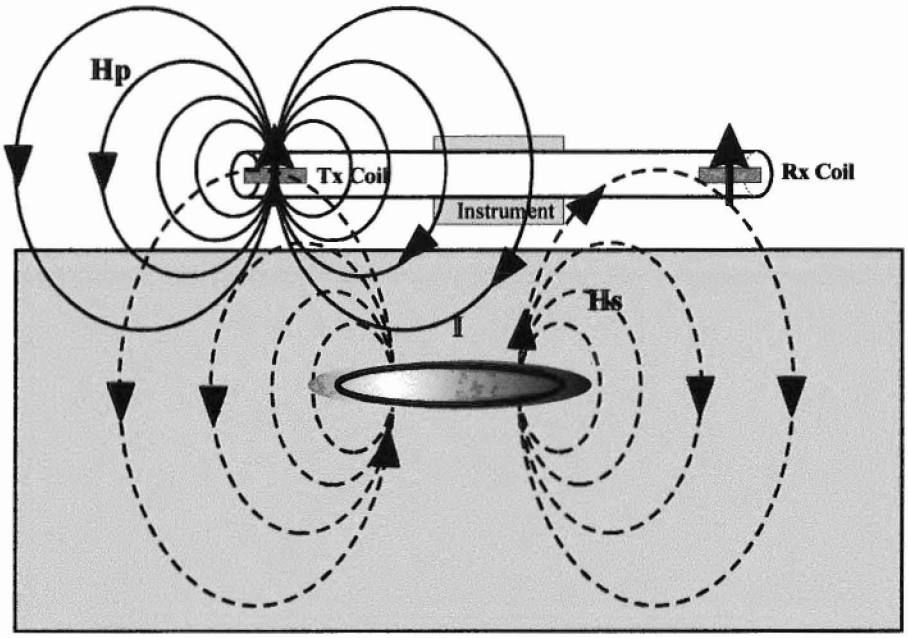

- Operating frequency is 9.8 kHz
- Coil separation is 3.66m
- Apparent conductivity is a linear function of conductivity, at low conductivities. Apparent conductivity displayed by the EM31 uses this relation:

$$\sigma = \frac{4[H_s/H_p]_Q}{\mu_0 \omega s^2}$$

where σ - conductivity (S/m)
H_s, H_p - magnetic field strength, secondary and primary (A/m)
Q - quadrature component (also called imaginary or out-of-phase)
μ_0 - magnetic permeability of free space (H/m)
ω - angular frequency (Hz)
s - coil separation (m)

Figure 2.10. *Sketch illustrating induction in a confined conductor for the EM31 conductivity meter.*

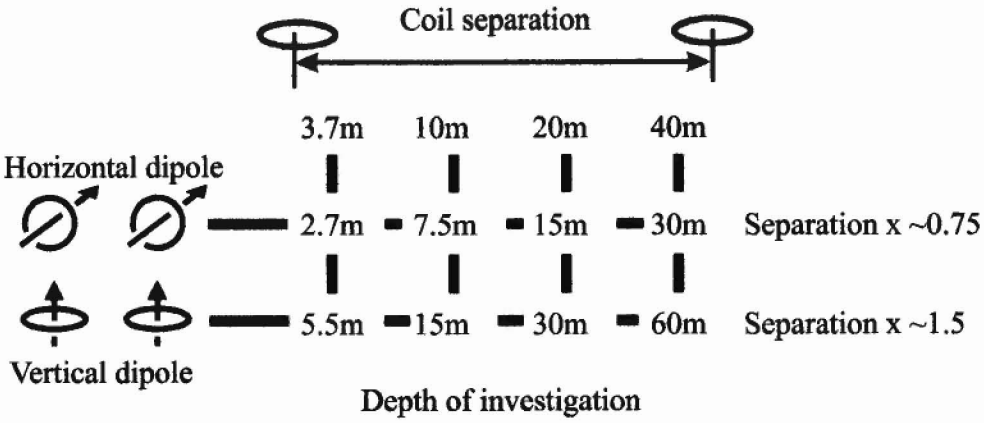

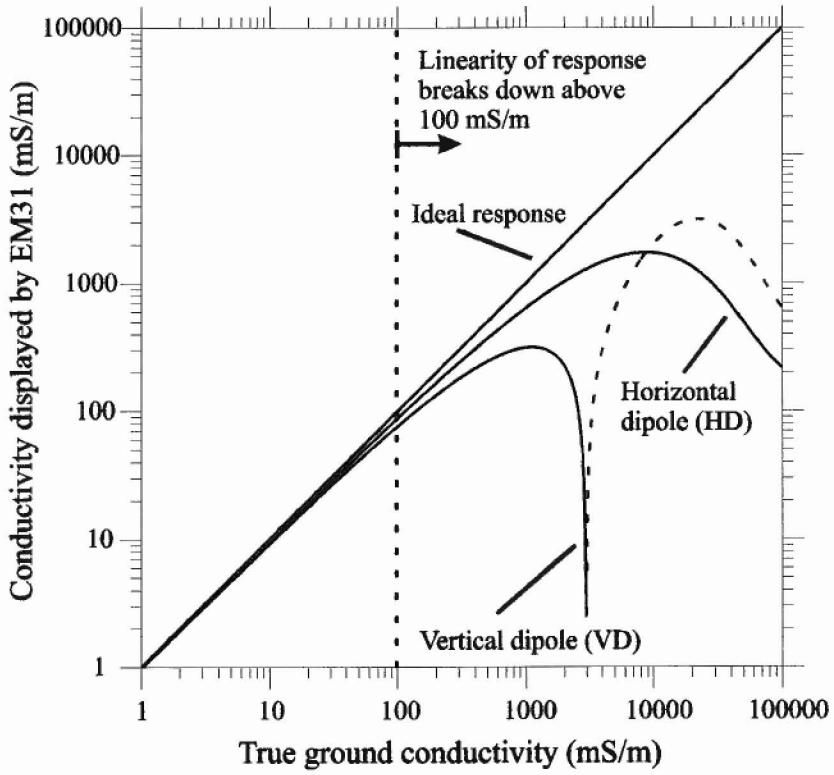

Figure 2.11. *Depth of investigation and linearity of the conductivity response of the EM31.*

Interpretation of EM data

The tools necessary for interpretation and analysis of EM data originate from a variety of sources. Most research in the study of EM interpretation is drawn from a combination of sources: field measurements, laboratory experiments, physical scale modelling and computer modelling. Field

measurements may include ground, airborne or borehole surveys in conjunction with ground-truthing drillhole information. Laboratory measurements involve either rock property measurements taken from field samples or scale-model studies which simulate both field instrument response and earth material properties. In recent years, computer modelling has dwarfed physical scale modelling as the dominant interpretation tool. These models can be divided into three major categories with increasing levels of complexity (Fig. 2.12).

1. 1-D: The physical properties of the earth vary only as a function of depth. These types of models are also called layered-earth models. The halfspace where the earth or the volume below surface exhibits uniform physical properties is one of the simplest forms of this model.

2. 2-D: In addition to physical properties such as conductivity varying with depth, physical properties may vary laterally. Features such as geological boundaries, topography, buried valleys and dipping beds may be modelled. A 2-D modelling example is described in the case study below.

3. 3-D: Three-dimensional objects may be modelled. Some classic analytical models developed from the 1950s to the 1970s are the EM response of a buried sphere and a buried cylinder. These models can be used to simulate buried drums, massive sulphide lenses or tunnels. Presently, much of the modelling research is focussed on developing efficient numerical techniques, in which the model is constructed with a 3-D grid to simulate geological models. These techniques, shunned in the past because of the intensive computer power required have become increasingly popular because of their ability to realistically model geological environments.

These geometric models can be formulated as forward problems, where the model is given and the synthetic EM data are calculated, or as inverse problems, where the EM field data are given and a synthetic model is calculated. Forward modelling software exists for all three model geometries described above, whereas inverse modelling software exists

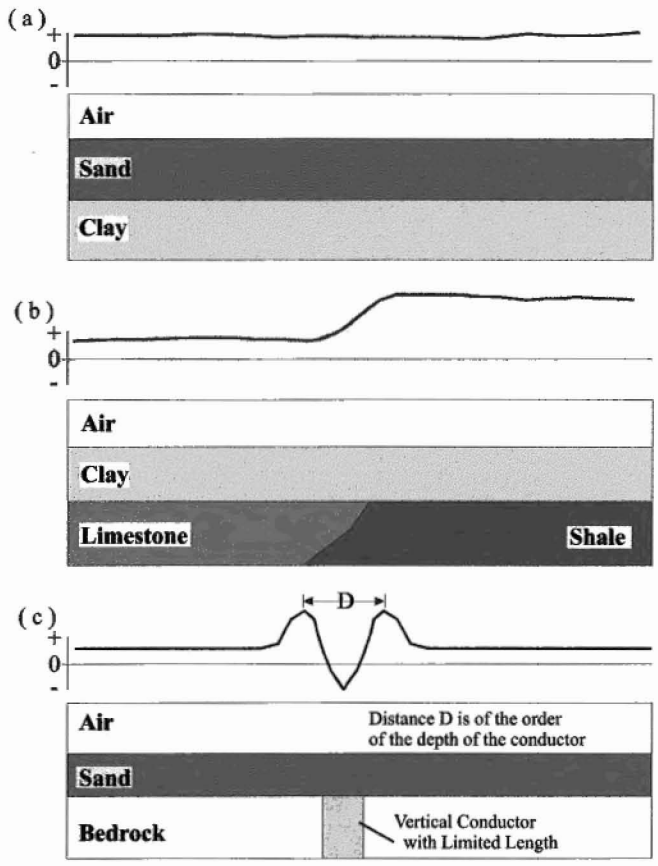

Figure 2.12. *EM interpretation: typical models and examples of survey profiles. (a) one-dimensional, layered-earth, (b) two-dimensional, and (c) three-dimensional*

commercially only in the 1-D and 2-D formulations.

Noise sources and cultural anomalies in EM surveys

Unfortunately, it is not only geological anomalies that produce EM signals. Unwanted signals may either be noise generated by an independent power source (e.g. a power transmission line) or cultural anomalies generated by currents in engineering structures (e.g. railway tracks) that swamp or interfere with the wanted signal. Noise sources may be natural such as sferics (Fig. 2.13) primarily generated by lightning discharge or artificial such as those caused by the 60 Hz (and odd harmonics) signal of power lines. The following list illustrates some typical noise sources:

1. Sferic (atmospheric) noise is usually not a problem for most EM surveys. In cases where symptoms of sferic noise such as erratic jumps or fluctuations in meter readings are observed, instrument malfunction is more likely to be the cause.
2. Power line noise: Although many frequency domain instruments use 60 Hz notch filters to remove power line noise, it often not sufficient to completely remove the effect of these strong unwanted signals. Surveying near power lines is often not possible.
3. Noise due to coil motion (e.g. wind): Unwanted angular motion of the receiver coil can cause an EM signal. Indeed, a coil rotating in the earth's DC magnetic field will induce a voltage in the sensor.
4. Interference from another EM (geophysical) instrument: Two instruments, if they transmit and are sensitive to similar frequencies or frequency ranges will interfere with each other. A good rule of thumb, based on the coil separation rule stated above is to keep the two instruments a minimum distance from each other, roughly two times their coil separation.
5. Interference from other EM transmitters: Other EM transmitters such as AM, FM and communication transmitters usually do not interfere with operation of EM equipment because they operate at much higher frequencies than the operating frequencies of typical EM instruments.

Cultural anomalies are caused by artefacts such as power lines, pipelines, railroads or any other metallic infrastructure or structure. Two EM prospecting concepts are useful in avoiding and recognizing cultural anomalies:

1. The distance at which a metallic structure or object is detected by the EM method is proportional to the size of that object. Currents induced on a metallic object circulate on its surface, the size of those current vortices is proportional to the surface area of the object. A closed loop of wire, or any closed path, can constitute a valid current path and produce a significant anomaly. For example, a power line in itself does not produce a sizeable anomaly. To do so, the power line must be grounded at least at two positions (it almost always is), thereby providing a return current path through the earth. Short power lines can be detected a short distance away, tall power lines can be detected a long distance away.
2. The angle at which the primary magnetic field couples with the surface of an object also determines the size of the EM anomaly. Primary magnetic fields that are perpendicular to the surface of a metallic object are maximum coupled and therefore maximize the response of that object. Conversely, primary magnetic fields that are parallel to the surface of a

metallic object are minimum coupled (or null coupled) and therefore minimize the response of that object. With large-loop EM instruments, it is sometimes possible to position the transmitter loop so as to provide minimum coupling with the unwanted object.

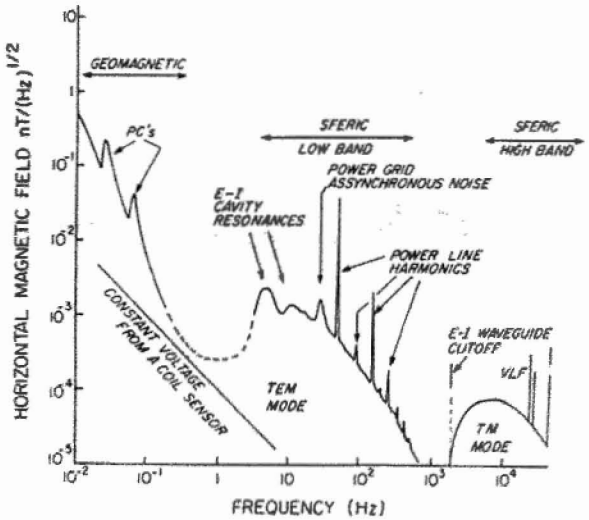

Figure 2.13. *Frequency range and amplitude of EM noise (Macnae et al., 1984).*

In general, it is preferable to stay a safe distance away from metallic conductors such as power lines, pipelines and fences etc. For large-loop or remote transmitter systems, a safe distance is 1.5 to 2 times the size of the unwanted object. For smaller loop-loop systems such as the EM31 and EM34, a safe distance is 1.5 to 2 times the coil separation. If avoiding the structure is impossible, measuring its effect is important. Running several profiles perpendicular and parallel to the structure can help determine its effect. It may then be possible to remove the effect of the cultural anomaly from the data. Table 2.5 lists typical cultural anomalies.

Table 2.5. *Cultural anomalies in EM measurements.*

1.	**Power lines** - grounded loops. If possible, stay away. Sometimes possible to obtain permission, for smaller power lines, to "un-plug" grounding cables.
2.	**Pipelines, railroads and u/g cables** - grounded metallic conductors. Typically can cause high amplitude but small spatial extent anomalies.
3.	**Fences**, chain-link - most serious in HD mode. Often useful to run several lines perpendicular and parallel to the fence to gauge its effect.
4.	**Tanks, Drums**, buried metallic objects. Typically cause 3-D anomalies with small spatial extent. Be cautious of these in old landfill sites, gravel pits, abandoned mine sites, etc.

A case study

Interpreting surveys in terms of a layered earth

The capability of EM techniques is illustrated by the following example of a survey and interpretation. In this example, variation in electrical conductivity is interpreted as a geological change according to a layered earth model. Many geological settings can be described as a horizontally layered series of units, each with its own electrical conductivity. The layers may vary in thickness, depth, and internal properties. All of these factors influence the electrical conductivity sensed at the surface. An accurate interpretation of an EM survey depends on prior knowledge of how the components of the layered system can vary. An unambiguous interpretation is most likely when the conductivity differences between layers are large, the conductivities of the different layers are known and constant, and the geology continuously conforms to the layered model.

Departures from the layered model, for example due to lateral changes in conductivity or the presence of a vertically-oriented unit, can be dealt with, but, again, prior knowledge of these departures from the horizontally layered geometry is necessary. Otherwise, such complexities in the geology will be interpreted as simply a change in the thickness of the components of the layered model. Because different geological situations can produce the same geophysical response, some first hand knowledge of the geological character of the survey area is necessary. This is obtained through subsurface observation by borehole, test pit, road cut or outcrop.

The simplest geological setting for an EM survey is the two layer case where a layer of given conductivity, σ_1, overlies another material of differing conductivity, σ_2, that extends to indefinite depth (at least beyond the sounding depth of the instrument in use). The apparent conductivity measured by EM techniques is determined by the conductivities of individual materials, weighted according to how the electromagnetic field induced by the particular instrument diffuses with depth. If the conductivity of each layer remains constant, the only variable capable of changing the apparent conductivity observed at the surface is the thickness of the upper material. If the upper material thins and disappears, then the apparent conductivity is the conductivity of the underlying material (σ_2). If the upper material becomes so thick that it extends beyond the sounding depth of the instrument, then the apparent conductivity is the conductivity of the overlying material (σ_1). Hence, variation in apparent conductivity is most likely caused by changes in the thickness of the upper layer. This thickness variation can be determined if the contribution of the layer to the apparent conductivity is known.

A two-layer example

Knowledge of thicknesses in a layered or stratigraphic sequence is necessary for many geomorphic and engineering applications. It may serve to define the geometry of a buried glacial feature or identify the depth to an aquifer. A strong contrast in electrical conductivity between layers makes EM techniques very effective in mapping the thickness of units in a layered setting. In the Kingston area, the Geonics EM31 has been used to map the thickness of a lacustrine clay overlying limestone. In this case, planning for housing construction required a knowledge of bedrock depth and an outline of areas where excavations in bedrock would likely encounter groundwater inflow. Basements of

houses in adjacent developed areas had been subject to seepage where excavations intersected bedrock at the base of bedrock slopes. Prior knowledge of bedrock topography permitted such hydraulic settings to be avoided in subsequent construction areas.

The land holding intended for residential development was surveyed by taking readings of apparent conductivity at predetermined locations on a grid (Fig. 2.14). The contoured results of this survey are shown in Figure 2.15. To interpret these data, a two-layer geological model was adopted. Boreholes and test pits on the property had demonstrated the existence of the lacustrine clay layer over bedrock. It was also reasonable to assume that the limestone bedrock extended well beyond the sounding depth of the EM31 instrument. Therefore, the clay comprised the upper layer and the limestone bedrock comprised the lower layer.

Interpreting the data consists of converting apparent conductivity to bedrock depth. To do this, a calibration curve for the particular geological setting under study is constructed. The equation for a 2-layer case expressing apparent conductivity in terms of the contributions of the different layers to apparent conductivity reading is used:

$$\sigma_a = \sigma_1(1 - R(z_1)) + \sigma_2 R(z_2)$$

where σ_1 is the conductivity of the lacustrine clay and σ_2 is the conductivity of the bedrock.

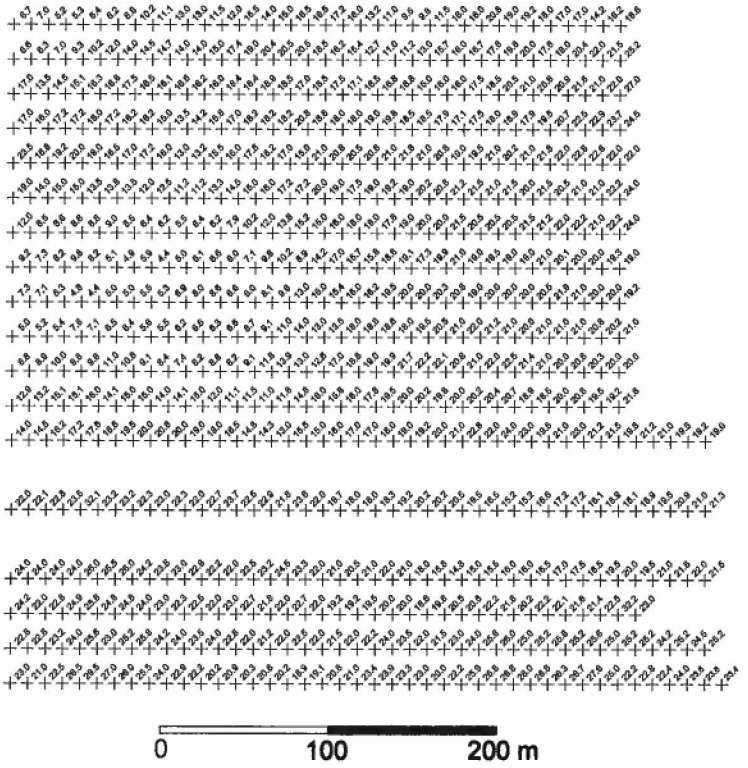

Figure 2.14. *EM31 survey grid, showing apparent conductivity readings in mS/m.*

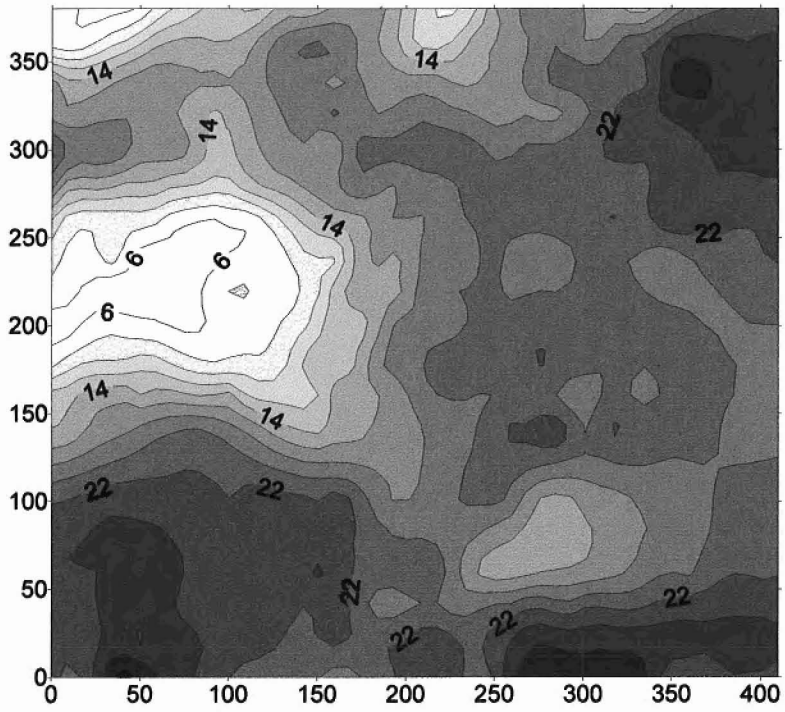

Figure 2.15. *Isopleth map of apparent conductivity for the survey area in Figure 2.14. Isopleth interval is 2 mS/m. Scales in metres.*

Apparent conductivity is calculated for a number of arbitrary depths to construct the calibration curve. *R(z)* is the cumulative relative contribution of all the material below a depth z to the instrument response. It represents the degree to which the conductivity of a material below a given depth contributes to the instrument reading. It is a characteristic of the particular instrument being used and for the EM31 is shown in Figure 2.16. $R(z_1)$ is the proportion of the sensitivity extending below the depth z_1 of the upper (first) layer and $(1-R(z_1))$ is the proportion extending down to the same depth z_1. Once the calibration curve is constructed, then the upper layer thickness for any apparent conductivity reading can be read from the curve.

Where bedrock is exposed at the surface, readings between 4 and 5 mS/m were obtained (this is σ_2). Where the clay is known to be at least 6 m thick, a reading of 31 mS/m was obtained (this is σ_1). These apparent conductivity readings are equivalent to the actual conductivities of each of the two layers because the readings are taken at locations where each layer extends from the surface to a depth effectively beyond the sounding depth of the instrument. Table 2.6 shows apparent conductivities calculated using the 2-layer equation, the above values for σ_1 and σ_2, and the multilayer response curve.

With the calibration curve constructed (Fig. 2.17), the apparent conductivities in Figure 2.14 can be converted to upper layer thicknesses. This has been done in Figure 2.18. These thicknesses can then be subtracted from the surface elevation to give elevations on the bedrock surface, if that is desired.

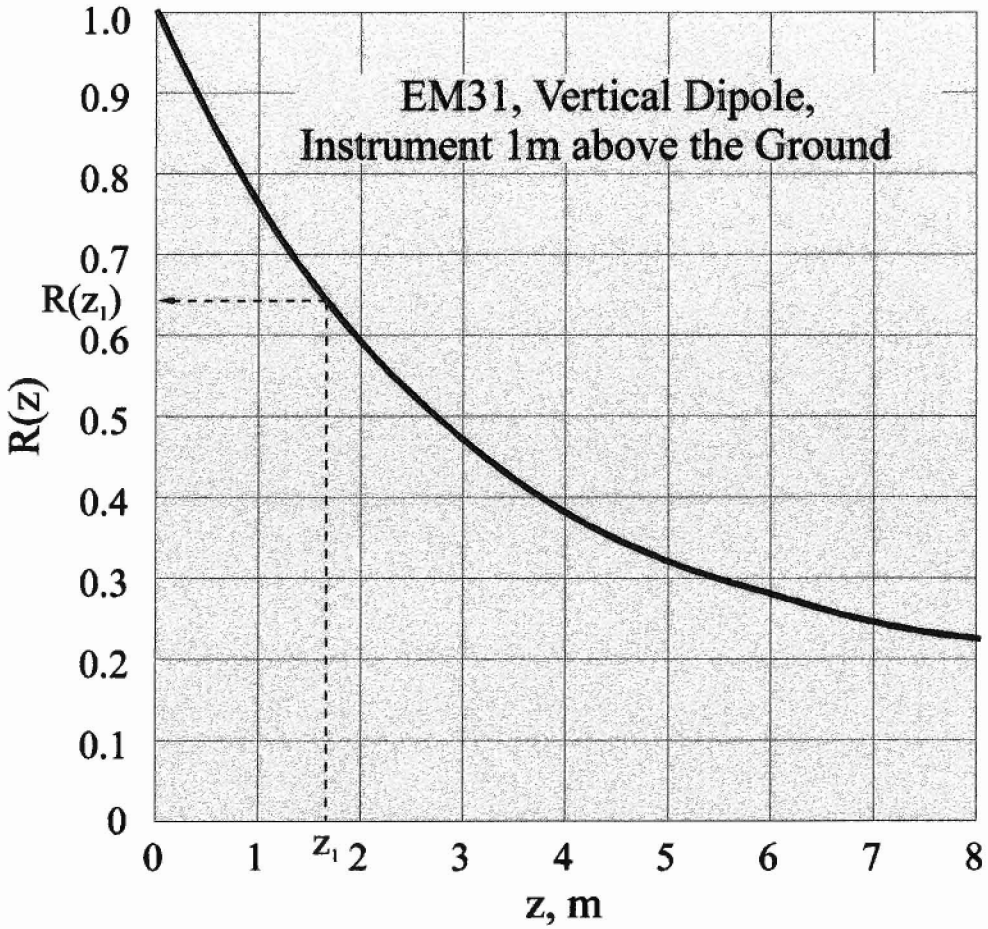

2 Layer Model

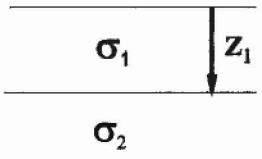

$$\sigma_a = \sigma_1(1-R(z_1)) + \sigma_2(R(z_1))$$

3 Layer Model

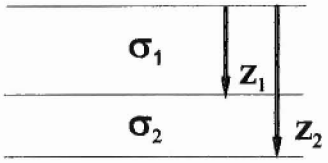

$$\sigma_a = \sigma_1(1-R(z_1)) + \sigma_2(R(z_1) - R(z_2)) + \sigma_3(R(z_2))$$

Figure 2.16. *Curve showing how the sensitivity of the EM31 decreases with depth. R(z) is the proportion that the ground below a given depth, z, contributes to the apparent conductivity reading. The equations allow apparent conductivity to be calculated given the conductivities of the layers and the portion of instrument sensitivity that each layer receives. (McNeill, 1980).*

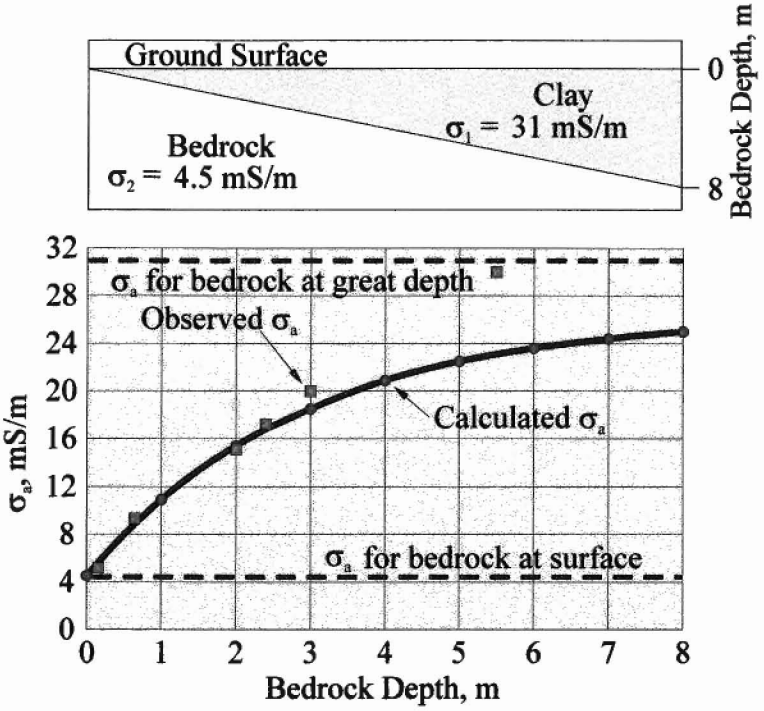

Figure 2.17. *Calibration curve for converting apparent conductivity (σ_a) to bedrock depth at the Kingston study site. Curve with circles indicates calculated apparent conductivities based on selected values for σ_1 and σ_2, squares are apparent conductivities observed at sites where the depth to bedrock was determined in excavations.*

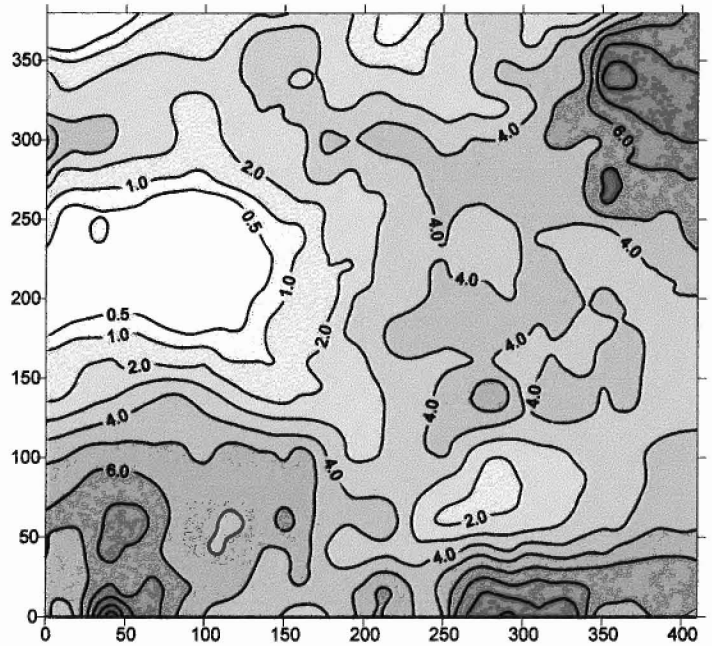

Figure 2.18. *Isopleth map of depth to bedrock (or clay layer thickness). Isopleth interval is 1 m with an extra level at 0.5 m. Scales in metres.*

Table 2.6. *Apparent conductivities calculated using 2-layer equation.*

Thickness of the σ_1 layer (m)	$R(z_1)$	σ_a (mS/m)
0	1.00	4.5
1	.76	10.9
2	.59	15.4
3	.47	18.5
4	.38	20.9
5	.32	22.5
6	.28	23.6

note: $\sigma_1 = 31$ mS/m
$\sigma_2 = 4.5$ mS/m

The technique would work in other geologic settings, such as a glaciofluvial-lacustrine sequence. In this case, deltas prograding onto silts and clays may be present and an EM survey would permit the thickness of the deltaic component to be determined, assuming that a reasonable contrast in conductivity between the deltaic and lacustrine sediments existed. An instrument with a sounding capability deeper than the EM31 would be necessary if the deltaic sediments were thicker than about 5 m but the survey and analysis procedure would be essentially the same.

Accuracy of the interpretation

As a check on the accuracy of the clay layer thickness determinations, apparent conductivity readings were taken at locations where test pits were subsequently dug to bedrock. Table 2.7 gives these readings along with the clay thicknesses and expected apparent conductivities based on the σ_1 and σ_2 values used in constructing the calibration curve.

Table 2.7. *Comparison of measured σ_a to calculated σ_a.*

Depth to Bedrock (m)	Actual σ_a (mS/m)	Calculated σ_a (mS/m)
0.15	5.2	5.4
0.64	9.3	8.5
2.0	15.1	15.4
2.4	17.2	17.4
3.0	20.0	18.5
5.5	30.0	24.1

The closeness of the agreement between interpreted and measured depths to bedrock can be seen in Figure 2.17. The explanation for the discrepancy below 3 m depth is most likely variability in the conductivity of the clay; 39 mS/m would be required to give the observed apparent conductivity at the 5.5 m location. Alternatively, the observed apparent conductivity could be interpreted as a clay thickness considerably in excess of 10 m. It is entirely possible that the clay

conductivity could show the required variation, due to changes in pore water salinity, moisture content, etc. It is less likely that the clay reaches such thicknesses, based on its habit in the area. It should be apparent how knowledge of the geology is necessary to resolve this ambiguity. It should also be emphasized that the instrument sensitivity to changes in clay layer thickness decreases as the layer thickens (see Fig. 2.17 which shows how little the apparent conductivity is changing for clay thicknesses beyond 5-6 m). As pointed out previously, the accuracy of the interpretation is likely to be determined by the familiarity with the geological setting.

Dealing with more than two layers

As long as the conductivities of each layer in a two layer case are reasonably uniform, there is little chance that difficulties in interpretation will arise. When a third layer is present, different combinations of layer thicknesses can give the same apparent conductivity. The equation giving σ_a in terms of the layer conductivities for any number of layers, n, is:

$$\sigma_a = \sigma_1(1 - R(z_1)) + \sigma_2(R(z_1) - R(z_2)) + \ldots + \sigma_n(R(z_n))$$

It should be obvious that as the number of layers increases, various combination of layer thickness can give the same σ_a value.

In a three-layer sequence with conductivities decreasing with depth, a decrease in apparent conductivity could be interpreted as a decrease in the uppermost layer thickness or an increase in the middle layer thickness. Selecting the correct interpretation would require knowledge of the geology sufficient that the most likely tendency would be known. Thus the possibility of more than one interpretation underlines the requirement that geophysical measurements must be used to extend geological knowledge rather than determine geology where no prior understanding exists.

Summary

In a suitable geological setting, a ground conductivity survey can be a very efficient way of mapping subsurface geology or a condition of the ground with a distinctive conductivity. The key to a useful outcome is 1) a prior understanding of the general geological character of a site or feature, 2) a geological setting or feature which can be described in terms of, at most, a few layers and 3) the existence of a discernable contrast in electrical conductivity between these elements.

Conclusion

EM methods can be used for a variety of applications to delineate conductivity contrasts and to assess material properties. It is a relatively quick and inexpensive survey method that offers both lateral mapping and depth sounding capability. Although it lacks the resolution of instruments that operate in the wave propagation regime such as GPR and acoustic techniques, the ability of EM to detect targets at great depths is one of its inherent advantages. As with all geophysical techniques, and in spite of the very powerful forward and inverse modelling tools available, interpretation of EM data should always be done in conjunction with reliable ground-truthing, be it drillhole logging, geological mapping, water sample analysis or any other independent assessment method.

REFERENCES

Jackson, P.D., Taylor-Smith, D., and Standford, P.N.
1978: Resistivity-porosity-particle shape relationships for marine sands; Geophysics, v. 43, p. 1250-1268.

Klein, J. and Lajoie, J.J.
1980: Electromagnetic prospecting for minerals; in Practical Geophysics for the Exploration Geologist; Van Blaricom R. (ed.); Northwest Mining Association, Spokane, Washington, p. 239-293.

Macnae, J.C., Lamontagne, Y., and West, G.F.
1984: Noise processing techniques for time-domain EM systems; Geophysics, v. 49, p. 934-938.

Marchand, N.
1990: A scale-model study of the borehole pulse electromagnetic response from two conductors; M.Sc. thesis, Queen's University, Kingston, Ontario.

McNeill, J.D.
1980: Electromagnetic terrain conductivity measurement at low induction numbers; Geonics Technical Note TN-6.
1990: Use of electromagnetic methods for groundwater studies; in Geotechnical and Environmental Geophysics, Volume I: Review and Tutorial, Ward S.H. (ed.); Society of Exploration Geophysicists, Tulsa, Oklahoma, p. 191-217.

Palacky, G.J.
1988: Resistivity characteristics of geological targets; in Electromagnetic Methods in Applied Geophysics, Volume 1: Theory; Nabighian M.N. (ed.); Society of Exploration Geophysicists, Tulsa, Oklahoma, p. 53-129.

Telford, W.M., Geldart, L.P., and Sheriff, R.E.
1990: Applied Geophysics, (2nd ed.); Cambridge University Press, Cambridge, p. 343-521.

Todd, D.K.
1964: Groundwater, handbook of applied hydrology; McGraw-Hill, New York.

Other publications of interest

Grant, F.S. and West, G.F.
1965: Interpretation theory in applied geophysics; McGraw-Hill, New York.
An early applied geophysics textbook. Somewhat out of date with respect to instrumentation, but still has an excellent EM theory section.

Nabighian, M.N. (ed.)
1987: Electromagnetic methods in applied geophysics, volume 1: theory, volume 2: applications; Society of Exploration Geophysicists, Tulsa, Oklahoma.
Very comprehensive technical textbook on EM methods and theory.

Sheriff, R.E. (ed.)
1984: Encyclopedic dictionary of exploration geophysics (2nd ed.); Society of Exploration Geophysicists, Tulsa, Oklahoma.
A good reference; a third edition is now available.

Telford, W.M., Geldart, L.P., and Sheriff, R.E.

1990: Applied geophysics (2nd ed.); Cambridge University Press, Cambridge.

Considered by many geophysicists to be a geophysical "bible". Mostly mineral and petroleum exploration applications. Good reference for theory and instrument design.

Van Blaricom, R. (ed.)

1980: Practical geophysics for the exploration geologist (1st ed.); Northwest Mining Association, Spokane, Washington.

Very basic and practical geophysics textbook. Written for the geologist, not as technical as the other texts; suitable the non-geophysicist. 2nd edition available with much expanded EM section.

Ward, S.H. (ed.)

1990: Geotechnical and environmental geophysics, volume I: review and tutorial, volume II: environmental and groundwater, volume III: geotechnical; Society of Exploration Geophysicists, Tulsa, Oklahoma.

Of all textbooks listed here, best suited for geomorphic, environmental and geotechnical applications.

CHAPTER 3 Land-based shallow seismic methods

Susan E. Pullan and James A. Hunter

Introduction

Land-based seismic methods are geophysical techniques which use measurements of the time taken for acoustic energy to travel from a source on the surface through the subsurface and back to a series of receivers on the ground. Energy is refracted or reflected at boundaries where there is a change in acoustic impedance (the product of material density and seismic velocity). Because contrasts in acoustic impedance are generally associated with lithological boundaries, seismic techniques can be used to obtain subsurface structural information. The purpose of this paper is to outline the application of land-based seismic methods to delineating the structure of unconsolidated sediments and the underlying bedrock surface.

Until the 1980s, refraction rather than reflection methods were used almost exclusively when shallow subsurface structural information was required (note that the situation was completely different for water-based studies - see Chapter 6). Refraction methods depend on the measurement of only the time of first arrival of seismic energy at each receiver location, and so do not require digitization of the seismic wave train or computer processing of the data. Thus, refraction surveys could be carried out with relatively simple and inexpensive equipment, and for many decades were the only shallow seismic method used to obtain estimates of the depth to bedrock, and if possible, to determine the major lithologic boundaries within the overburden.

Seismic reflection methods have been the primary geophysical tool used in oil and gas exploration for over 60 years. Because of the tremendous commercial importance of oil, much industrial research and development has been invested in this branch of geophysics. By the 1960s, specialized field procedures, digital magnetic tape recording, and computer processing of the data had become standard in the industry. More recently, the need for more accurate and detailed subsurface structural information for petroleum exploration was one of the driving forces behind the development of supercomputers. Conventional seismic reflection techniques are highly sophisticated, but require considerable investment in both data acquisition and processing.

In the early 1980s, the development of digital enhancement engineering seismographs with high-pass filtering capabilities and the proliferation of increasingly powerful microcomputers, began to make the application of seismic reflection methods to "shallow" problems a viable alternative. Over the last 15-20 years, much experience and expertise in the application of shallow high-resolution reflection techniques have been gained, and today these methods are not only technologically viable, but are also becoming accepted and proven shallow geophysical tools.

Both refraction and reflection techniques have potential applications in geomorphological research, where information on the depth to bedrock, the bedrock topography or the overburden stratigraphy would be useful (e.g. Hunter et al., 1989; Roberts et al., 1992). Both techniques can be applied using compressional (P-wave) or shear (S-wave) energy (compressional waves are those in which the particle motion and direction of wave propagation are the same, whereas shear waves are those in which the particle motion is normal to the direction of wave propagation). The use of seismic methods and the choice of refraction or reflection surveys depend on the particular geological setting, the desired information, and the range of depths that are of interest. In this paper both these techniques are discussed briefly (assuming the use of compressional waves), and some examples of survey data are presented. The objective is to describe the type of information that can be obtained with these methods and the conditions under which the best results might be expected, as well as the limitations of shallow seismic refraction and reflection techniques.

Seismic refraction methods

Seismic refraction methods involve the measurement of the time of first arrival of seismic energy at a series of source-receiver separations. Energy is radiated downwards into the ground from a seismic source on or near the ground surface (hammer striking a plate, falling weight, in-hole shotgun, explosives, etc.). At subsurface interfaces across which there is a change in seismic velocity (V_1 to V_2), energy is refracted according to Snell's law:

$$(\sin i_1) / V_1 = (\sin i_2) / V_2$$

where i_1 is the angle (with the normal to the interface) of the incident wave travelling with a velocity V_1 in layer 1, and i_2 is the angle of the refracted wave travelling with a velocity V_2 in layer 2. When V_2 is greater than V_1 there is a critical angle of incidence i_c where the angle of refraction $i_2 = 90°$ and $\sin i_2 = 1$:

$$\sin i_c = V_1 / V_2 \qquad \text{(critical angle of incidence)}$$

For angles of incidence greater than i_c, the energy is totally reflected into the upper layer. Energy that is critically refracted travels along the interface at a velocity V_2, and is continuously radiated back to the surface where it can be detected by geophones (Fig. 3.1). As the source-receiver separations increase, energy that has been refracted from deeper (i.e. higher velocity) horizons overtakes the shallower refractions and becomes the first arrival. The arrival times and source-receiver distances are used to determine layer velocities and depths to the refracting horizons.

As can be seen from the above analysis, refraction methods are based on the assumption that velocity increases with depth, as energy is refracted *away* from the surface at an interface where velocity decreases. Velocity contrasts must also be large for an interface to be definitively identified in a refraction analysis.

The theory and various methods of collecting and interpreting seismic refraction measurements can be found in basic textbooks on exploration geophysics (e.g. Dobrin, 1976; Telford et al., 1976), in more detail in textbooks devoted to refraction methods (Sjögren, 1984; Palmer, 1986), and in a summary by Lankston (1990). With the development of digital engineering seismographs and the advent of microcomputers, seismic refraction records are now interactively picked and analyzed using software developed for personal computers. Techniques such as delay time methods and the GRM (generalized reciprocal method; Palmer, 1981; see also Lankston, 1990), which yield more detailed information on subsurface structure than the simple dipping layer interpretation, can now be applied more easily and cost-effectively. As the application of shallow seismic reflection methods becomes more common (see below), attempts are being made to utilize the first arrival data from these large data sets to determine detailed near-surface velocity information (e.g., using refraction tomography, Lanz et al., 1998).

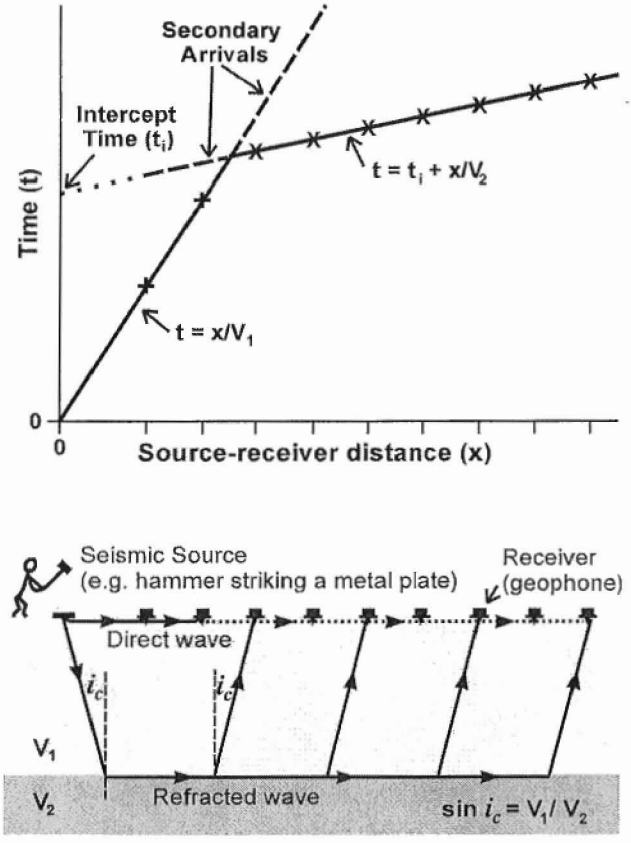

Figure 3.1. *Time-distance graph (top), and direct and critically refracted raypaths (bottom) in the ideal two-layer case. First break times are noted by crosses on the time-distance graph. Solid lines are defined by first breaks. Dashed lines on the time-distance graph are secondary arrivals that might not be visible on the field record or might be difficult to time accurately. The dotted line is the projection to the intercept time based on critically refracted arrival times. (Adapted from Lankston, 1990).*

In general, refraction methods are very useful for determining the depth to bedrock particularly where it is within approximately 30 m of the surface and where this interface is characterized by a large velocity increase (Table 3.1). As the depth to bedrock increases, and/or the velocity contrast at this horizon decreases, longer spread lengths (series of source-receiver separations) and larger sources (e.g. explosives) are required to measure refracted energy from the bedrock surface. As a rule of thumb, spread lengths of approximately 3-5 times the depth to a target horizon characterized by a strong velocity increase are required to observe refractions from that horizon as first arrivals.

Table 3.1. Compressional- and shear-wave seismic velocities for a variety of sediment/rock types.

Compressional Velocity (m/s)	Shear Velocity (m/s)	Sediment/Rock Description
300-1500	50-400	Unconsolidated clays and silts; unsaturated sands and gravels
1500-2000	200-800	Saturated sands and gravels; compacted clays and silts; glacial tills; completely weathered rocks
2000-2500	800-1200	Partially consolidated sediments; compacted glacial tills; highly weathered metamorphic/igneous rocks; weathered and/or jointed sandstones and shales
2500-3700	1200-2000	Partially weathered to fresh shales and sandstones; weathered and/or sheared metamorphic, igneous or limestone rocks
3700-4500	2000-2500	Slightly weathered and/or fractured metamorphic or igneous rocks or limestones; some very hard or indurated sandstones and shales
4500-6000	2500-3500	Unweathered metamorphic and igneous rocks; some limestones and dolomites

Since velocity contrasts within water-saturated overburden materials are usually relatively small, refraction methods are not particularly suited to providing information on overburden stratigraphy unless significant velocity increases exist within the sequence. For example, refraction methods could possibly be used to detect a thick, coarse-grained unit or diamict (typical velocity of >1700 m/s) beneath a fine-grained unit such as silt or clay (typical velocity of 1500-1600 m/s). However, any user of refraction methods must be aware of the "hidden layer" problem, where refracted energy from a layer sandwiched between lower and higher velocity units may never appear as first arrivals (Fig. 3.2).

Within unconsolidated sediments, very significant velocity contrasts are found at the boundary between dry and water-saturated materials (Table 3.1). This makes the water table a good target for refraction surveys (e.g. Haeni, 1986).

Refraction surveys yield fairly accurate estimates of velocities of subsurface units, which are related to lithology (Table 3.1) and the physical state of the sediment. For example, lateral changes in bedrock velocity may indicate a change in bedrock lithology or a change in physical

characteristics (e.g. weathering) of the bedrock unit. Thus, refraction can be an appropriate geophysical technique for delineating lateral changes in stratigraphy or structure with associated changes in seismic velocity (e.g. fracture/shear zones in bedrock surface, kimberlites?).

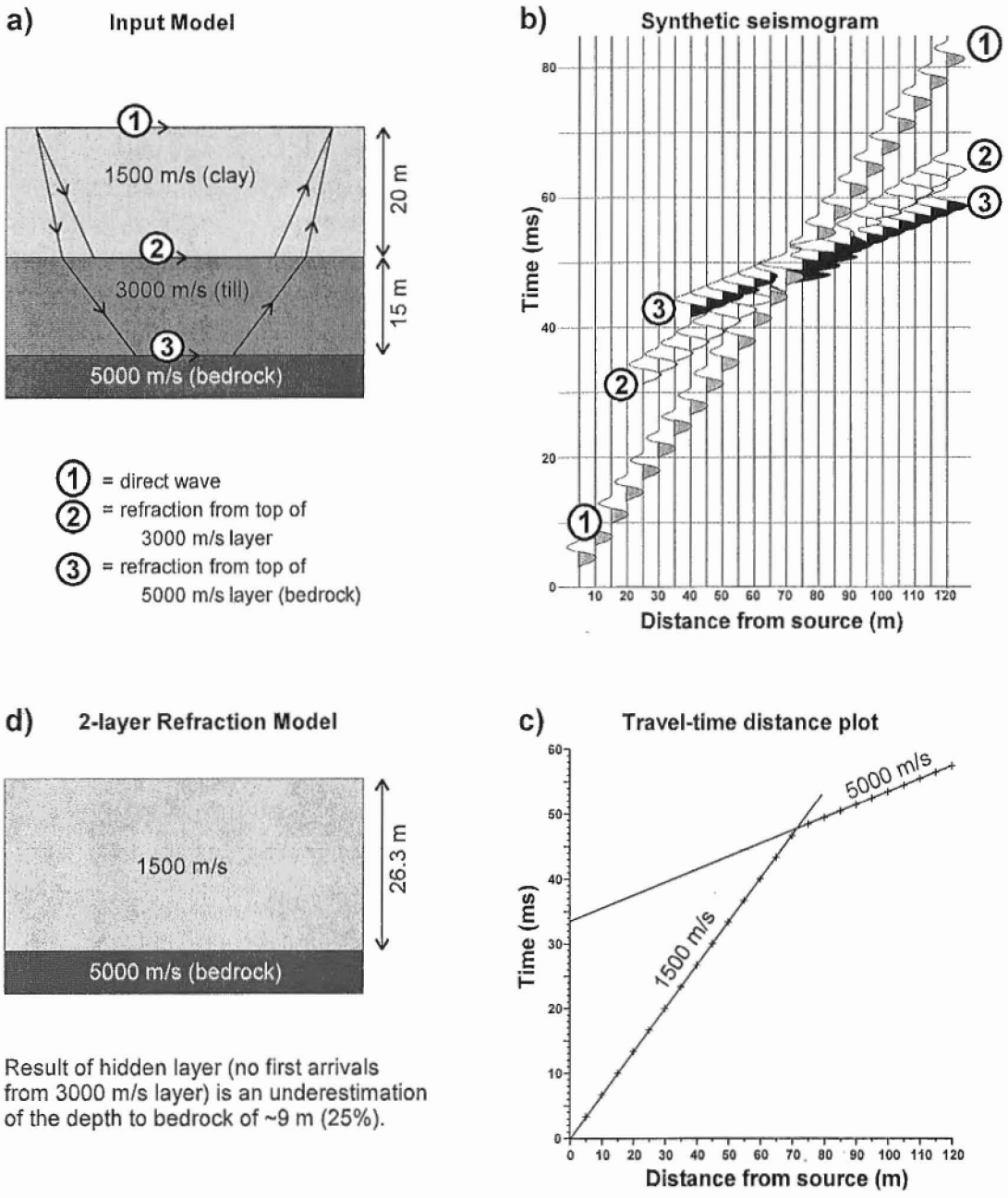

Figure 3.2. *Model and time-distance plot demonstrating the "hidden layer" problem. a) Input 3-layer model. b) Resulting synthetic seismogram showing direct and refracted arrivals. c) Corresponding travel-time plot. d) Interpreted 2-layer subsurface model. In this case, 15 m of high-velocity (3000 m/s) overburden could not be detected using first-arrival times, resulting in a 25% error in depth-to-bedrock estimates.*

Before embarking on a refraction survey, the problem should be modelled to ensure that the survey has a reasonable chance of providing the desired information. Velocities for each major stratigraphic unit can be estimated (Table 3.1). These velocities and estimated unit thicknesses can be input to simple modelling programs (e.g. Ayers, 1996) to help design the recording parameters (e.g. spread lengths and geophone spacings) for the refraction survey, and indicate potential problems such as a hidden layer. Contractors should be able and willing to provide such modelled results prior to setting up a survey.

Summary of refraction methods

Refraction surveys can often be used very effectively to provide estimates of the depth to bedrock, depth to water table, and in some cases, information on major stratigraphy within the overburden sequence. The velocity information derived from these surveys provides an indication of lithology and can be used to map lateral changes in bedrock or overburden conditions. The limitations of refraction techniques are a) the basic assumption that velocity increases with depth, b) the possibility of "hidden layers" which may lead to significant errors in depth estimates to underlying units, c) the large source energies and long spread lengths required to obtain refractions from horizons deeper than 20 or 30 m below surface, and d) the difficulty in resolving detailed structure on the target horizon.

Examples of refraction data

Interpretation of refraction data from Shubenacadie, Nova Scotia

Figure 3.3 shows the time distance plot and interpreted depth section for a refraction spread in the Shubenacadie basin in Nova Scotia. The survey was one of a series of test spreads shot to delineate the extent and depth of the Carboniferous basin, and to map the stratigraphy of the overlying Cretaceous and Quaternary sediments.

The data were acquired by laying out 24 geophones at 5-m spacings, and shooting 5 m off each end as well as in the centre of the spread. The 120-m spread length was sufficient to observe refracted arrivals from high-velocity bedrock (unit 4) at a depth of approximately 30 m. Above bedrock is a 15-20 m thick layer (unit 3) with a velocity of approximately 2200 m/s, which could be Cretaceous sediments or a Quaternary till sequence. Tills with velocities in this range are widespread in the area. The interface between units 2 and 3 is not well defined by the data, and therefore the topography shown on this interface in the depth section of Figure 3.3 may not be realistic. The upper two units (units 1 and 2) are interpreted to be Quaternary sediments, with unit 1 representing the weathered or unsaturated zone. A drillhole would be required to determine the lithologies of the units identified in the section.

Refraction surveys such as the simple one discussed in this example can be carried out quickly and are relatively inexpensive. They can provide estimates of the depth to bedrock and gross stratigraphy of the overburden materials to constrain models of subsurface structure or to allow the optimum siting of boreholes.

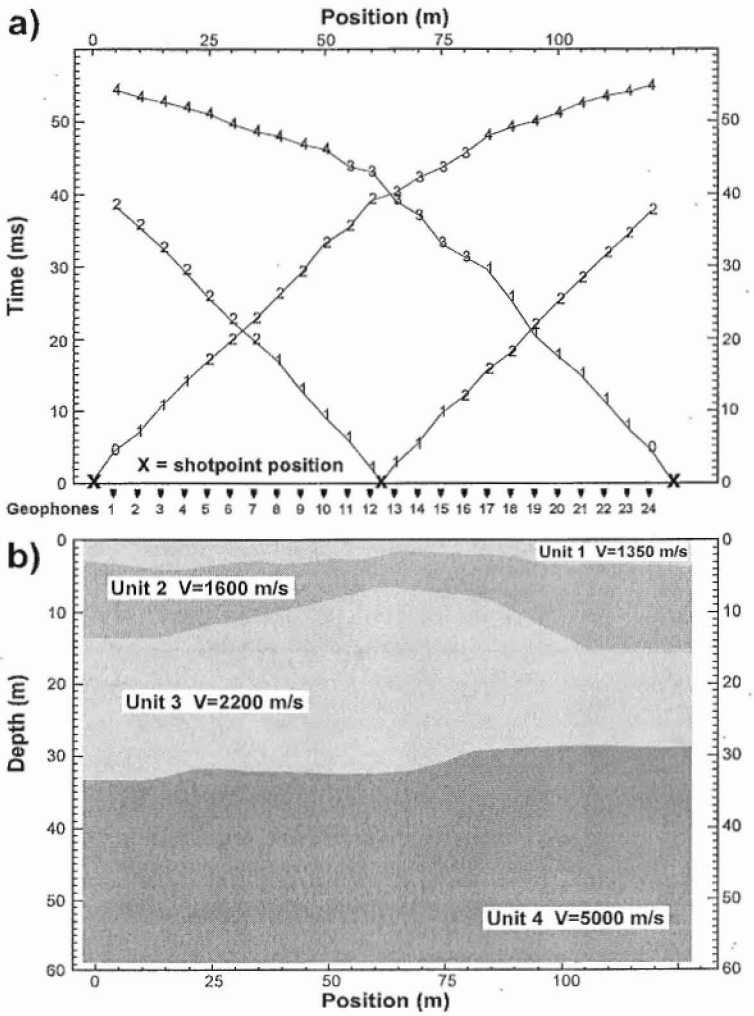

Figure 3.3. *a) Time distance plot showing the layer assignments for each of the first arrivals from a simple refraction survey from Shubenacadie, Nova Scotia. b) The depth section that was interpreted from the time-distance data using a refraction analysis program (SIPQC) from Rimrock Geophysics Inc.*

Interpretation of shear wave refraction data from Richmond, B.C.

Figure 3.4 shows a reversed time-distance plot of shear wave refraction first arrivals and the interpretation for a refraction spread in the Fraser River delta, British Columbia (Hunter et al., 1998b). The objective of the survey was to delineate the boundary between Holocene and Pleistocene materials. The data were obtained using low frequency horizontal geophones placed at 3-m intervals on surface and shear wave sources (a hammer striking the end of a truck-loaded beam) at each end of the spread. Shear-wave first-arrival times were identified and plotted versus source-geophone offset. From inspection of the plot, a high-velocity refractor was identified from both the forward and reversed source locations. Differing apparent velocities and intercept-times indicated that the high-velocity refractor was dipping. Using the arithmetically averaged refractor velocity, simple layered-case interpretation methods were employed (e.g. Dobrin, 1976) to estimate depths to the refractor at either end of the spread. The interpreted depth of 19.6 m to the refractor at the north end of the spread was later confirmed by drilling as the boundary between Holocene sand (high porosity) and Pleistocene sand (lower porosity). Although shear wave velocities are relatively unaffected by water content (unlike P wave velocities), they can be strongly affected by porosity of materials and degree of consolidation.

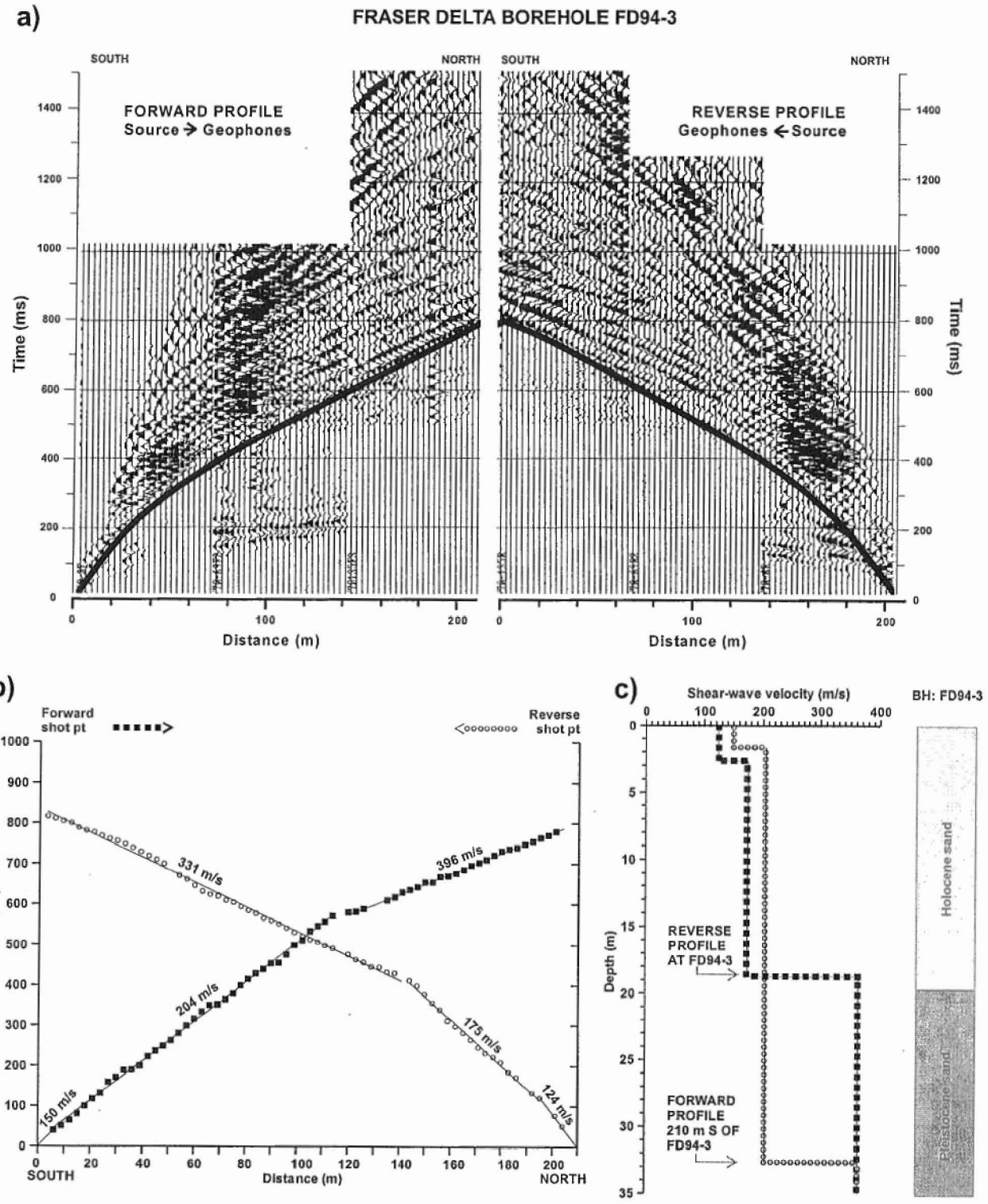

Figure 3.4. *Shear wave reversed refraction profile, Richmond, B.C. (from Hunter et al., 1998b) a) Composite seismic record. b) First arrival travel-time plots and apparent velocities. c) Velocity-depth plot.*

Seismic reflection methods

Seismic reflection methods involve measurement of the time taken for seismic energy to travel from the source at or near the surface, down into the ground to an acoustical discontinuity, and back up to a receiver or series of receivers on the ground surface (Fig. 3.5a). These methods require digitization of the seismic wave train and at least some degree of computer processing of the data. Data are usually acquired continuously along a survey line, and processed to produce a seismic section which is a two-way travel time cross-section of the subsurface (Fig. 3.5b). Velocity-depth functions calculated from the data, or seismic logging of a nearby borehole(s) are used to translate the two-way travel time into depth.

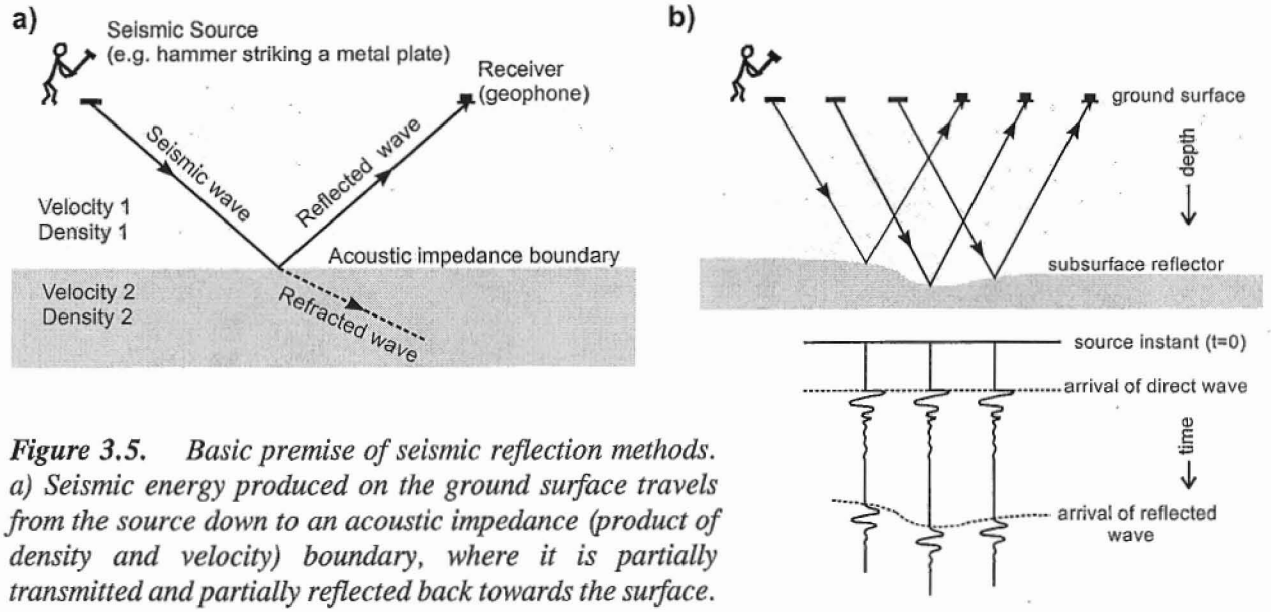

Figure 3.5. *Basic premise of seismic reflection methods. a) Seismic energy produced on the ground surface travels from the source down to an acoustic impedance (product of density and velocity) boundary, where it is partially transmitted and partially reflected back towards the surface. b) Data are usually acquired continuously along a survey line and the record of ground motion as a function of time is related to the subsurface structure.*

Details on the development and early application of shallow seismic reflection methods can be found in Hunter et al. (1989), Pullan and Hunter (1990) and Steeples and Miller (1990). These papers summarize the development of two different shallow seismic reflection methods - the "optimum offset" technique, which in its simplest form is a single channel, constant offset profiling technique requiring a minimum of data processing (Fig. 3.5b), and the common midpoint (CMP) method (often also referred to as the common-depth-point, or CDP, method) which is an adaptation of the methods used by the petroleum industry. In CMP surveys, multi- (12, 24, or more) channel data are recorded for each shotpoint. During processing these data are sorted according to their common midpoints or common depth points (Fig. 3.6), and all data with the same CMP are corrected for offset and stacked (summed) in order to enhance subsurface reflection signals. The stacking process yields a potential improvement in the signal to noise ratio proportional to the square root of the "fold" (number of traces summed to form one trace on the final section).

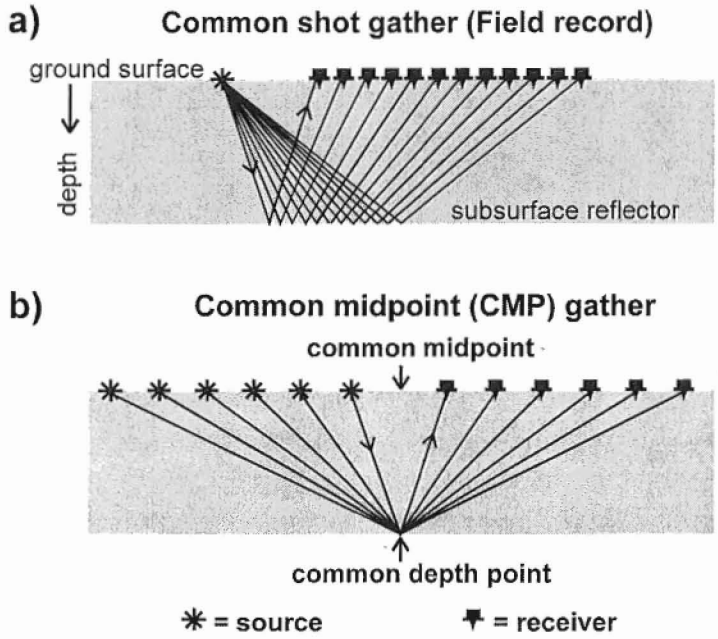

Figure 3.6. Schematic diagram showing a) the subsurface travel paths of reflections from a field record and b) a common midpoint gather. The traces in the CMP gather will be processed and stacked together to form a single trace on the final CMP section (6-fold).

The profound technological improvements in engineering seismographs, personal computers and data storage capabilities over the last 10-15 years have overcome many of the limiting factors that led to the development of the "optimum offset" technique (i.e. collection of single-fold data), and that technique is now essentially obsolete. CMP data are routinely collected in the field, now often using 48 or more channels. Engineering seismographs have a greatly increased dynamic range (>96 dB) and are now capable of recording data from vibratory sources. Researchers are starting to look at shallow three-dimensional surveys, using three-component recording, and examining more than one seismic mode at a time. Steeples (1998) provides an overview of the development of shallow seismic reflection techniques, and the suite of papers in that special issue (Geophysics, v. 63, p. 1210-1450) provides a summary of the state-of-the-art of shallow seismic reflection as it exists today.

Advantages and limitations of reflection methods

Reflection methods overcome many of the limitations associated with refraction methods. First, energy is reflected back to the surface from any interface across which there is a change in the acoustic impedance, whether it is associated with an increase or a decrease in seismic velocity. Thus, even though no energy is refracted from the top of a low-velocity layer, a reflection does exist. Another advantage of reflection methods is the large amplitude of a reflection in comparison to the refracted signal from the same interface; reflected waves may be as much as an order of magnitude greater in amplitude than the refracted wave. This means that smaller, non-destructive sources can be effectively used to obtain reflections from depths of several tens or hundreds of metres, while it might require the use of explosives or heavy, truck-mounted seismic sources to obtain refractions from the same horizons. Finally, reflection techniques have the potential of providing considerable detail on the overburden structure and bedrock topography depending on the frequencies of the reflection signals that are recorded. For example, small bedrock depressions or rugged bedrock topography would be difficult to resolve with refraction techniques, but may be well delineated by a reflection survey.

Shallow seismic reflection methods do, however, have their own limitations. First, the successful application of any shallow reflection survey depends on the detection of high-frequency energy reflected from velocity discontinuities within the subsurface. Unfortunately, earth materials, and especially unconsolidated overburden materials, are strong attenuators of high-frequency energy. Thus, seismic waves in the 10-90 Hz range commonly used in petroleum exploration may be reflected from depths of thousands of metres, but energy with frequencies above 100 Hz normally only have travel paths on the order of tens or hundreds of metres. The ability of a particular site to transmit high-frequency energy is a major factor in determining the quality and the ultimate resolution of a shallow reflection survey (Fig. 3.7).

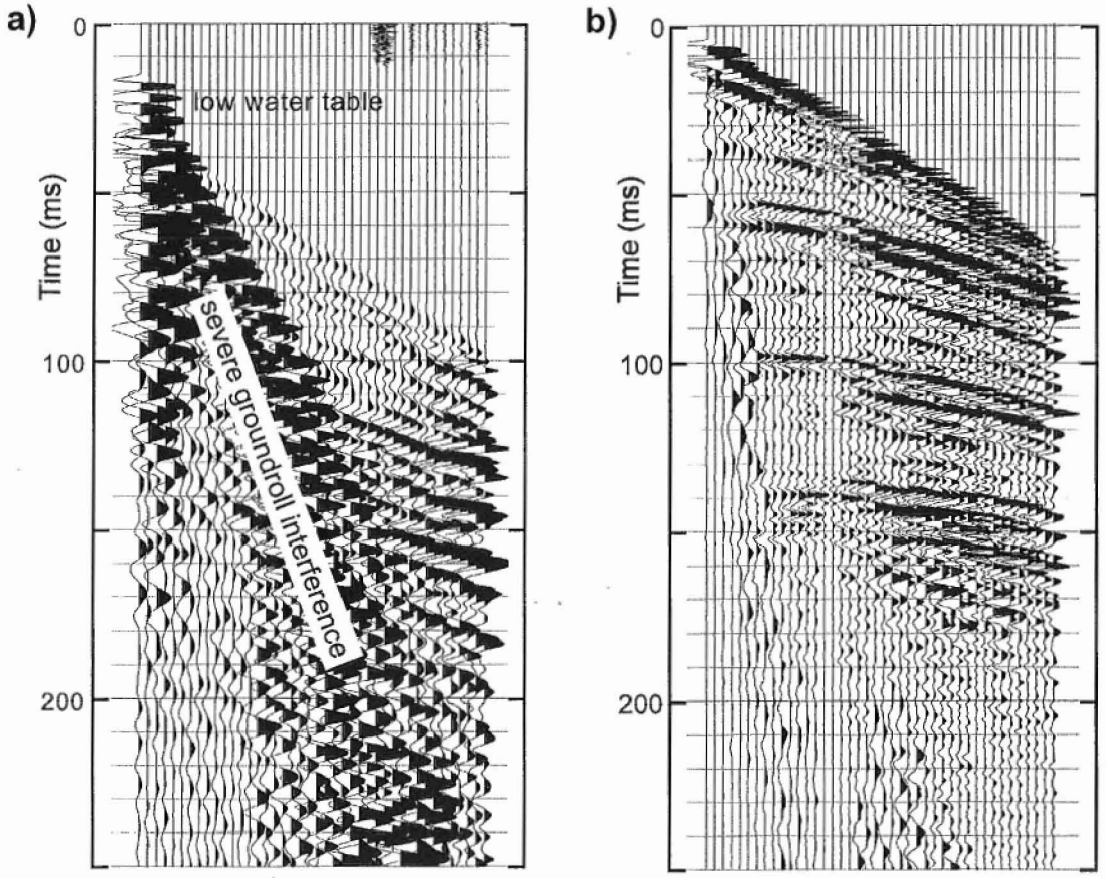

Figure 3.7. *Two field records with similar subsurface geology but differing surface conditions. a) Where the surface sediments are composed of a dry sand, the seismic record shows a relatively low-frequency reflection signal, a low signal-to-noise ratio, and considerable interference from groundroll. b) In contrast, where the surface sediments are damp and fine-grained, the seismic record shows excellent high-frequency reflection energy, and essentially no groundroll interference.*

Much of the attenuation of high-frequency energy occurs in the near surface materials where the seismic energy is produced (Fig. 3.8). The optimum conditions for shallow reflection surveys are usually when the surface materials are fine-grained and water-saturated; reflections with dominant frequencies of 300-500 Hz can be obtained in such field situations. These

frequencies correspond to seismic wavelengths in unconsolidated overburden materials on the order of 3-5 m (Fig. 3.9), with a potential subsurface structural resolution of approximately 1 m (Miller et al., 1995). However, when the surface materials are coarse-grained and dry, the dominant frequencies of reflection data can be less than 100 Hz. In such areas, seismic wavelengths may exceed 15 m, and the resolution of the data may not be sufficient to obtain the desired subsurface information (Figs. 3.7, 3.9).

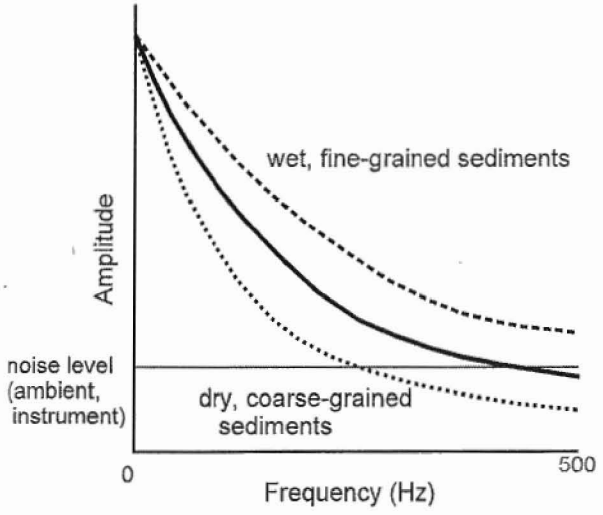

Figure 3.8. *Schematic diagram representing attenuation of high-frequency seismic signals in unconsolidated sediments. Attenuation can be extreme when the surface sediments are dry and coarse-grained.*

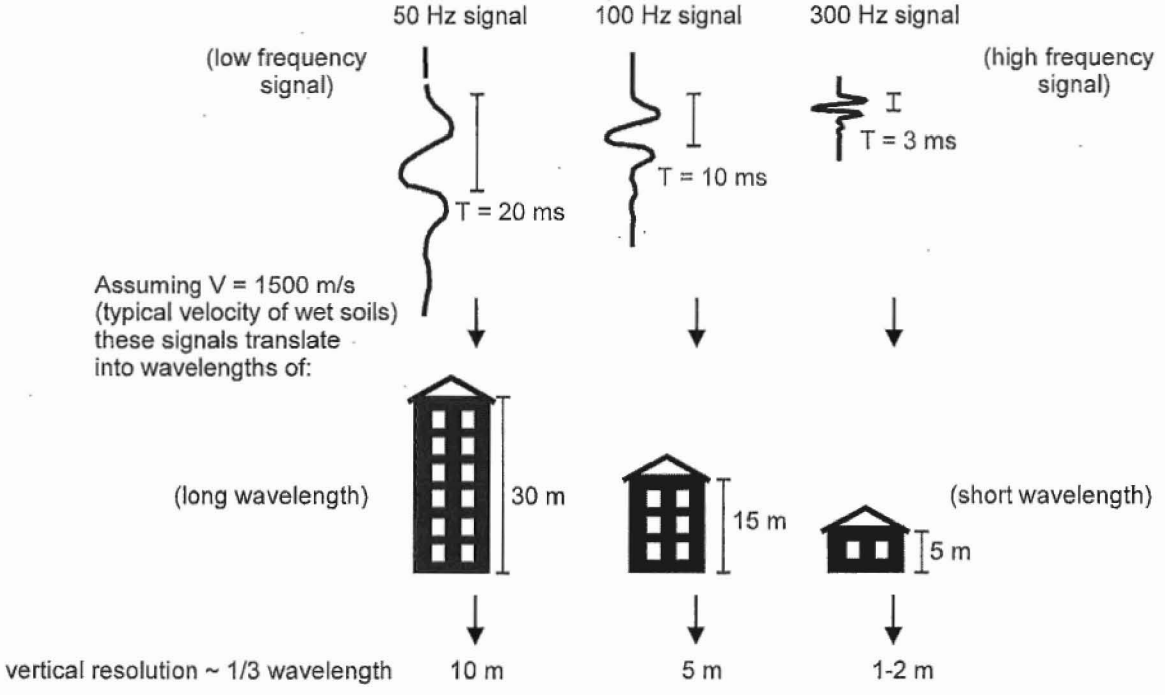

Figure 3.9. *The resolution (typically estimated to be 1/3 wavelength; Miller et al., 1995) of a shallow seismic reflection section depends on the wavelength of the recorded signal (wavelength = velocity/frequency). Most shallow targets require dominant reflection frequencies >100 Hz.*

The ability to produce and record high-frequency energy for shallow seismic reflection surveys has improved significantly over the years with the development and testing of various seismic sources (Miller et al., 1986, 1992; Pullan and MacAulay, 1987) and with the technological improvements in engineering seismographs. Today state-of-the-art engineering seismographs use instantaneous-floating-point analog-to-digital (A/D) convertors, reducing or even removing the necessity to use high-frequency geophones and pre-A/D low-cut filters in the field in order to enhance the high-frequency components of the seismic signal. This has substantially improved the potential of shallow seismic reflection surveys, but site characteristics are still crucial in determining the suitability and chance of success of the survey.

Reflections from very shallow interfaces arrive at times that are close to the arrival times for energy that has travelled directly along the surface of the ground or been refracted from shallow interfaces such as the water table. For this reason it is often not possible to separate very shallow reflection signals from other interfering events. The depth to the first separable reflection horizon depends on the frequency of the signals and the source-receiver offsets but in general, horizons within 10-15 m of the surface require short wavelengths (high dominant frequencies) and very tight source-receiver geometries to be successfully imaged (e.g. Bachrach and Nur, 1998; Ghose et al., 1998).

Shallow seismic reflection surveys are expensive (commercially $5000 or more per line-km depending on the size of survey, site location, type of data collection and processing, and density of shot/receiver locations). For this reason, such surveys are best suited to problems where detailed knowledge of the subsurface structure is required (e.g. to save drilling costs in drift prospecting exploration programs, identification of buried valleys in groundwater investigations, and site characterizations for environmental assessments). It is strongly recommended that modelling and a test survey be carried out prior to any major reflection survey, to establish whether shallow seismic reflection methods can provide the desired resolution of the target horizon at that site.

Summary of reflection methods

Shallow seismic reflection surveys are recommended for detailed mapping of overburden stratigraphy and bedrock topography below depths of 15-20 m below surface. Data quality and resolution are critically dependent on the surface conditions, with the best results usually associated with fine-grained, water-saturated surface materials, and the poorest results with coarse-grained, dry surface sediments. Large variations in surface topography along a survey line can be corrected for during the processing sequence; however, surface conditions and the depth to water table are likely to vary along with the topography and these changes may affect the frequency characteristics and the resolution of the data. High-resolution seismic reflection surveys should not be attempted in areas where the surface sediments are gas-charged (e.g. on fill, peat, or swamps), as the attenuation of high-frequency energy in such areas is extreme.

Carrying out a shallow seismic reflection survey

Before starting a seismic reflection survey the goals and targets of the survey should be clearly

defined and modelled (e.g. Ayers, 1996). The operator should also be aware of the possible "pitfalls" of collecting shallow seismic reflection data, which can include an inappropriate choice of seismic source, or of source-receiver geometries, and spatial aliasing of groundroll (Steeples and Miller, 1998). Once in the field, test data should be acquired at a number of sites located throughout the survey area, and covering the full range of geological conditions expected to be encountered. For these tests it is recommended that at least two different sources be tried (Miller et al., 1986, 1992; Pullan and MacAulay, 1987), with small geophone spacings (1/2 that expected to be used in the final production survey) and offsets that reach at least 1.5 times the maximum depth of the primary target horizon (Steeples and Miller, 1998). The objective of these tests is to evaluate the quality of reflected energy (frequency and signal strength), to determine the depths from which reflection signals were recorded, and to establish the recording parameters (source/receiver geometry, recording timescale, input filter settings) and line priorities for the production phase. In some cases, these tests may indicate that it is not possible to acquire the high-frequency reflection signals required to meet the goals of the survey, and the survey should be terminated.

In the production phase of a CMP survey, multi-channel (12, 24, or more) data are recorded for each shotpoint, usually with a consistent source-receiver geometry that is moved continuously along a survey line. The source-receiver layout may be an off-end (source located off one end of the geophone spread) or split-spread (source located within the geophone spread) geometry, depending on the number of recording channels available, target depths, and the geophone and shot spacings used. Recording such data are usually accomplished by laying out a large number of geophones and using a "rollalong" switching box (either internal or external to the recording seismograph) that allows a chosen suite of geophone outputs to be input to the recording seismograph (Fig. 3.10). It is critical that detailed and accurate records of the source and receiver locations for each shot are maintained throughout the survey, as it is this information that allows the field records to be resorted into CMP gathers and processed to produce the final seismic section. An elevation survey should also be conducted after the seismic data are collected so that topographic corrections may be applied.

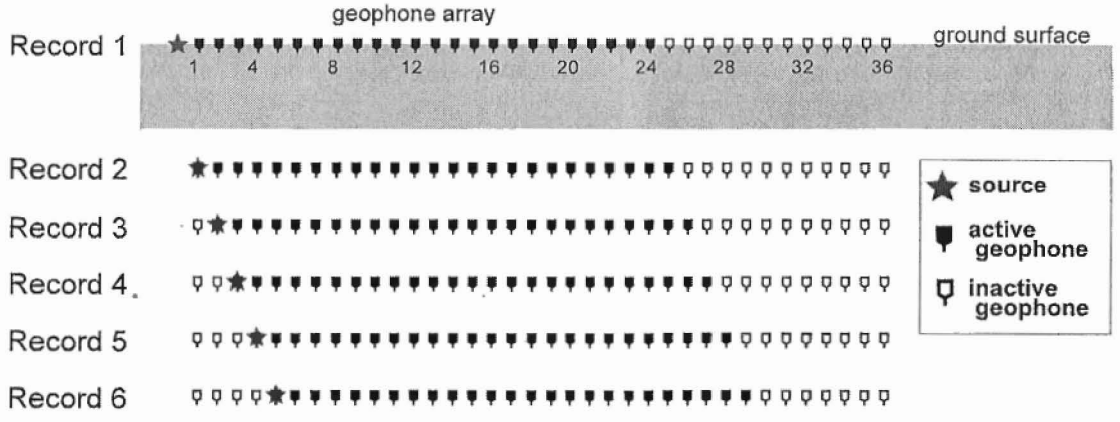

Figure 3.10. *Schematic layout of 36 geophones on the ground surface, and the source and receiver (active geophone) geometry for 6 consecutive 24-channel records (off-end shooting geometry). Activating each set of 24 geophones would be accomplished through the use of a "rollalong" switch.*

Data processing

A standard sequence of CMP processing steps includes trace editing, static corrections, bandpass filtering, gain scaling, velocity analyses, normal moveout corrections and stacking of the corrected traces (Fig. 3.11). During processing, the data are sorted according to their common midpoints or common depth points (Fig. 3.6). Each trace is corrected for offset according to a velocity-depth function determined from the data (normal moveout, or NMO, corrections). Finally, the NMO-corrected traces in each CMP gather are stacked. This stacking procedure is the essence of the CMP technique, and allows a potential improvement in the signal-to-noise ratio of the data according to the square root of the fold.

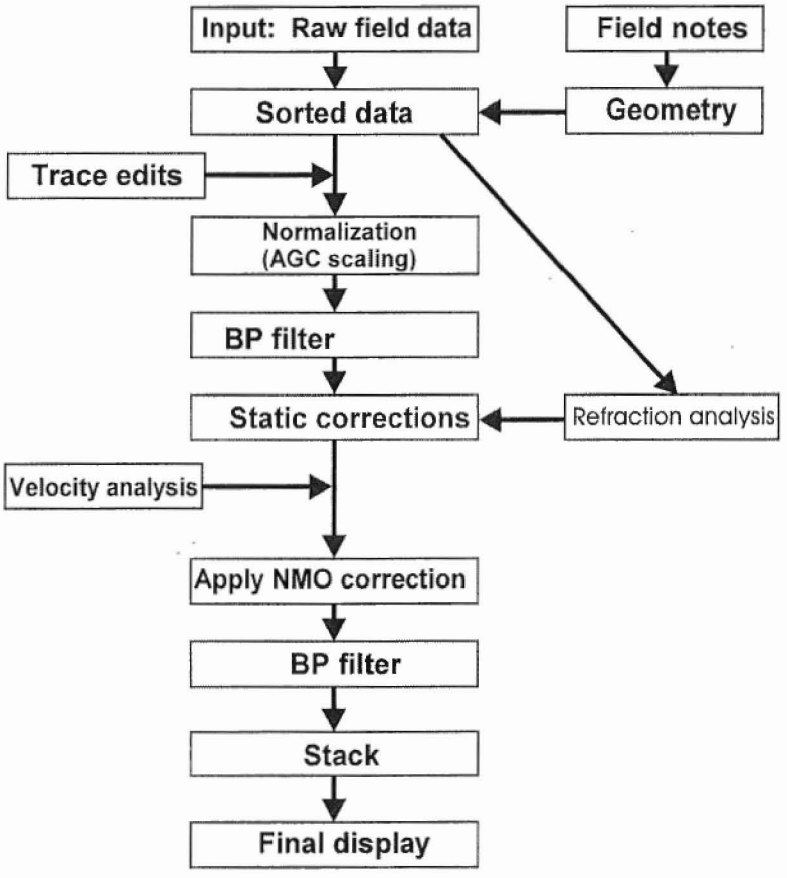

Figure 3.11. A standard sequence of processing steps for CMP data.

Many seismic reflection processing packages are now commercially available, some of these with advanced data processing techniques developed in the petroleum industry such as surface-consistent deconvolution, scaling and residual static analysis, and structural modelling to enhance velocity and static analysis (see Yilmaz, 1987; Schieck and Pullan, 1995; Pasasa et al., 1998).

CMP processing involves considerable data manipulation and the interpreter must be careful that this does not degrade the reflection signal or produce artifacts (Steeples and Miller, 1998). It is still recommended that common offset panels, raw field records and/or CMP gathers be pulled from the data set and examined during processing. This procedure allows the interpreter to assess the reflection quality along the seismic line, and ensure that the CMP processing does not result in any degradation of the reflection signal (Pullan et al., 1991; Miller et al., 1998).

Two-way time to depth scale

Seismic profiles are sections in two-way travel time (not depth). Velocity functions are estimated from the seismic data at intervals along the line during the processing sequence, in order to calculate the normal moveout corrections applied to the data before the stacking procedure, and these velocities can also be used to convert the two-way travel time section to a depth section. However, velocities determined from reflection data can be subject to large uncertainties, especially as the moveout of reflection events decreases down the record. Whenever possible, accurate downhole velocity data from borehole logging should be obtained in support of the seismic reflection survey (Hunter et al., 1998a).

Examples of reflection data

Mapping shallow foreset sequence, Fraser River delta, B.C.

The Fraser River delta lies just south of the city of Vancouver in an area of rapid urbanization and development. The delta is an extremely complex sedimentary system, and shallow seismic reflection surveys provide one means of delineating its three-dimensional structure (Jol, 1988; Jol and Roberts, 1988, 1992; Pullan et al., 1989, 1998; Roberts et al., 1992).

An example "optimum offset" (i.e. single-fold) shallow seismic reflection section is shown in Figure 3.12. The fine-grained, water-saturated surface conditions of the Fraser River delta provide an excellent environment for shallow seismic reflection profiling; in general, reflection signals in excess of 300 Hz could be obtained and groundroll was almost completely suppressed with a low-cut filter. These data were recorded with an in-hole shotgun source and 100 Hz geophones, both planted in the bottom of water-filled drainage ditches alongside a road. The source-receiver offset was 12 m, and shot and receiver spacings were 1.5 m. The depth scale on Figure 3.12 has been calculated from a velocity analysis of multi-channel records. This section shows the high quality of reflection data that can be obtained even with a very simple reflection technique in areas where the conditions are optimum. The vertical resolution of these data is on the order of 1-2 m.

The topsets (Unit 1) are clearly depicted in this section. The unit is approximately 20 m thick and is separated from the underlying foreset sequence by a sharp, nearly planar surface. Just to the right of the centre of this figure is a shallow channel-like feature cut into the foreset deposits. The channel is approximately 100 m wide and 5 m deep, and may represent an old distributary channel of the Fraser River. The higher-amplitude, south-dipping reflections (Unit

2) below the topset beds are interpreted to be a progradational sequence of foreset beds deposited on the foreslope of the ancestral Fraser delta (Jol and Roberts, 1988; Clague et al., 1991). The foreset sequence is shown to be at least 50 thick along the profile shown in Figure 3.12.

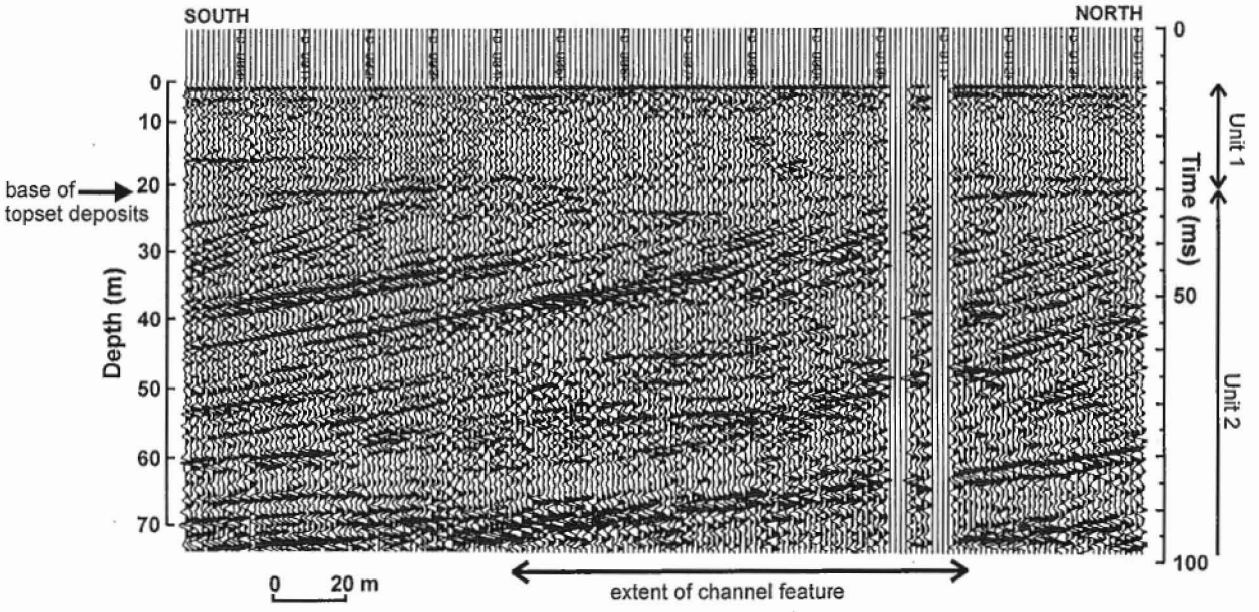

Figure 3.12. *Optimum offset shallow seismic reflection section from the Fraser River delta, B.C., recorded with an offset of 12 m and a geophone spacing of 1.5 m. These parameters allow for high resolution in the uppermost few tens of metres of the sediment sequence. This section shows the interface between the uppermost flat-lying topset sediments (unit 1) and the underlying foreset sequence (unit 2) at a depth of 20-25 m.*

Buried channel, Oak Ridges Moraine, Ontario

Several shallow seismic reflection CDP surveys have been carried out in conjunction with a major program to study the hydrogeologic setting of the Oak Ridges area north of Toronto (Sharpe et al., 1996). The Oak Ridges Moraine (a topographically high surface feature) is a major groundwater recharge area which stretches more than 160 km across south-central Ontario. The three-dimensional structure and the hydraulic connectivity of geologic units beneath the Moraine were largely unknown. The results from seismic reflection surveys (approximately 50 line-km), in conjunction with data obtained from strategically placed boreholes, are contributing to a better understanding of the subsurface structure and its effect on regional groundwater flow (Pullan et al., 1994; Pugin et al., 1996, 1999).

Figure 3.13 shows an example of 12-fold CMP high-resolution surveying from north of the Oak Ridges Moraine (Pugin et al., 1996). The geophone and shot spacings were 5 m, and the active geophone array consisted of 24 geophones which were "rolled" through 48 traces, giving subsurface horizontal coverage of 2.5 m. A 12-gauge in-hole shotgun was used as the seismic

source. The data were recorded on an EG&G Geometrics 2401 engineering seismograph and processed on an IBM compatible personal computer.

The seismic reflection profile (Fig. 3.13) crosses a topographic valley, one of a network of large northeast-trending valleys in the area. These valleys are eroded into the regional Newmarket Till sheet and in this case, through older stratified glacial sediments below the till to close to the bedrock surface. The erosion is thought to be the result of catastrophic sub-glacial events (Pugin et al., 1996; Sharpe et al., 1996). Coarse-grained channel fills in the valley bottoms are potential aquifers confined by overlying fine-grained glaciolacustrine sediments.

Information such as that provided by this seismic section has been used to site drill holes in an efficient manner in order to obtain representative geological sampling of the overburden as well as to investigate the potential for aquifers.

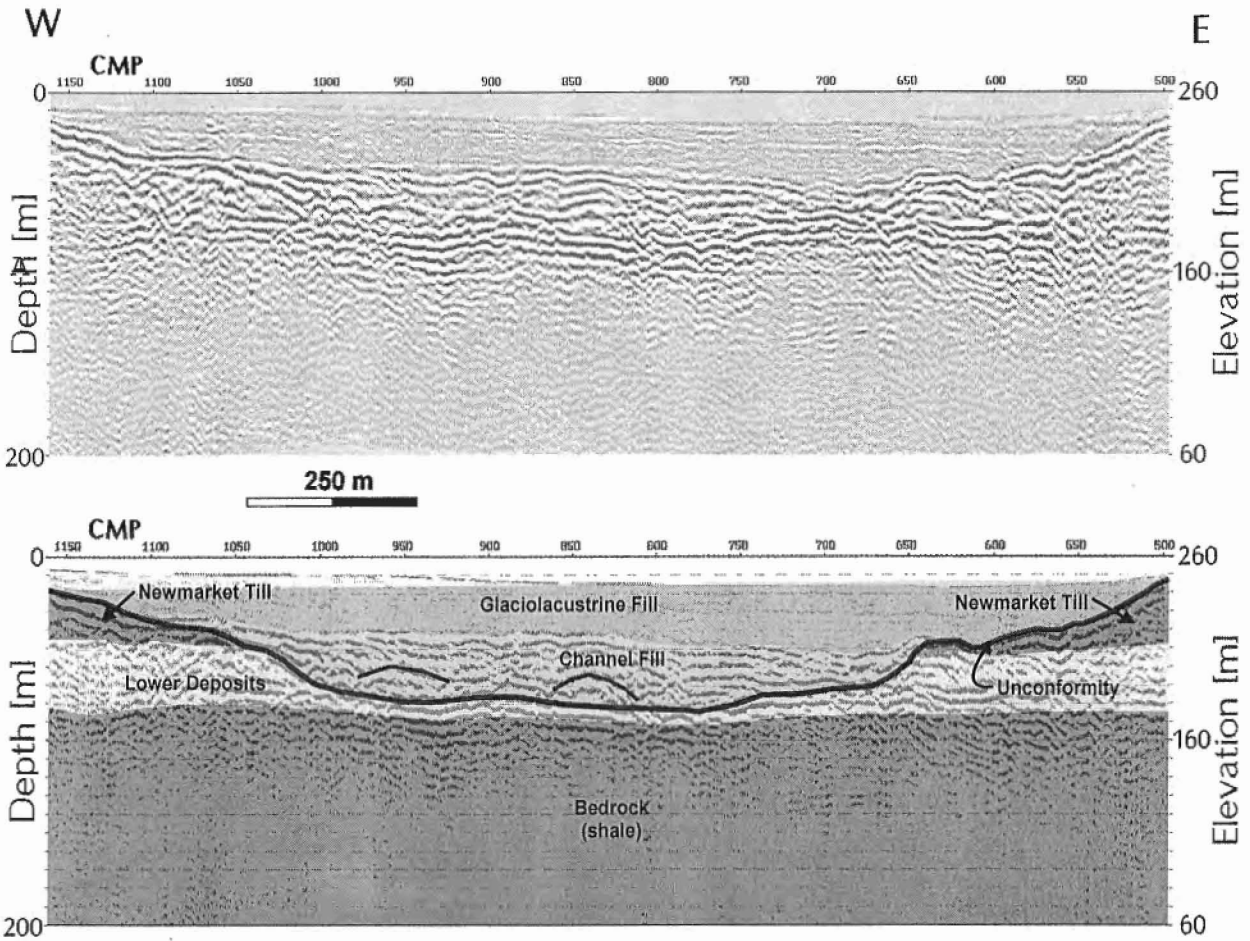

Figure 3.13. *12-fold CMP seismic section from north of the Oak Ridges Moraine, southern Ontario, showing a deeply incised buried channel. The channel is ~1.5 km wide and 80 m deep. It is interpreted to have cut through the high-velocity Newmarket Till exposed on either side of the surface expression of the channel and been infilled with 30-40 m of coarse-grained sediments overlain by ~30 m of finer-grained glaciolacustrine deposits.*

Mapping overburden stratigraphy and structure, Waterloo Moraine, Ontario

The Waterloo Moraine in southern Ontario is an important groundwater resource in the Waterloo area and has been the subject of extensive studies. However, these studies have been based on drilling programs, with relatively little use of surface geophysics. In 1993, a short reflection profile was obtained in the area as a test of the applicability of shallow seismic reflection method to groundwater resource and modelling studies.

The profile shown in Figure 3.14 was acquired using a 12-gauge in-hole shotgun source, and a 120 m spread consisting of 24 geophones (50 Hz) at 5 m spacings. Twelve-fold CMP coverage was obtained by shooting into each spread from offsets of 5 and 2.5 m from the nearest receiver, resulting in a trace spacing on the final stacked section of 1.25 m. The data were recorded on an EG&G Geometrics 2401 engineering seismograph. The survey was preceded by a short trial phase in which test records were shot at a number of locations in the survey area to establish recording parameters, and to determine the expected data quality and its variation according to terrain type and elevation. The entire survey was recorded in two days by a three-person crew.

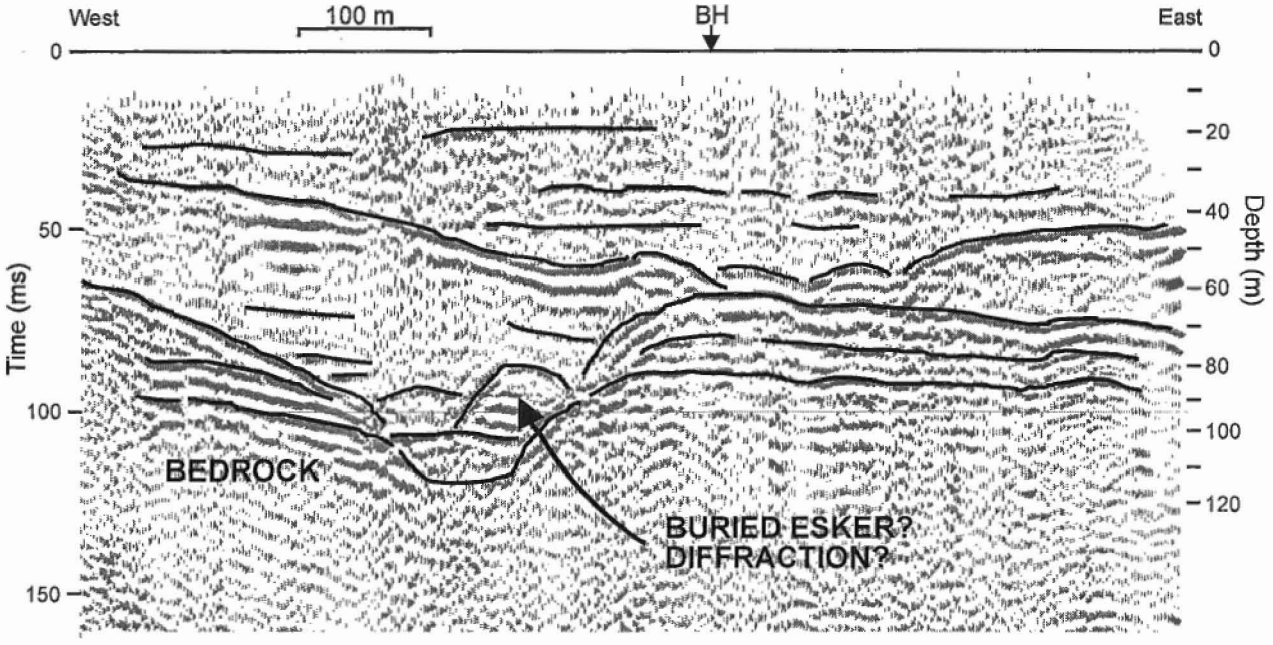

Figure 3.14. *A 12-fold CMP seismic reflection profile from the Waterloo Moraine area, southern Ontario. The subsurface architecture is enhanced by the overdrawn lines. This profile is less than 1 km in length. The variation in overburden stratigraphy along this section could not be predicted from borehole information unless the boreholes were very closely spaced.*

Excellent high-frequency data were obtained at this site (Fig. 3.14), with the dominant frequency of the reflection signal of between 250 and 300 Hz (implying a subsurface vertical resolution on the order of 2 m). Reflections are evident from depths of approximately 20 m below ground surface to the bedrock interface, which varies along the profile from 70-100 m depth. The seismic

section clearly shows a bedrock valley, 30 m deep and approximately 400 m across. Overlying the bedrock is a complex sequence of sediments, with the most striking feature being a broad depression that is not coincident with the bedrock valley.

This profile demonstrates the potential of shallow seismic reflection surveys for providing detailed subsurface structural information. Such information can be valuable input to hydrogeological studies where the continuity of stratigraphic units between boreholes is of critical importance. Rapidly changing subsurface structures, such as imaged in this profile can be effectively delineated by shallow seismic reflection methods, but are extremely difficult to infer from a limited number of boreholes.

Delineating a buried Cretaceous basin, central Nova Scotia

In 1993, the Geological Survey of Canada and the Nova Scotia Department of Natural Resources initiated a project to examine the Cretaceous to Quaternary stratigraphy in the Shubenacadie and Musquodoboit valleys in cental Nova Scotia. Isolated occurrences of economically valuable silica sand and kaolin clays were known to occur in these basins. The object of the project was to use drilling and geophysical techniques (shallow seismic reflection surveying and borehole logging) to better delineate the extent of these deposits and allow an assessment of their economic potential (Pullan et al., 1997).

The production phase of the seismic program involved the recording of continuous 12-fold common-midpoint-point (CMP) profiles. On the basis of earlier test spread results, these lines were located where substantial thicknesses of Cretaceous infilling of buried basins were suspected. In these surveys, 5 m shot and geophone spacings, and a 5 m source-to-nearest receiver offset were used. All data were recorded on an OYO DAS-1 engineering seismograph with instantaneous-floating-point amplifiers and 24-bit analog-digital conversion. Acquisition rates averaged 0.5 km (200 records) per day with a four-person field crew.

Figure 3.15 shows a 2 km north-south seismic profile across the western limit of the Musquodoboit Valley. It is striking example of a buried basin structure, infilled with Cretaceous sediments reaching an estimated thickness of 140 m. The data are of excellent quality, except for a poor record area in the centre of the valley where boggy surface conditions caused a severe deterioration in ground coupling. The Quaternary sequence appears to consist essentially of a till that thins from a maximum thickness of 40 m in the south to <20 m in the north. This rests unconformably on the Cretaceous sediments except at the south edge of the bedrock valley where a large channel has been eroded into the Cretaceous deposits. The draped structure of the Cretaceous sediments is clearly shown by a series of strong, concave reflections that conform to the curvature of the bedrock surface. Correlation of these reflections with borehole logs suggests that these large-amplitude reflections are related to packages of thin fine-grained layers including lignite, marcasite, and distinctive calcareous sandstone beds (Hunter et al., 1998a).

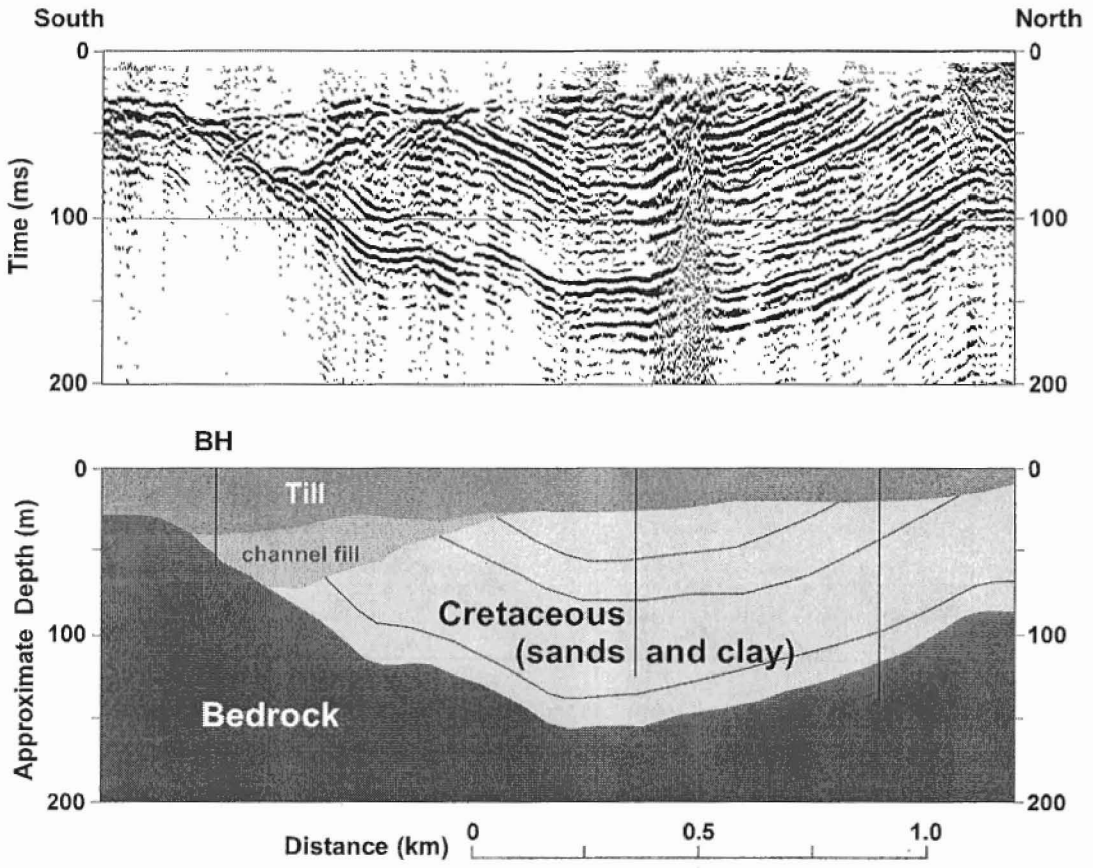

Figure 3.15. *Seismic profile across west end of Musquodoboit Valley, central Nova Scotia, showing a cross-section of a bedrock valley infilled with >100 m of Cretaceous sands and clays (from Pullan et al., 1997).*

Summary

Shallow seismic methods are geophysical tools that are capable of mapping bedrock topography and overburden stratigraphy, and which have applications to geomorphic research. The choice between refraction and reflection methods depends on the geological or structural target of the survey, the depth of interest, and the degree of subsurface resolution required. This paper has attempted to provide a simple description of these methods, and Table 3.2 summarizes their advantages, limitations and major applications. It must be emphasized that the quality of seismic data (especially of shallow reflection data) is site-dependent, and it is always prudent to conduct a small test survey before embarking on a major seismic program.

Shallow seismic reflection methods have been emphasized in this paper because their application to Quaternary research is relatively new, and therefore perhaps less known, and because they have the potential to provide a particularly powerful component to geomorphic

Table 3.2. Summary of major applications of shallow seismic refraction and reflection techniques (adapted from Blackhawk Geometrics, Technical Note).

	Advantages	Limitations	Major Applications
Refraction	Allows determination of both depth to, and velocity of, subsurface interfaces characterized by significant velocity increases (e.g. bedrock, water table (P-waves))	May require large impact sources or explosives to map features at depths >30 m	Determining depth to bedrock
			Determining depth to water table
		Cannot detect (no first arrival) low velocity layer beneath higher velocity layer	Using velocity information to grossly estimate lithologies, or rock properties (weathering, fractures)
	Quality of data not strongly site dependant	Possibility of "hidden" layer(s) which can result in errors in depth calculations	
	Acquisition and processing costs significantly less than reflection methods	Spatial resolution ~5-10 times less than reflection data	
	Advantages	**Limitations**	**Major Applications**
Reflection	Does not require increasing velocity with depth; reflection from interfaces characterized by either velocity increase or decrease	Acquisition of high quality data dependent on site conditions. Best results usually where surface sediments are fine-grained and water-saturated	Mapping detailed subsurface structure (bedrock topography and overburden stratigraphy) - potential resolution ~1 m
			Preferred technique for targets depths >30 m when site conditions are favourable
	Large amplitude of reflection signal (in comparison to refracted energy from same horizon) means that smaller, non-destructive sources can be used	Limited resolution of very near surface (depending on source-receiver geometries)	
		Velocity-depth information derived from data subject to large uncertainties, especially as depth increases (i.e. as moveout on reflection records decreases)	
	Can map reflecting boundaries with spatial resolution 5-10 times better than refraction data		
		Acquisition and processing costs greater than refraction methods	

studies with continuous two-dimensional "pictures" of the shallow subsurface. The few examples provided in this paper show that shallow seismic reflection sections can provide information of the depth and nature of the bedrock surface, and on the thickness, two-dimensional structure, and lateral continuity of different units within the overburden. It is important to keep in mind that accurate interpretation of a seismic section requires at least some degree of ground truth from surface observations or borehole information, and that the quality of seismic reflection data depends very strongly on near-surface conditions. However, where seismic reflection methods do work, they can make a substantial contribution to Quaternary or geomorphic studies by delineating subsurface structure.

REFERENCES

Ayers, J.

1996: Synthetic seismogram generation for designing shallow seismic surveys; Journal of Environmental and Engineering Geophysics, v.1, p. 109-118.

Bachrach, R. and Nur, A.

1998: High-resolution shallow-seismic experiments in sand, Part 1: Water table, fluid flow and saturation; Geophysics, v. 63, p. 1225-1233.

Blackhawk Geometrics (Golden, CO)

Seismic refraction and reflection in engineering and environmental investigations; Technical Note.

Clague, J.J., Luternauer, J.L., Pullan, S.E., and Hunter, J.A.

1991: Postglacial deltaic sediments, southern Fraser River delta, British Columbia; Canadian Journal of Earth Sciences, v. 28, p. 1386-1393.

Dobrin, M.B.

1976: Introduction to Geophysical Prospecting; McGraw-Hill Book Co., New York, N.Y.

Ghose, R., Nijhof, V., Brouwer, J., Matsubara, Y., Kida, Y., and Takahashi, T.

1998: Shallow to very shallow, high-resolution reflection seismic using a portable vibrator system; Geophysics, v. 63, p. 1295-1309.

Haeni, F.P.

1986: Application of seismic refraction methods groundwater modelling studies in New England; Geophysics, v. 51, p. 236-249.

Hunter, J.A., Pullan, S.E., Burns, R.A., Gagné, R.M., and Good, R.L.

1989: Applications of a shallow seismic reflection method to groundwater and engineering studies; in Proceedings of Exploration '87: Third Decennial International Conference on Geophysical and Geochemical Exploration for Minerals and Groundwater, (ed.) G.D. Garland; Ontario Geological Survey, Special Volume 3, p.704-715.

Hunter, J.A., Pullan, S.E., Burns, R.A., Good, R.L., Harris, J.B., Pugin, A., Skvortsov, A., and Goriainov, N.N.

1998a: Downhole seismic logging for high-resolution reflection surveying in unconsolidated overburden; Geophysics, v. 63, p. 1371-1384.

Hunter, J.A., Douma, M., Burns, R.A., Good, R.L., Pullan, S.E., Harris, J.B., Luternauer, J.L., and Best, M.E.

1998b: Testing and application of near-surface geophysical techniques for earthquake hazard studies, Fraser River delta, British Columbia; in Geology and Natural Hazards of the Fraser River Delta, British Columbia, (eds.) J.J. Clague, J.L. Luternauer, and D.C. Mosher; Geological Survey of Canada, Bulletin 525, p. 123-145.

Jol, H.M.

1988: Seismic stratigraphic analysis of the southeastern Fraser River delta, British Columbia; M.Sc. thesis, Simon Fraser University, Burnaby, B.C.

Jol, H.M. and Roberts, M.C.

1988: The seismic facies of a delta onlapping an offshore island: Fraser River delta, British Columbia; in Sequences, Stratigraphy, Sedimentology: Surface and Subsurface, (eds.) D.P. James and D.A. Leckie; Canadian Society of Petroleum Geologists, Memoir 15, p. 137-142.

1992: The seismic facies of a tidally influenced Holocene delta: Boundary Bay Fraser River delta, B.C.; Sedimentary Geology, v. 77, p. 173-183.

Lankston, R.W.

1990: High-resolution refraction seismic data acquisition and interpretation; in Geotechnical and Environmental Geophysics, v.I, Tutorial, (ed.) S.H. Ward; Society of Exploration Geophysicists, Tulsa, Oklahoma, p. 45-73.

Lanz, E., Maurer, H., and Green, A.G.
1998: Refraction tomography over a buried waste disposal site; Geophysics, v. 63, p. 1414-1433.

Miller, R.D., Pullan, S.E., Waldner, J.S., and Haeni, F.P.
1986: Field comparison of shallow seismic sources; Geophysics, v. 51, p. 2067-2092.

Miller, R.D., Pullan, S.E., Steeples, D.W., and Hunter, J.A.
1992: Field comparison of shallow seismic sources near Chino, California; Geophysics, v. 57, p. 693-709.

Miller, R.D., Anderson, N.L., Feldman, H.R., and Franseen, E.K.
1995: Vertical resolution of a seismic survey in stratigraphic sequences less that 100 m deep in southeastern Kansas; Geophysics, v. 60, p. 423-430.

Miller, R.D., Xia, J., and Steeples, D.W.
1998: Shallow seismic reflection does not always work; Expanded Abstracts with Biographies, 1998 Technical Program; 68th Annual International Meeting of the Society of Exploration Geophysicists, New Orleans, Louisiana, p. 852-855.

Palmer, D.
1981: An introduction to the generalized reciprocal method of seismic refraction interpretation; Geophysics, v. 46, p. 1508-1518.
1986: Refraction seismics: The lateral resolution of structure and seismic velocity; Handbook of Geophysical Exploration, Section I. Seismic Exploration, (eds.) K. Helbig and S. Treitel; Volume 13, Geophysical Press, London, U.K.

Pasasa, L., Wenzel, F., and Zhao, P.
1998: Prestack Kirchhoff depth migration of shallow seismic data; Geophysics, v. 63, p. 1241-1247.

Pugin, A., Pullan, S.E., and Sharpe, D.R.
1996: Observations of tunnel channels in glacial sediments with shallow land-based seismic reflections; Annals of Glaciology, v. 22, p.176-180.
1999: Seismic facies and regional architecture of the Oak Ridges Moraine area, southern Ontario; Canadian Journal of Earth Sciences, in press.

Pullan, S.E. and Hunter, J.A.
1990: Delineation of buried bedrock valleys using the optimum offset shallow seismic reflection technique; in Geotechnical and Environmental Geophysics, v.III, Geotechnical, (ed.) S.H. Ward; Society of Exploration Geophysicists, Tulsa, Oklahoma, p. 75-87.

Pullan, S.E. and MacAulay, H.A.
1987: An in-hole shotgun source for engineering seismic surveys; Geophysics, v. 52, p.985-996.

Pullan, S.E., Jol, H.M., Gagné, R.M., and Hunter, J.A.
1989: Compilation of high resolution "optimum offset" shallow seismic reflection profiles from the southern Fraser River delta, British Columbia; Geological Survey of Canada, Open File 1992.

Pullan, S.E., Miller, R.D., Hunter, J.A., and Steeples, D.W.
1991: Shallow seismic reflection surveys - CDP or "optimum offset"?; Expanded Abstracts, 61st International Meeting of the Society of Exploration Geophysicists, Houston, Texas, v.1, p. 576-579.

Pullan, S.E., Pugin, A., Dyke, L.D., Hunter, J.A., Pilon, J.A., Todd, B.J., Allen, V.S., and Barnett P.J.
1994: Shallow geophysics in a hydrogeological investigation of the Oak Ridges Moraine, Ontario; Proceedings of the Symposium on the Application of Geophysics to Engineering and Environmental Problems (SAGEEP'94), Boston, Massachusetts, v. 1, p.134-161.

Pullan, S.E., Stea, R.R., Finck, P.W., Burns, R.A., Douma, M., and Good, R.L.
1997: Seismic exploration for Cretaceous kaolin deposits in glaciated terrains: Example from Nova Scotia, Canada; Proceedings of the Symposium on the Application of Geophysics to Engineering and Environmental Problems (SAGEEP'97), Reno, Nevada, p. 133-142.

Pullan, S.E., Hunter, J.A., Jol, H.M., Roberts, M.C., Burns, R.A., and Harris, J.B.
1998: Seismostratigraphic investigations of the southern Fraser River delta; in Geology and Natural Hazards of the Fraser River Delta, British Columbia, (eds.) J.J. Clague, J.L. Luternauer, and D.C. Mosher; Geological Survey of Canada, Bulletin 525, p. 91-122.

Roberts, M.C., Pullan, S.E., and Hunter, J.A.
1992: Applications of land-based high resolution seismic reflection analysis to Quaternary and geomorphic research; Quaternary Science Reviews, v. 11, p. 557-568.

Schieck, D.G. and Pullan, S.E.
1995: Processing a shallow seismic CDP survey: An example from the Oak Ridges Moraine, Ontario, Canada; Proceedings of the Symposium on the Application of Geophysics to Engineering and Environmental Problems (SAGEEP'95), Orlando, Florida, p.609-618.

Sharpe, D.R., Dyke, L.D., Hinton, M. J., Pullan, S.E., Russell., H.A.J., Brennand, T.A., Barnett, P.J., and Pugin, A.
1996: Groundwater prospects in the Oak Ridges Moraine area, southern Ontario: application of regional geological models; in Current Research 1996-E; Geological Survey of Canada, p. 181-190.

Sjögren, B.
1984: Shallow refraction seismics; Chapman and Hall, New York, N.Y.

Steeples, D.W.
1998: Special issue: Shallow seismic reflection section - Introduction; Geophysics, v. 63, p. 1210-1212.

Steeples, D.W. and Miller, R.D.
1990: Seismic reflection methods applied to engineering, environmental, and groundwater problems; in Geotechnical and Environmental Geophysics, v.I, Tutorial, (ed.) S.H. Ward; Society of Exploration Geophysicists, Tulsa, Oklahoma, p. 1-30.
1998: Avoiding pitfalls in shallow seismic reflection surveys; Geophysics, v. 63, p. 1213-1224.

Telford, W.M., Geldart, L.P., Sheriff, R.E., and Keys, D.A.
1976: Applied geophysics; Cambridge University Press, New York, N.Y.

Yilmaz, O.
1987: Seismic data processing: Series - Investigations in geophysics, vol. 2; Society of Exploration Geophysicists, Tulsa, Oklahoma.

CHAPTER 4 Borehole geophysical logging

Marten Douma, James A. Hunter and Ron L. Good

Introduction

Borehole geophysical logging techniques have been important tools in the search for oil and gas for many years. A large array of such methods has been developed to yield both qualitative and quantitative estimates of such parameters as rock type and mineral composition, density, porosity, permeability, as well as dynamic elastic properties. Such equipment and techniques are usually applied in large diameter oil and gas bore holes reaching depths of several kilometers.

It is only in the last forty years that "slim-hole" equipment and techniques have become available for potential applications in other areas such as hard rock mining and investigations within unconsolidated overburden (Rutter and Wyder, 1969; Killeen, 1986). With the advent of digital technology, along with increased use of geophysics in environmental, hydrological and geotechnical engineering problems, a new generation of portable, lightweight "slim-hole"(<10 cm diameter) equipment has emerged on the world market. Such equipment is generally designed for use in shallow boreholes (<100 m depth) and commonly in field situations where plastic casing has been installed.

The Terrain Sciences Division of the Geological Survey of Canada owns and operates some "slim-hole" sondes which are used on a routine basis to provide additional detailed stratigraphic and physical property data for the "third dimension" in various GSC projects. This paper provides an overview of the operation of these sondes along with example borehole logs from current work illustrating their role in geomorphological studies in the subsurface.

Most modern field equipment is lightweight, rugged and compact; shallow boreholes can be logged by a single operator working from a small field vehicle. Figure 4-1 shows an example of the Geonics EM-39 logging system (total count natural gamma, electrical conductivity, and magnetic susceptibility) set up over an engineering borehole.

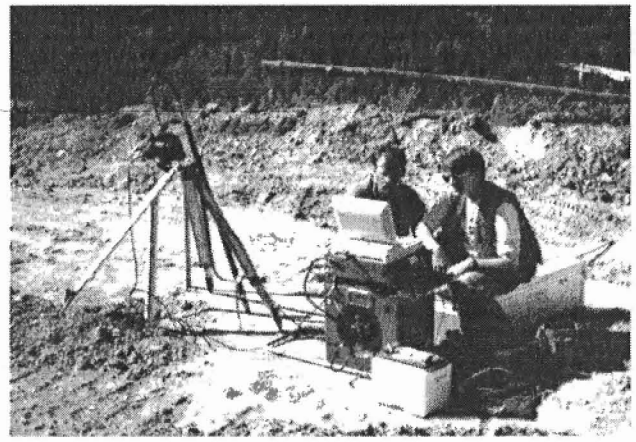

Figure 4-1. *Geonics EM-39 borehole logging system (gamma, conductivity, magnetic susceptibility sondes) in field use.*

Terrain Sciences Division borehole sondes

Natural gamma

Radioactive isotopes of potassium, uranium and thorium occur naturally in unconsolidated sediments and the decay of these elements produces gamma rays. Changes in the measured count rate of gamma rays emitted from a formation can be used in a qualitative manner to estimate grain size, and to accurately indicate lithological boundaries. In most sedimentary environments, high count rates are associated with fine-grained units such as silts and clays, whereas low count rates are associated with sand and gravel (there are of course both exceptions and additional modifying conditions which may be area dependent).

In modern sondes, a sodium iodide scintillation detector is used to detect gamma radiation. The simplest form of a such a system monitors total count rate over a broad energy band (0-3 Mev). Spectral systems, on the other hand, examine count rates of gamma energy peaks associated with radioactive uranium, thorium and potassium to ascertain the relative amounts of each element, hence the gamma "footprint" of the formation. Presently, spectral data are routinely gathered only in mining exploration in rock and few measurements have been made in unconsolidated overburden for stratigraphic evaluation.

Gamma radiation is measured from the earth material immediately surrounding the borehole (out to a distance of approximately 30 cm from the sonde). The overall count rate level can be strongly affected by hole diameter, type of casing (steel vs. plastic), integration time (summing time per measurement), logging speed and sensitivity of the sonde; these factors must be considered when comparing logs done as part of different surveys in the same area.

Figure 4-2 shows several gamma ray examples from GSC boreholes illustrating common stratigraphic boundaries.

Electrical conductivity (resistivity)

The electrical conductivity of a porous unconsolidated material is a function of the combined electrical conductivity of the matrix or framework and the pore fluid. If the pore fluid conductivity is low (such as air or fresh water in the pore spaces) then the bulk conductivity of the material mainly reflects that of the matrix material; for example, definitive conductivity differences exist between sand and clay. If, however, the porewater fluid is highly conductive (e.g. saline water) and the porosity is relatively high (40-50%), then the bulk conductivity of the material mainly reflects that of the pore fluid, and the matrix contribution to the bulk conductivity is small. Hence conductivity differences between clay and sand with high porewater salinity may be subdued.

In logging programs in overburden for groundwater studies (usually in fresh pore-water conditions), conductivity values are commonly expressed in terms of resistivity (inverse of conductivity); high resistivities are associated with coarse-grained materials (sand and gravel) and lower values with silt and clay (due to conductive clay minerals). Figure 4-3(a) shows an example of resistivity contrasts between sand and clay where the materials are saturated with fresh pore water.

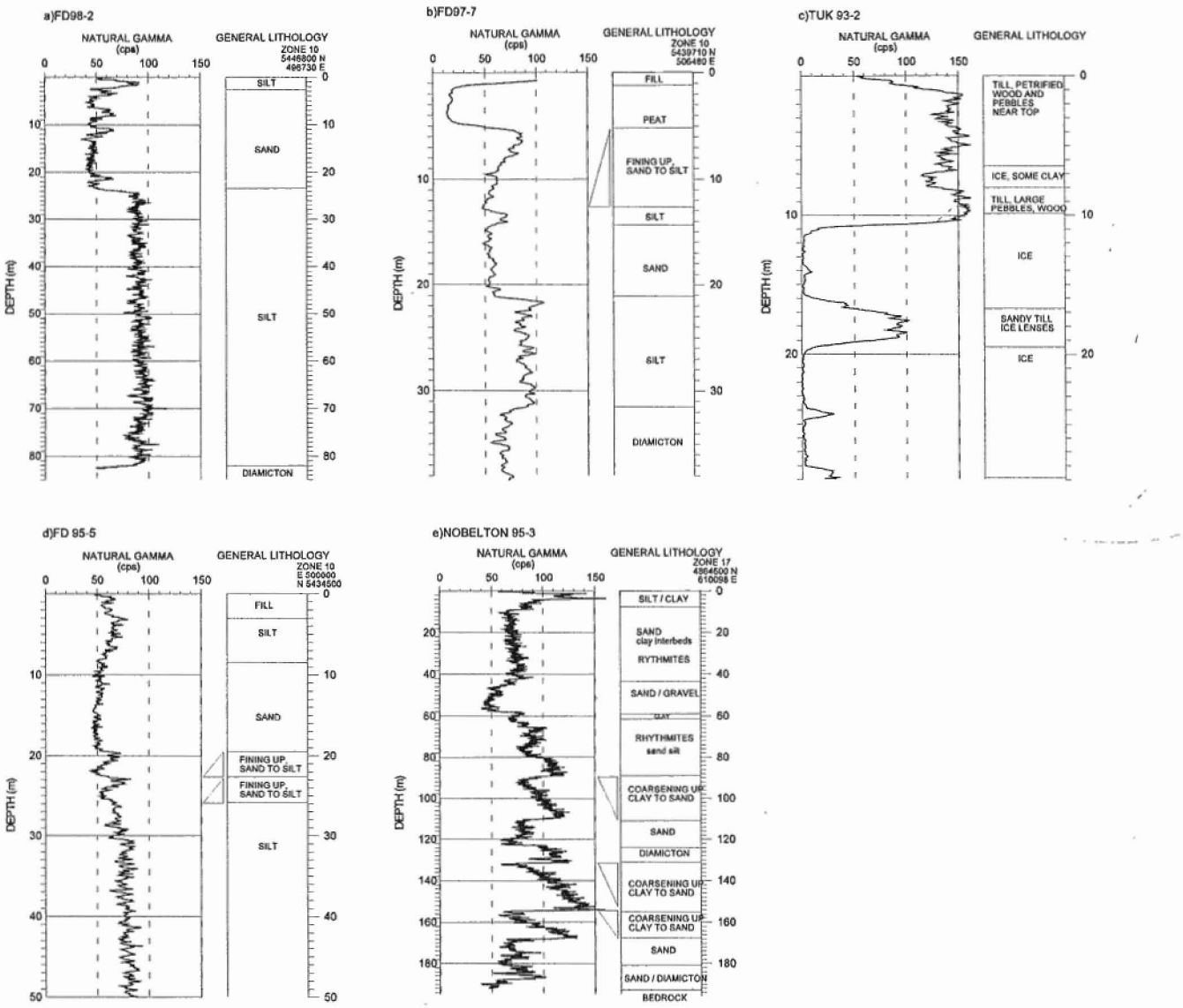

Figure 4-2. *Example natural gamma total count-rate borehole logging data: (a) an example of an abrupt sand-silt boundary in Holocene deltaic sediments, Fraser River delta, B.C. (b) an example of a peat-silt boundary, Fraser river delta, B.C. (c) a permafrost example showing a segregated ice lense (count rate near zero) imbedded between a silt above and a sand beneath, Tuktoyaktuk, N.W.T. (d) an example of fining upward sequence (sand to silt) in Holocene sediments over 3 meters, Fraser River delta, B.C. (e) coarsening upwards sequences (silt to sand) within Pleistocene materials, Oak Ridges area, southern Ontario.*

In overburden logging studies directed towards detection of groundwater contaminants (e.g. leachate monitoring studies, or salt water invasion), electrical results are given in terms of conductivities. Figure 4-3(b) shows a conductivity contrast between sand and clay where the pore water is saline (similar to seawater).

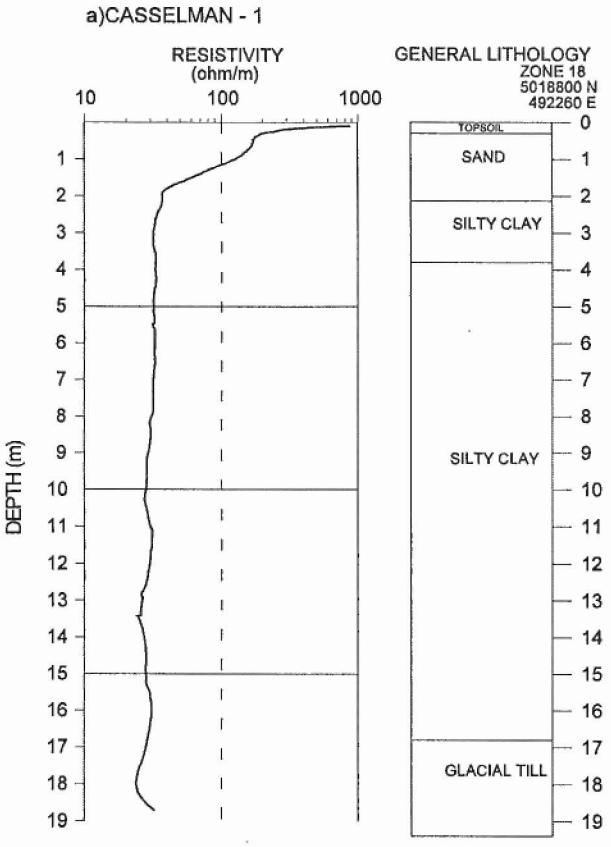

Figure 4-3(a). *An eastern Ontario borehole log example of electrical resistivity contrast across a silt- sand lithological boundary where the pore fluid is fresh water. The horizontal scale is logarithmic to emphasize resistivity contrast at low values.*

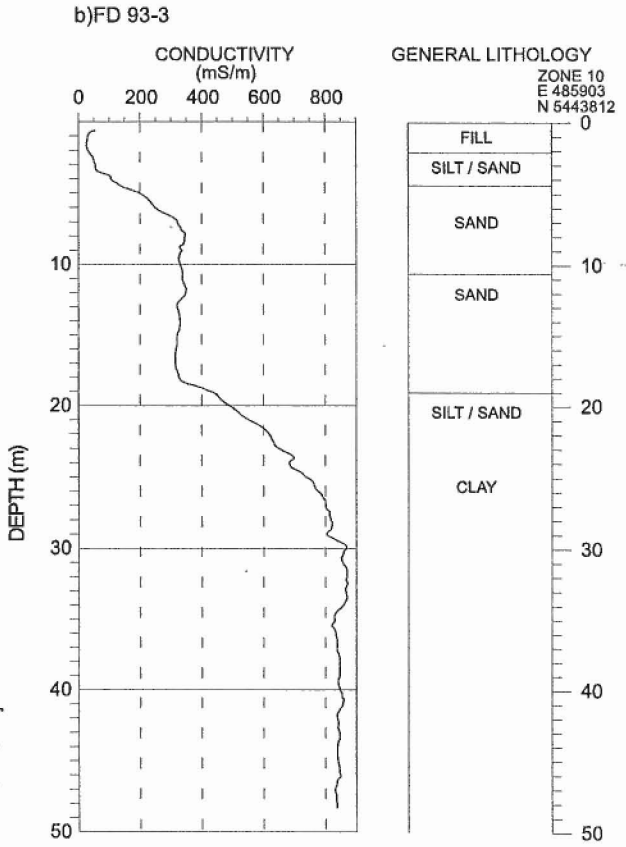

Figure 4-3(b). *A borehole log example of electrical conductivity contrast across a silt-sand lithological boundary where the pore fluid consists of sea-water, Fraser River delta, B.C.*

Induction electromagnetic conductivity loggers do not require contact with the formation or fluid in the borehole; hence, they are commonly used in plastic-cased boreholes in engineering and environmental surveys (the method does not work in steel casing). A high frequency electromagnetic is signal transmitted from, and received by two coils in the sonde. The magnitude of the induced electromagnetic field (the so-called out-of-phase or quadrature response) is proportional to formation electrical conductivity (at relatively low conductivities). The necessary spacing between transmission and receiving coils in the sonde results in the observed conductivity being the average of a large volume of material around the sonde, the extent of which is governed by the inter-coil spacing; hence, a form of smoothing is imposed on the conductivity log. As well, most induction logging sondes have been designed to be relatively insensitive to near effects (such as change in hole size or saline drilling fluids), and most of the conductivity response comes from 15-100 cm out from

the tool. Further details can be found in Taylor et al. (1989).

Induction logging systems have non-linear response at high formation conductivities (measured values 20% less than actual ones). For example, using the Geonics EM-39 system in boreholes where formation conductivities exceed 200 mS/m, it is necessary to perform post-acquisition correction (McNeill, 1986).

Figure 4-4 shows examples of high formation conductivities and a conductivity gradient associated with Holocene sediments overlying Pleistocene materials from boreholes in the Fraser River delta. In this case, it has been interpreted that the Holocene delta sediments were laid down in a seawater environment; subsequent groundwater flow associated with the more permeable Pleistocene materials has resulted in salt diffusion resulting in a salinity gradient. Where pore water samples were available for boreholes in Holocene sediments, salinity-electrical conductivity relationships have been attempted (Hyde and Hunter, 1998). Throughout the Fraser River delta, conductivity gradients in the lower part of the Holocene sediments are prevalent (Hunter et al., 1998*a*). In Champlain Sea sediments in eastern Ontario, high or low electrical conductivity values are also correlatable with presence or absence of saline pore water, and are associated with either stable or "sensitive clay" conditions.

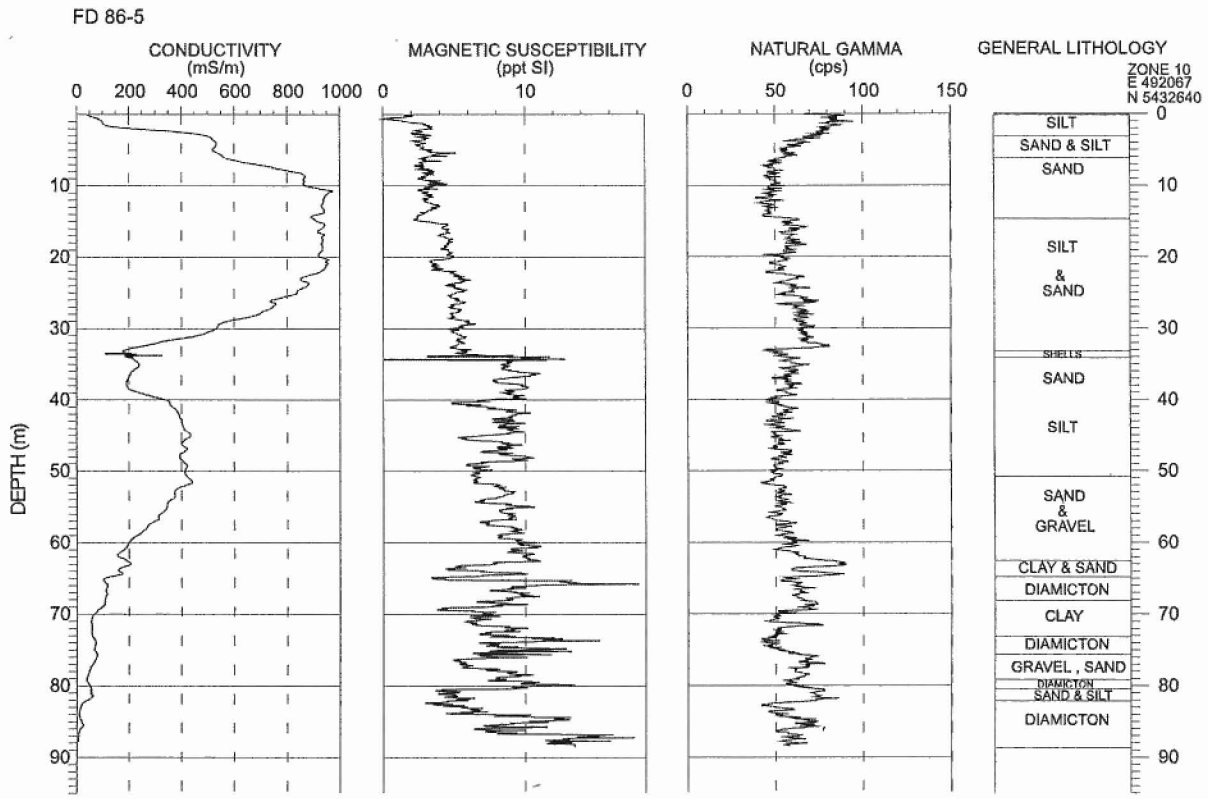

Figure 4-4. *Example borehole logs from the Fraser River delta showing high conductivities in the upper Holocene deltaic materials due to saline porewater, and conductivity gradients down to the top of the Pleistocene materials (fresh-water, permeable).*

Magnetic susceptibility

Magnetic susceptibility is a measure of the magnetization capacity of a material and is a dimensionless quantity (i.e. in effect, the ratio of the induced to the applied magnetic field). In unconsolidated earth materials most of the response results from small quantities of magnetite. Hence, anomalously large values of bulk magnetic susceptibility in a formation are an indirect indication of increased heavy mineral content.

The magnetic susceptibility sonde is similar in design to that of the induction electrical conductivity sonde; the so-called "in-phase" response of the instrument is a measure of the formation magnetic susceptibility and hence has a similar (but slightly less) depth of penetration into the formation as well as limitations in resolution. Where earth materials exhibit high electrical conductivity (>200 mS/m) a correction for conductive effects must be made to the raw magnetic susceptibility field data. A detailed description of the tool is given by McNeil et al. (1996).

In borehole logging in overburden the magnetic susceptibility tool can be used as an aid in identifying layer boundaries (e.g. clay versus sand) and, in some cases, to identify differing origins of similar materials (e.g. magnetite-rich sand). Figure 4-5 shows some examples of magnetic susceptibility logs in unconsolidated sediments.

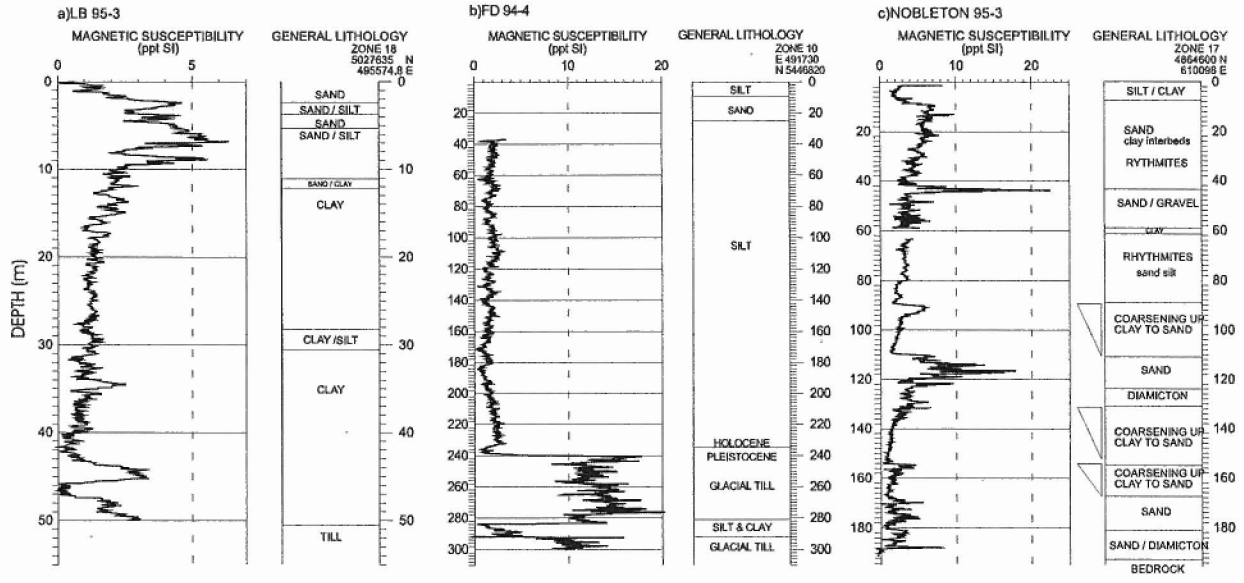

Figure 4-5. *Example borehole logs of magnetic susceptibility data showing: a) a sand-clay boundary (Holocene materials), eastern Ontario. b) the Holocene - Pleistocene boundary in borehole FD94-4, Fraser River delta. Magnetite content of Pleistocene sediments in many Fraser River delta boreholes is relatively high. c) high magnetic susceptibility associated with a sand unit in Pleistocene materials from the Oak Ridges area, southern Ontario.*

Spectral gamma-gamma density log

Slim-hole gamma-gamma density logs have been available for many years; such tools generally use a collimated radioactive gamma ray emission source (e.g. Cesium 137, Cobalt 60) and a collimated receiver to measure total count rate of radiation after penetration into the formation, assuming that such radiation is scattered proportionally to the bulk density of the formation (Compton scattering). Currently, using measurement of gamma radiation levels over a spectrum of gamma ray energies (0 to 3 Mev) it is possible to refine the energy window over which the Compton scattering phenomenon is predominant (Killeen and Mwenifumbo, 1988).

Considerable experience with this type of tool has been acquired in hard rock mining exploration, and open-hole calibrations between observed count rates and rock densities are available. However, for borehole logging in unconsolidated overburden, where the tool is generally run in a small diameter PVC casing, density calibrations have not yet been attempted. Hence, density variations are relative and are values are given in units of count rate (e.g. high count rate equivalent to low density, and vice versa). Examples of spectral gamma density logging in overburden are given in Figure 4-6.

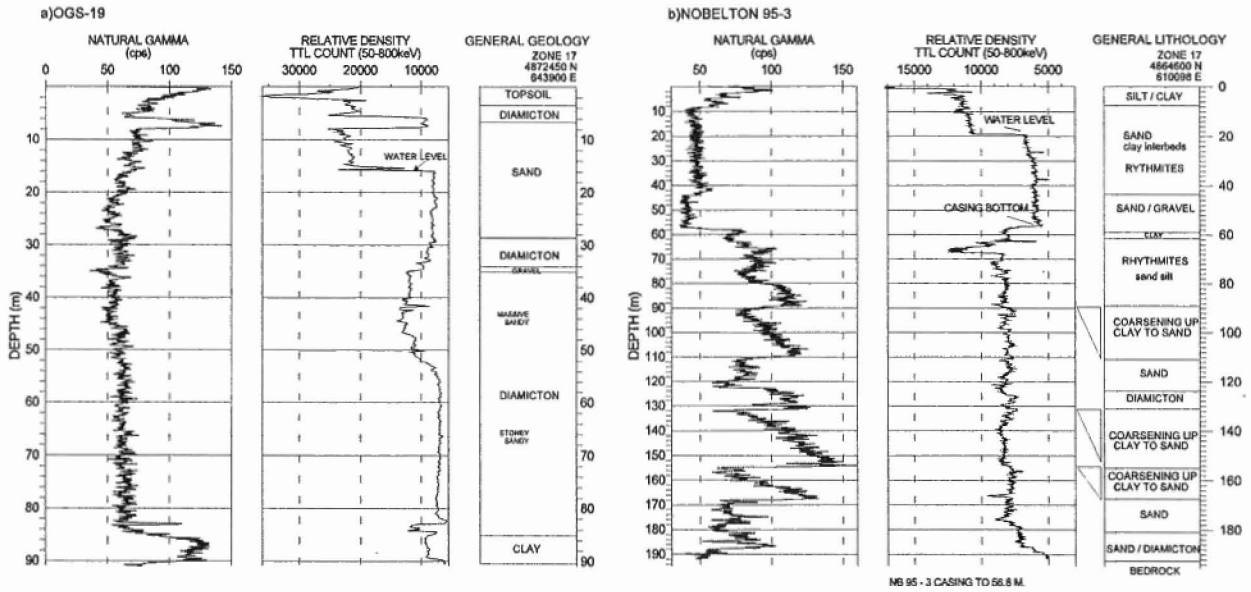

Figure 4-6. *Examples of gamma-gamma relative density borehole logs showing density variations: a)across an aquifer in Pleistocene materials, borehole OGS-19, Oak Ridges area, southern Ontario. b)within Pleistocene materials, borehole Nobelton 95-3, Oak Ridges area, southern Ontario.*

Spectral gamma-gamma ratio log

The low energy end (<180 keV) of the observed gamma ray spectrum of earth materials obtained by using one of the above-mentioned sources in a sonde, is particularly sensitive to the average atomic number (Z) of the formation (due to photoelectric absorption). Hence, by choosing a low energy and a high energy window, vertical changes in the count-rate ratio of these windows would reflect

changes in Z but would be insensitive to changes in formation density. In overburden materials, such changes in average Z might result from variation in heavy mineral content, void ratio, or moisture content.

The spectral gamma-gamma tool can be used to obtain relative density as well as qualitative estimates of changes in average Z. An example of such a log, in Figure 4-7, shows variations in porosity in a water-saturated Pleistocene aquifer in the Oak Ridges moraine.

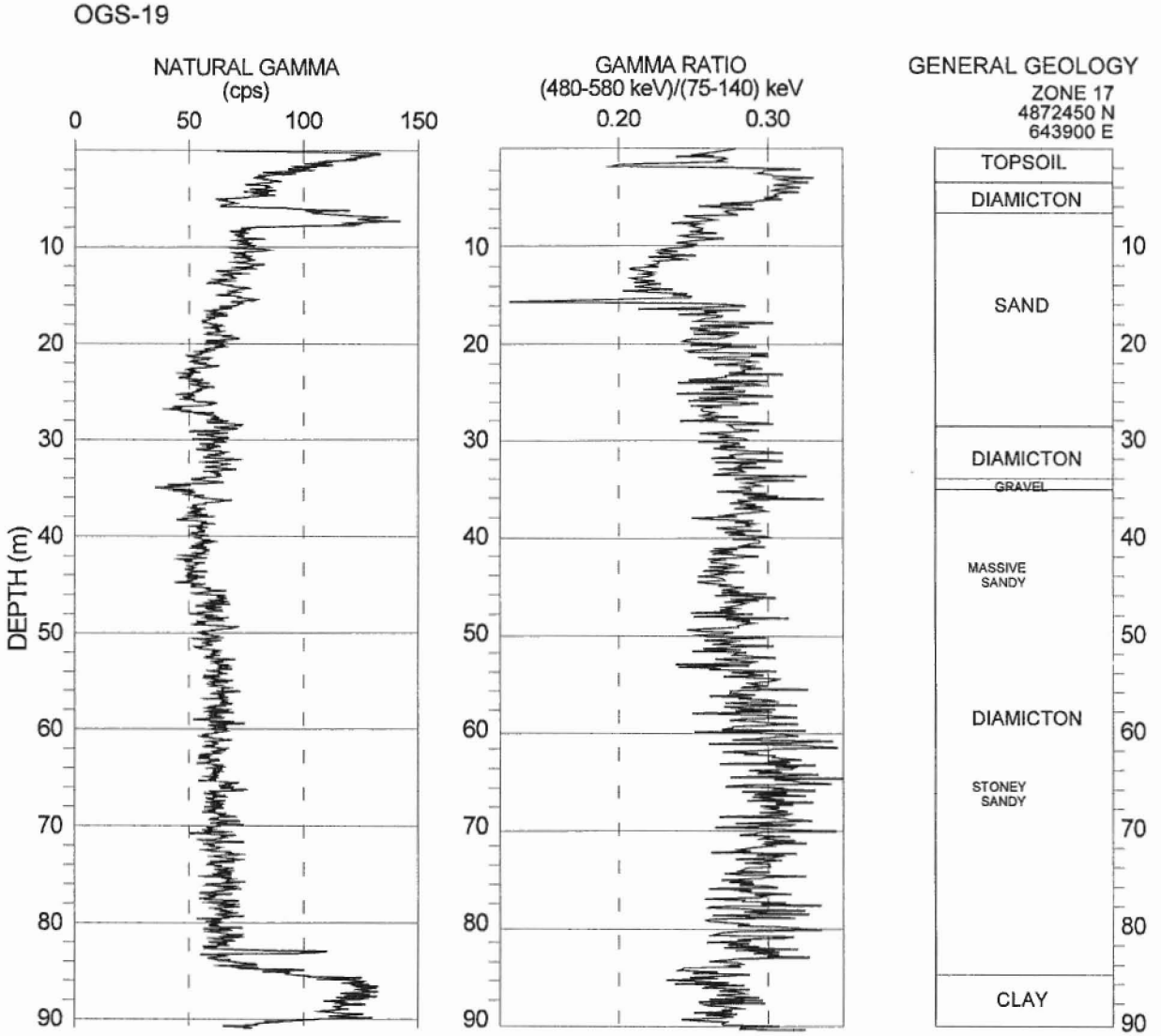

Figure 4-7. *Spectral gamma-gamma ratio (high energy/low energy) in coarse grained, Pleistocene materials, borehole OGS-19, Oak Ridges area, southern Ontario.*

Seismic downhole logs

Compressional and shear wave velocities of unconsolidated formations can be used to identify changes in moisture content (top of water table) and strengths of materials, and to provide qualitative

estimates of over-consolidation.

Compressional wave (P -wave) surveys are commonly done using a multichannel hydrophone array deployed in a borehole, along with a surface source (hammer and plate, or in-hole seismic gun) deployed adjacent to the borehole. For successive source shots, the array is moved down the borehole at intervals. Travel times of P-waves between the source and the hydrophone detectors are measured and interpreted for interval velocities. Details of such work can be found in Hunter et al. (1998*b*). Such hydrophone arrays can consist of 12 or 24 detectors with spacings in the range of 0.5 or 1 m so as to provide detailed vertical velocity coverage.

In a similar manner, downhole shear wave interval velocities can be measured using a single (or an array of) well-lock, 3-component geophone(s), and a surface horizontally polarizing shear wave source (commonly, a loaded plank, hammered end-on).

P- wave velocities in unconsolidated materials are strongly affected by the pore fluid velocity. For most near-surface, normally consolidated, water-saturated materials, the P-wave velocity is approximately 1500 to 1800 m/s, slightly higher than that of water (1480 m/s).

Figure 4-8 shows both compressional (P-wave) and shear wave velocities in a deep stratigraphic borehole in the Fraser River delta. The P-wave log indicates the presence of low water content in the pore spaces in the upper portion of the hole (in this case a small quantity of methane gas is present in the pore space) resulting in low velocities. The boundary between Holocene and Pleistocene sediments is marked by an abrupt increase in velocity (resulting from an increase in bulk density, bulk modulus, as well as increased age-related consolidation).

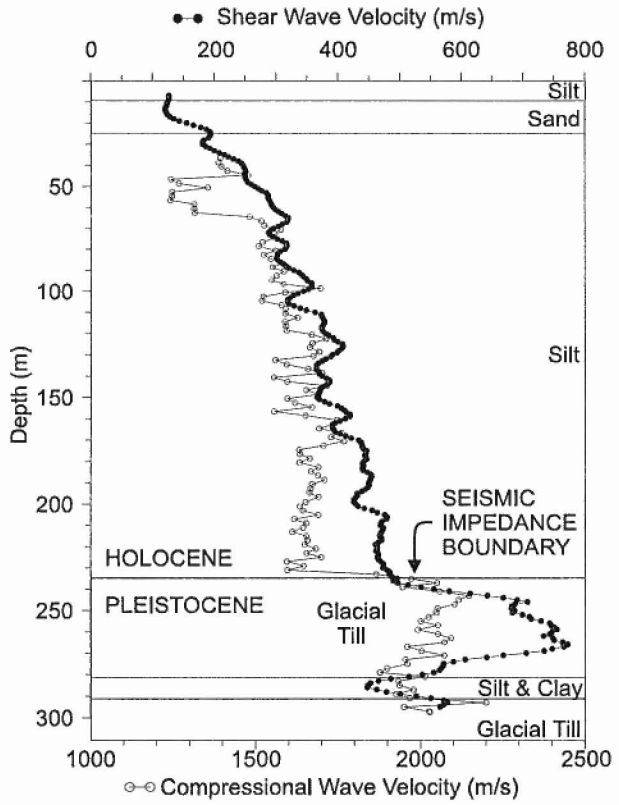

Figure 4-8. *Compressional and shear wave velocities in Holocene and Pleistocene materials, borehole FD94-4, Richmond, B.C.*

Shear waves are transmitted through the framework of the material and are much less affected by pore fluid composition. On the other hand, shear wave velocities are affected by load pressure (depth of burial), and degree of consolidation.

The shear wave velocity-depth section shown in Figure 4-8 indicates an increasing shear wave velocity, with depth, in the upper portion of the hole, in response to overburden load pressure. At the Holocene-Pleistocene boundary, the abrupt shear wave velocity anomaly is associated with over-consolidated glacial materials (with increased bulk density and shear modulus).

Summary

Geophysical logging of boreholes drilled in overburden can be used to augment the observed geological sample descriptions. Such data can reveal subtleties of grain size, mineralogy and pore-water content that are not readily observable during normal specimen examination in the field. Borehole stratigraphy may be more accurately constrained and hole-to-hole correlations more easily visualized with the aid of geophysical logs.

REFERENCES

Hunter, J.A., Burns, R.A., Good, R.L., and Pelletier, C.F.

1998a: A compilation of shear wave velocities and borehole logs in unconsolidated sediments of the Fraser River delta; Geological Survey of Canada, Open File D3622.

Hunter, J.A., Pullan, S.E., Burns, R.A., Good, R.L., Harris, J.B., Pugin, A., Skvortsov, A., and Goriainov, N.N.

1998b: Downhole seismic logging for high-resolution reflection surveying in unconsolidated overburden; Geophysics, v.63, p.# 1371-1384.

Hyde, C.F.B. and Hunter, J.A.,

1998: Formation electrical conductivity-porewater salinity relationships in Quaternary sediments from two Canadian sites; Proceedings, Symposium on the Application of Geophysics to Engineering and Environmental Problems (SAGEEP'98), Chicago, Illinois, p.# 499-510.

Killeen, P.G.

1986: Borehole geophysics for mining and geotechnical applications; Geological Survey of Canada, Paper 85-27.

Killeen, P.G., and Mwenifumbo, C.J.

1988: Interpretation of a new generation geophysical logs in Canadian mineral exploration; 2nd International Symposium on Borehole geophysics for Minerals, Geotechnical and Groundwater Applications, Golden, Colorado, p.#167-178.

McNeill, J.D.

1986: Geonics EM-39 borehole conductivity meter, theory of operation: Geonics Technical Note TN-20.

McNeill, J.D., Hunter, J.A., and Bosnar, M.

1996: Application of a borehole induction magnetic susceptibility logger to shallow lithological mapping; Journal of Environmental and Engineering Geophysics, v. 0, no. 2, p.# 77-90.

Rutter, N.W. and Wyder, J.E.
1969: Application of borehole stratigraphic techniques in areas of mountain glacial drift in Alberta, Canada; Geological Survey of Canada, Paper 69-35.
Taylor, K.C., Hess, J.W., and Mazzela, A.
1989: Field evaluation of a slim-hole borehole induction tool; Ground Water Monitoring Review, Winter Issue, 1989, p.#100-104.

CHAPTER 5 Ground penetrating radar

Stephen D. Robinson and Yves Michaud

Introduction

Ground penetrating radar (GPR) has been gaining wide acceptance in the geomorphic community as a fast, reliable, portable, and relatively inexpensive tool for non-destructive high-resolution mapping of subsurface materials. In many applications, GPR is the only geophysical method that can provide the resolution and depth of penetration required by geomorphologists. GPR surveying and interpretation are relatively simple, and although a good knowledge of the geophysical theory behind GPR is useful to understand system response, it is not always a requirement for the production of successful surveys. GPR surveying is in many ways similar to shallow seismic reflection (Chapter 3), but whereas seismic methods generally yield limited information in the upper 10 m and have poor resolution, GPR is especially adept at delineating near-surface features and provides much improved resolution (McCann et al., 1988).

This paper is intended as an introduction to the application of GPR to various aspects of geomorphic research, and as such the geophysics are kept to a minimum, and the basics of successful GPR surveying and case studies are stressed. Those wishing to delve deeper into the physics behind GPR are encouraged to read Annan and Davis (1977), Daniels et al. (1988), Davis and Annan (1989), and Peters et al. (1994).

Basic geophysical concepts of ground penetrating radar

GPR surveying involves the transmission of short bursts of high frequency (10 to 1000 MHz) electromagnetic (EM) energy into the ground. The frequency of the transmitted pulse is dependent upon the antennas being used in the survey. A part of the energy is radiated into the ground where it travels with a velocity controlled by the geological properties of the ground (typically 1/2 to 1/10 of the speed of light). Depth of signal penetration is controlled by attenuation losses within the ground. Subsurface changes in material, density, water content, or temperature can cause a portion of the energy to be reflected back towards the surface, where it is detected by a receiving antenna (Fig. 5.1). The proportion of the signal that is reflected at a given subsurface change is dependent upon the magnitude of electrical changes at the boundary. A contact that causes energy reflection is called a *reflector*. The response of the receiving antenna as a function of time at one survey station is termed a *trace*. The radar system records both strength and return time of the reflected pulse at successive survey stations, making it possible to compile a *profile* and non-destructively map features beneath the ground surface. Figure 5.2 is a sample profile compiled from traces collected every 0.5 m for 114 m. Note that the horizontal axis represents position along the profile, and the vertical axis is the two-way travel time (in nanoseconds) of the radar wave. Individual reflectors are shaded black and often appear in many successive traces, allowing the delineation of subsurface features.

The theory behind *propagation velocity, depth of penetration, attenuation, reflection coefficients,* and *resolution* is key to understanding the basics of ground penetrating radar.

Velocity

GPR systems measure the "distance" to a reflector in terms of the *two-way travel time* between the emission of the transmitted pulse and its return to the receiver. The *wave propagation velocity* is required in order to convert two-way travel times to depth estimates. *Relative permittivity*[*], or *dielectric constant* (K) is related to the ability of a material to electrically polarize, and is the main factor controlling wave velocity through a material. Higher velocities related to lower values of dielectric constant (Table 5.1). As the permittivity of water is typically at least 20 times higher than

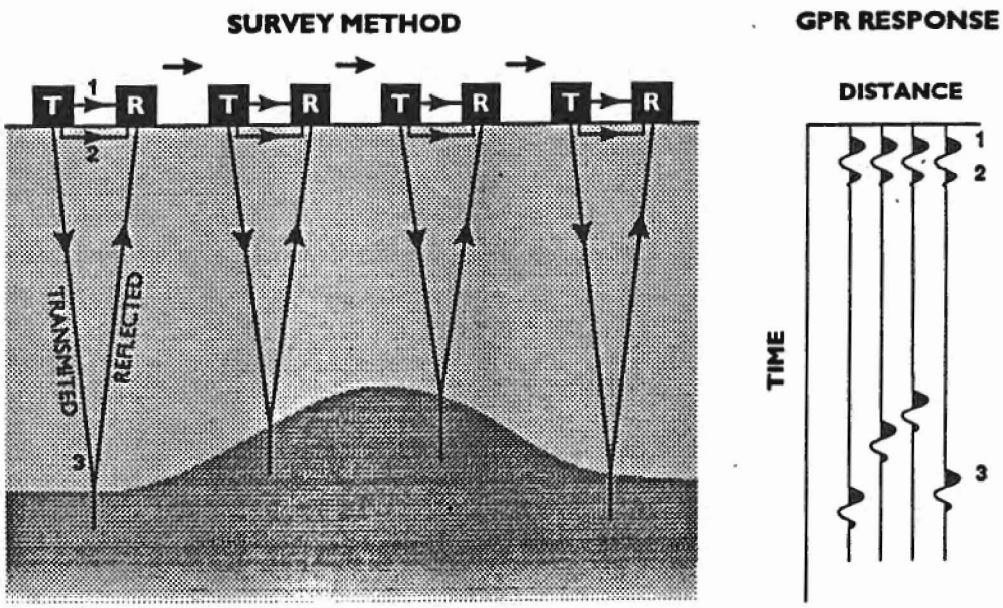

Figure 5.1 *Reflection survey method with electromagnetic energy transmitted from the transmitter (T) and received at the receiver (R) after reflecting off a contrast in material, density, or water content. One trace is collected at each survey station, with a collection of traces from evenly spaced stations forming a profile. The GPR response at right shows the 1) air wave, 2) ground wave, and 3) reflector from the contact. Successive traces are shown as a response to moving the antennas during profile collection. The air wave travels through the air between the transmitter and receiver and acts as a zero time marker. The ground wave travels through the surface skin of the ground at a slightly lower velocity. Responses received after the air and ground waves are most often from the subsurface.*

[*] The relative permittivity or dielectric constant (K) is the ratio of the dielectric permittivity of the material to that of free space.

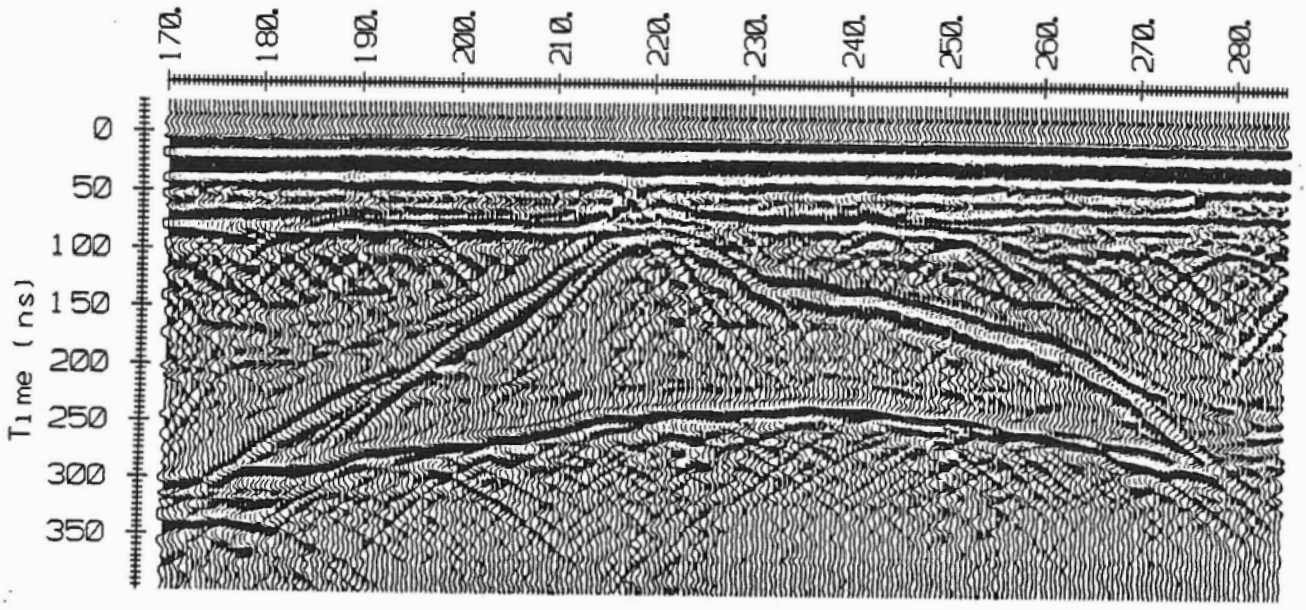

Figure 5.2 *A sample GPR profile with traces collected every 0.5 m for 114 m to form a profile. The horizontal axis represents position along the profile, and the vertical axis is the two-way travel time (in nanoseconds) of the radar wave. In this case, the positive pulses representing individual reflectors are shaded black and often appear in many successive traces, allowing the delineation of subsurface features. This examples shows massive ground ice, enclosing sediments, and bedrock topography near Contwoyto Lake, N.W.T. Source: modified from Wolfe et al. (1997).*

most solid components, this factor completely dominates propagation velocity in many saturated environments (e.g. peat). Propagation velocities should always be measured during a radar survey, but in general the velocity of a radar wave in a material can be calculated from the following relationship:

$$\text{Velocity} = \frac{\text{Velocity of the radar wave in air}}{\sqrt{\text{dielectric constant of material}}}$$

The most common technique for conducting a velocity measurement (CMP survey) is explained in detail in the section on interpretation.

Depth of penetration

The *depth of signal penetration* is controlled by the *attenuation rate* of the material, which is in turn primarily influenced by *electrical conductivity*. The dielectric constant of the material has minor effects upon the attenuation rate. The attenuation rate (α - expressed in dB/m) exponentially reduces the initial signal amplitude (A_0) with depth (z), and follows the equation of:

$$A = A_o e^{-\alpha z}$$

where A is the pulse amplitude at depth z.

The amplitude is reduced at some depth to a point where it is indistinguishable from background noise when it arrives at the receiver. This depth is considered the depth of penetration. The depth of penetration within which reflectors may be still distinguished can be predicted from radar range equations supplied by Davis and Annan (1989). However, for many applications, familiarity with the material electrical conductivity can be used to estimate the potential depth of penetration, and therefore success, of a survey. Referring to Table 5.1, materials with high conductivities have high rates of attenuation and accompanying shallow depths of penetration. As a general rule, GPR is of limited use when the soil conductivity is greater than about 20 mS/m.

Table 5.1 *Typical dielectric constant, electrical conductivity, velocity and attenuation values observed in common geologic materials.*

Material	Dielectric constant (K)	Electrical conductivity (mS/m)	Velocity (m/ns)	Attenuation (dB/m)
Air	1	0	0.30	0
Distilled water	80	0.01	0.033	0.002
Fresh water	80	0.5	0.033	0.1
Sea water	80	3000	0.01	1000
Dry sand	3-5	0.01	0.15	0.01
Saturated sand	20-30	0.1-1.0	0.06	0.03-0.3
Limestone	4-8	0.5-2.0	0.12	0.4-1.0
Shale	5-15	1-100	0.09	1-100
Silt	5-30	1-100	0.07	1-100
Clay	5-40	2-1000	0.06	1-300
Granite	4-6	0.01-1.0	0.13	0.01-1.0
Dry salt	5-6	0.01-1	0.13	0.01-1.0
Ice	3-4	0.01	0.16	0.01

Reflection coefficients and resolution

Reflections of the transmitted pulse occur when there is sufficient contrast in dielectric constant at a boundary between materials. If the dielectric constants at an interface are K_1 and K_2, a downward

moving wave of amplitude A travelling in material 1 is reflected at the interface with material 2 with an amplitude of RA, where the *reflection coefficient* R is given by:

$$R = \frac{\sqrt{K_1} - \sqrt{K_2}}{\sqrt{K_1} + \sqrt{K_2}}$$

The remaining energy transmits through the interface with a reduced amplitude, and is available for reflection at subsequent interfaces.

Gradual changes in dielectric constant often do not produce reflections. For a boundary to be considered abrupt, the change in dielectric constant must occur in roughly one quarter of a wavelength ($\lambda/4$ in metres), and is obviously dependent upon operating frequency (f in MHz) and the velocity of the material. Thus, with proper choice of antennas, gradational boundaries (e.g. the water table in fine-grained soils) may become distinct reflectors if the frequency is reduced to the point that the wavelength of the propagating radar pulse is long compared to the thickness over which the boundary occurs.

Resolution is the ability of the radar system to distinguish two signals that are close to each other in time. Higher frequency antennas yield greater resolution than antennas of lower frequency, but have lower depths of penetration. Note the resolution also deteriorates with depth, as it is often the higher frequency energy in the pulse that is attenuated. Figure 5.3 outlines the expected resolution (resolvable thickness) as a function of propagation velocity and antenna frequency. Figure 5.4 presents the exact same radar profile conducted with 50, 100, and 200 MHz antennas for depth of penetration and resolution comparisons.

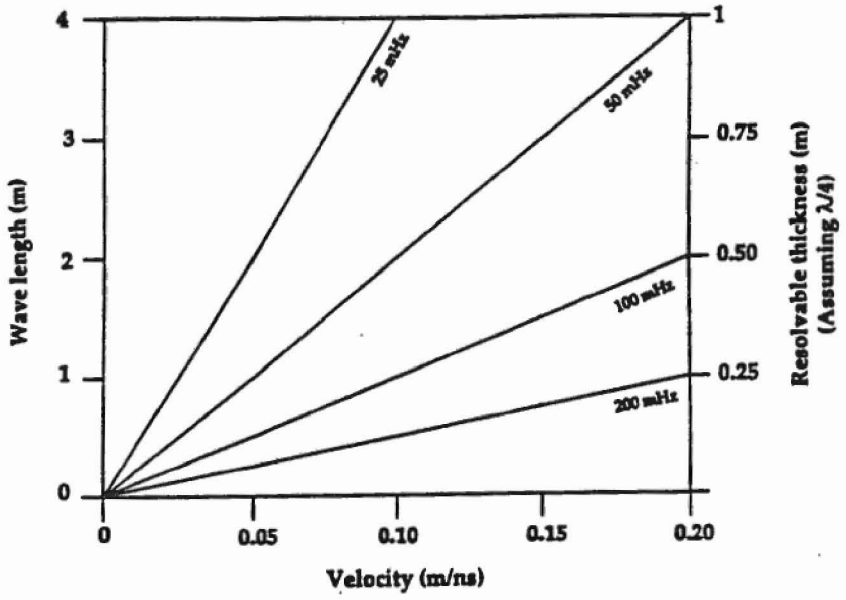

Figure 5.3 *Resolution, or resolvable thickness, as a function of radar wave velocity and wavelength for antenna frequencies of 25 to 200 MHz. Source: Jol (1995).*

Jol (1995) used antennas of different frequencies to examine stratigraphy within a saturated freshwater delta and found that vertical resolution ranged from 0.15 m (200 MHz antennas) to 0.76 m (25 MHz), and depths of penetration ranged from 14 m (200 MHz) to 28 m (25 MHz). In the less ideal case of Figure 5.4 from the Norman Wells pipeline route, resolution ranged from 0.14 to 0.52 m (V=0.10 m/ns), yet penetration was limited to about 4 m with 50 MHz antennas and to less than 2 m with 200 MHz antennas.

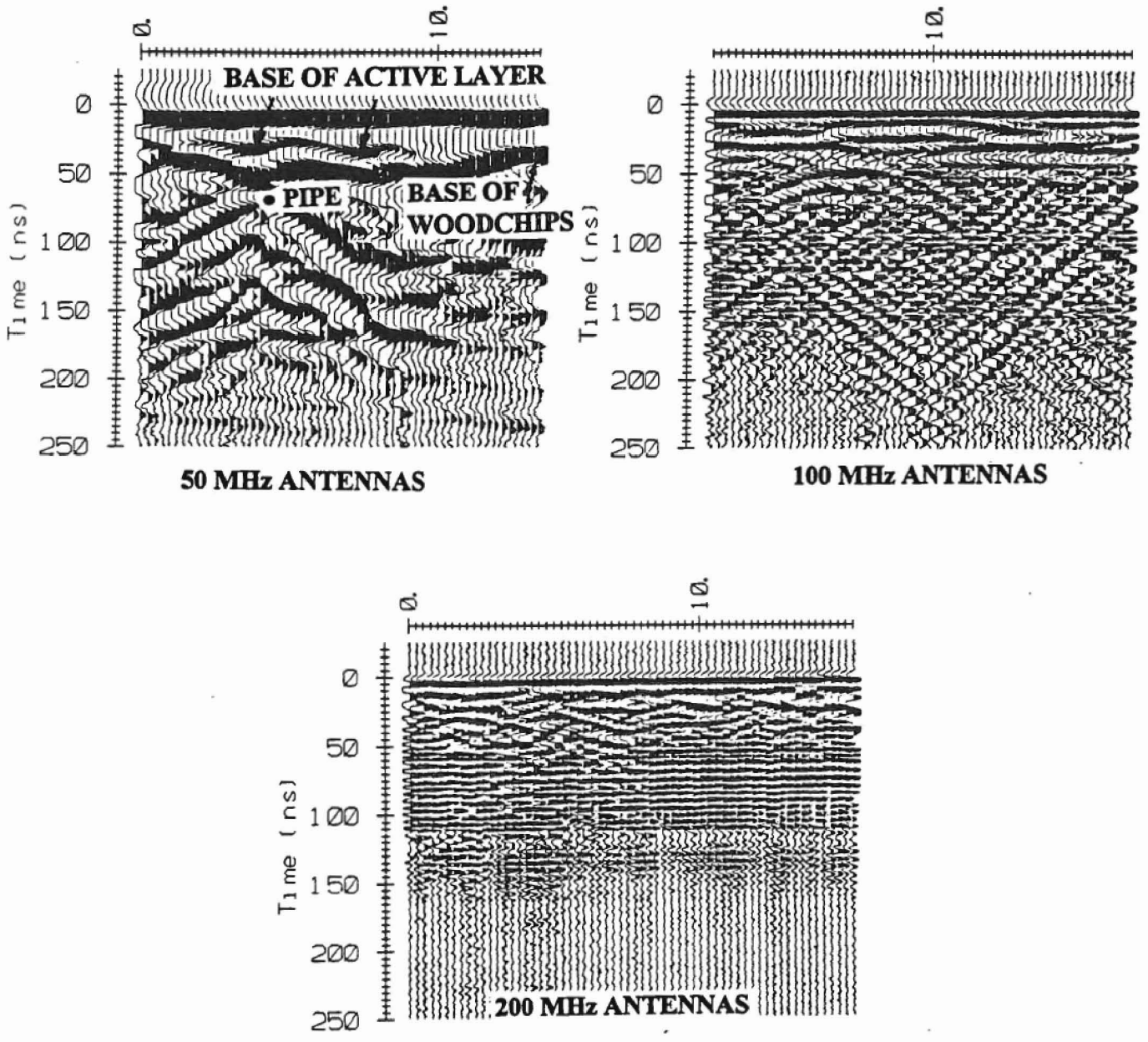

Figure 5.4 *The same radar profile surveyed with 50, 100, and 200 MHz antennas. These surveys were conducted across a slope on the Norman Wells pipeline, N.W.T., with a 1.5 m thick woodchip insulation layer to protect permafrost. Note that the reflectors of interest in this case, the base of annual thaw, base of woodchip insulation, and the pipe itself are only readily apparent in the 50 and 100 MHz surveys. The 200 MHz surveys returned too many additional reflectors that confuse the interpretation. Source: Robinson and Moorman (1995).*

To put all of this in a geomorphic context, Table 5.2 lists a variety of geomorphic applications along with the reasons why they were successful (or unsuccessful) based upon the GPR basics outlined above. The table is not a complete list of GPR applications, and is heavily weighted towards successful results as those are the most likely to appear in the literature.

Assessing various GPR applications

Years of radar experience have allowed the development of several "rules of thumb" for determining the potential success of GPR applications. If detailed background information on electrical properties (especially conductivity and dielectric constant) exists for the site, then the potential for success can be assessed by using the radar range equations provided by Annan and Davis (1977). Otherwise it is best to either 1) review the literature pertinent to your application, or 2) review parameters crucial to GPR to estimate success. Under ideal penetration conditions (dry sand or ice), signals from 50 MHz antennas can penetrate 30-50 m. This value is drastically reduced in a saturated clay, often to less than 1 m. Maximum penetration within saturated peat appears to be about 8-10 m with 50 MHz antennas.

Conditions to assess prior to conducting a survey include the following:

Soil conductivity
Low conductivity soils yield low attenuation rates, and as a general rule GPR will not be successful in terms of penetration if the conductivity is >20 mS/m. Surveying in tidal flats or other marine-derived sediments is rarely successful. In some instances however, the delineation of high conductivity zones is the survey objective (contaminant spills or the mapping of saline soils).

Cultural interference
Buildings, overhead or buried electrical cables, and cars will all cause interference if they are too close to the survey line. In addition to being transmitted into the ground, radar wave are also transmitted in the air (antenna are only poorly directional) and reflections can falsely appear as subsurface features in a profile. The same warning applies to natural objects that may be close to the survey, such as cliffs or large boulders. In many cases reflectors caused by such interference can be identified and accounted for during interpretation. Any reflector that arrives with a velocity of 0.30 m/ns has an above ground source. Proximity to radio transmitters should also be avoided, as external radio signals may saturate the receiver.

Material morphology
Sand and gravel are often of low conductivity, and different stratigraphic units commonly have high dielectric contrasts due to different water contents or bulk densities, resulting in deep penetration (low attenuation) and excellent discrimination of bedding features. Clays are most often highly conductive due to high dissolved ion concentrations, resulting in high rates of signal attenuation. Large boulders often cause hyperbolic reflections; that is, the radar unit "sees" them before it is over top of the boulder (c.f. Fig. 6.6). This pattern commonly obscures surrounding

Table 5.2. Some geomorphological applications of ground penetrating radar.

Geomorphological GPR Application	Reasons for Success	Comments	References
Internal morphology of freshwater fluvial deposits (coarse-grained)	•low conductivity results in excellent penetration (up to 50 m with 25 MHz antennas) •strong dielectric contrasts resulted in excellent discrimination of internal morphology •deeper penetration if the deposits are dry (see Smith and Jol, 1992)	•Smith and Jol (1992) mapped delta architecture (thickness, internal structure, angle of bedding) in fairly coarse-grained material (an ideal environment), while others have attempted to map finer-grained, poorly sorted, and higher conductivity deposits with more moderate results (e.g. Bridge et al., 1995; Fisher et al., 1995)	Jol and Smith (1991) Smith and Jol (1992) Jol (1995) Olsen and Andreason (1995) van Overmeeren (1998)
Mapping thickness, basal topography, and internal morphology of peatlands	•marked dielectric contrast (due to changes in water content) at the peat-mineral contact and among peat layers results in excellent delineation of basal topography and internal stratigraphy •low velocity (<0.04 m/ns) in unfrozen peat results in high resolution •frozen peat has a velocity 2-3 times higher than unfrozen peat, facilitating permafrost delineation (see Kettles and Robinson, 1996: Horvath, 1998)	•high velocity decreases resolution in frozen peat, and weakens peat-mineral reflectors •high attenuation rates are found in peatlands developed on marine deposits (e.g. Theimer et al., 1994) •with ancillary coring data, peat types can be mapped over large areas (as can changes in water content)	Theimer et al. (1994) Jol and Smith (1995) Kettles and Robinson (1996) Warner et al. (1990) Hanninen (1992) Lapen et al. (1996) Horvath (1998) Robinson and Kettles (unpub. data in this paper)
Permafrost mapping, including the distribution and thickness of massive ground ice and enclosing sediments	•excellent propagation depths (up to 30 m) due to permafrost if sediments are coarse (Wolfe et al., 1997) •large dielectric contrasts between ice-bonded sediments and pure ice result in excellent reflector delineation •excellent discrimination of internal sediment features and bedrock topography	•best results in winter with thin snow cover and without active layer development •much of the ground ice in the High Arctic is enclosed in marine sediments, resulting in high attenuation (Robinson, 1994)	Annan and Davis (1976) Wolfe et al. (1997) Lawson et al. (1991) Dallimore and Davis (1992) Robinson (1993) Arcone et al. (1998) Robinson, Burgess, and Wolfe (unpub. data in this paper) Michaud et al. (1994)
Delineation of permafrost along a pipeline route, including locating the buried pipe.	•good delineation of thawed depth and extent due to large variation in dielectric constant between frozen and unfrozen material •location of buried pipe (≈2m depth) easy using 50 and 100 MHz antennas	•difficulty was encountered due to spatial changes in velocity (frozen vs. unfrozen) •poorer results in clay due to high unfrozen water content	Burgess et al. (1995) Robinson and Moorman (1995)

Table 5.2, continued

Soil horizon delineation	•high frequency GPR with high resoultion, in conjunction with soil pits, can be used to delineate soil horizons and soil types, and clay content •can also map depth to bedrock in some cases	•variable moisture content (temporal and spatial) produces correlation problems • Tarussov et al., (1994) present an interesting application of airborne soils mapping using GPR	Dominic et al. (1995) Doolittle (1982) Collins and Doolittle (1987)
Internal morphology of coastal raised beaches	•stong dielectric contrasts resulted in excellent discrimination of internal morphology •low velocity resulted in high resolution	•slope of reflectors provided useful information to reconstruct shoreline locations	Parent and Michaud (1996)
Bathymetry and limnological studies	•strong dielectric contrast often exist between water column and lake bed material •low velocity in saturated material increases resolution	•easiest to conduct survey when frozen (see Moorman and Michel, 1997) •useful to find optimal sediment coring sites, water depths >10m may become problematic	Lowe (1985) Moorman and Michel (1997) Robinson, Burgess and Wolfe (unpub. data in this paper)
Hydrogeological investigations (incl. water table and aquifer delineation)	•excellent delineation of the water table and aquifer dimensions in fairly coarse-grained material	•marked loss of signal in clay and water table have a thick capillary fringe (non-abrupt reflector) •sinkhole mapping (Clasen, 1989)	Michaud et al. (1997) Davis and Annan (1992) Clasen (1989) Arcone et al. (1998) van Overmeeren (1998)
Fracture mapping within granite	•very low attenuation results in penetration to over 50 m •high dielectric contrast at water-filled fractures, give strong reflector signature	•high conductivities were noted in some water-filled fractures at depth	Holloway (1992) Stevens et al. (1995)
Glacial ice thickness and internal stratigraphy	•very low attenuation (≈ 0.01 dB/m) and high velocity (0.16 m/ns) can result in signal penetration to several hundred metres •strong reflector at base of glacier (dramatic decrease in water content) and at points of different ice density	•mapping glaciers was the original application for which GPR was developed	Behrendt et al. (1979) Evans (1963) Bently et al. (1979)

reflectors. Remember that in many cases the dielectric properties of the pore water overwhelm the material dielectric properties.

Moisture content
Moisture content is often the overwhelming control on dielectric constant, and therefore velocity and resolution. A high water content slows the velocity and increases resolution. However, attenuation rates are higher in wet materials than dry materials. Dissolved ions in the pore water increase conductivity, resulting in a further increase in attenuation rate. Clays have especially high dissolved ion concentrations.

Frozen or unfrozen material
Permafrost represents one of the best transmissive media for radar (especially if it is ice-rich), although propagation velocities are high (0.10 to 0.16 m/ns). Large dielectric contrasts exist at frozen-unfrozen contacts, making radar ideal for mapping the active layer or thaw contacts. Frozen clay often contains a high unfrozen water content, resulting in the same conductivity problems as with unfrozen clay.

Top-down reflector potential
The sequence and strength of potential reflectors and reflectors of interest must be kept in mind when planning radar surveys. Very strong near-surface reflectors (snow-ground, water table or active layer reflectors) may result in a large proportion of energy being reflected prior to reaching the depth of interest. In many geomorphic applications, this can be partially solved by careful selection of antenna frequency or survey season.

Depth of interest and resolution required
An idea of the desired penetration depth and resolution is required prior to surveying for survey design. There is a trade-off between depth of penetration and resolution (Jol, 1995). However, it is possible to repeat a survey using different antenna frequencies. Practical experience has shown that often the reflectors of interest are obscured if antenna frequency is too high, as too many "minor" or unimportant reflectors overwhelm the profile. Also remember that near-surface geometry is often distorted when using a large antenna separation as is common with low frequency antennas. Target geometry (height, length and width) and orientation (strike and dip) should also be estimated prior to surveying. For example, if the survey objective is to measure the dip of a reflector, the general direction of strike and dip should be known prior to surveying. Conducting two perpendicular survey lines will aid in finding the true dip direction.

Note that many of these parameters often go hand in hand. For example, clays are generally of high conductivity while sands are not, unless local groundwater is highly conductive.

Conducting a GPR survey

GPR surveys can be conducted in three different modes. By far the most common is *reflection profiling mode*, in which both antennas are moved at a set distance in the same direction, with a

trace being collected at each survey station. This type of survey results in the cross-section plot as seen in Figure 5.2. Other surveys types include *common mid-point (CMP) mode* for calculating velocity, and *transillumination mode*, in which the transmitter and receiver are set up on opposite sides of a medium to "look" through the material (*e.g.* antennas set up on opposite sides of a pillar in a mine shaft to examine fractures). CMP surveying and interpretation are dealt with in a subsequent section, while transillumination surveying is beyond the scope of this paper.

Reflection profiling

Antennae are always kept a set distance apart, usually 1 to 2 m depending on the antennae frequency and survey target. Keeping the antennae close together minimizes near-surface geometric distortion, but may result in interference between the transmitting and receiving antennae. As a general rule of thumb, antennae should be kept apart the same distance as the length of one antenna (i.e. 1 m for 100 MHz, 2 m for 50 MHz etc.). Remember that antennae selection should be made based upon target depth and required resolution. However, as surveying a 200 m line usually requires less than an hour, it does not require significant additional effort re-survey a section with a different set of antennae. Currently available radar units are portable enough to be carried in a backpack; however, many users pull the radar unit and batteries on a sled or in a wheelbarrow. To cover larger areas, radar surveys have been successfully conducted by towing the antennae behind a truck, snowmobile or a all-terrain vehicle. Conducting a survey "on the move" can decrease lateral resolution as the antennae may be moved faster than the unit can collect the data.

Station spacing, or the distance between each collected trace, is also a key parameter to successful GPR surveying, and should be determined by the required horizontal resolution. If the survey target is a continuous reflector that likely does not vary much along its length, then a survey using 1, 2 or even 5 m spacing may be adequate. However, if the survey is attempting to pinpoint small lateral changes in a subsurface reflector, then a station spacing as small as 0.25 m is recommended. As a general rule, if time permits, surveying at 0.25 or 0.5 m station spacing is always beneficial.

Several other factors must be considered when setting up a survey, the most important of which are time window and number of stacks. The *time window* is the length of time that the receiver stays on, or waits for received pulses, from the start of the transmitted pulse. It is suggested that this value be set at least 50% greater than the anticipated depth of penetration (in nanoseconds). Setting this value lower results in smaller data files and slightly faster surveying, yet valuable data may be not collected. It would be wise to collect a few sample traces prior to actual surveying to check depth of signal penetration at a site.

At each survey station, it is advisable to collect more than one trace in a process called *stacking*. Stacking collects numerous traces at one station, and presents the average of these traces as the actual recorded data. Stacking acts to subtract out unwanted random noise, and effectively increases the depth of penetration. Over 2000 stacks can be obtained; however, it is adequate to collect 32 or 64 stacks in most situations (a higher number of stacks increases survey time). The above are simply rules of thumb determined from years of GPR surveying. There are also

geophysical criteria for selecting antenna separation, station spacing, and stacking criteria, all of which are outlined in more detail in Annan (1992).

A survey chain with metre markings should be extended the length of the profile to maintain both antenna separation and station spacing. Surveys can be planned as a single line, multiple lines, or as grids for 3-dimensional surveying (Bridge et al., 1995). Survey lines should generally be as straight as possible, otherwise reflector continuity may be affected. From a starting point of the line, collect one trace before moving both antennas in the same direction (maintaining the same antenna separation) to the next station along the survey line (Fig. 5.5)(the required number of stacks will be collected and stored automatically if properly set in the software). As additional traces are collected, the radar software combines them into a profile, with a horizontal axis of survey position and a vertical axis of two-way travel time.

Note that with most commercially available radar systems, the profile can be viewed on the computer screen as the survey progresses. It is a good idea to check the profile on the screen every so often to make sure that everything is operating correctly (*e.g.* fibre optic cables are not broken and batteries are still good). Each trace is stored on the computer hard drive as it is collected. As the survey progresses, you will want to note the ground conditions over which the survey passes (e.g. slopes, nearby features, vegetation, soils, roads). It is very important to note topography, as corrections can be applied directly to the profile during data processing. At the end of the survey the file is closed and is ready for post-survey processing and plotting.

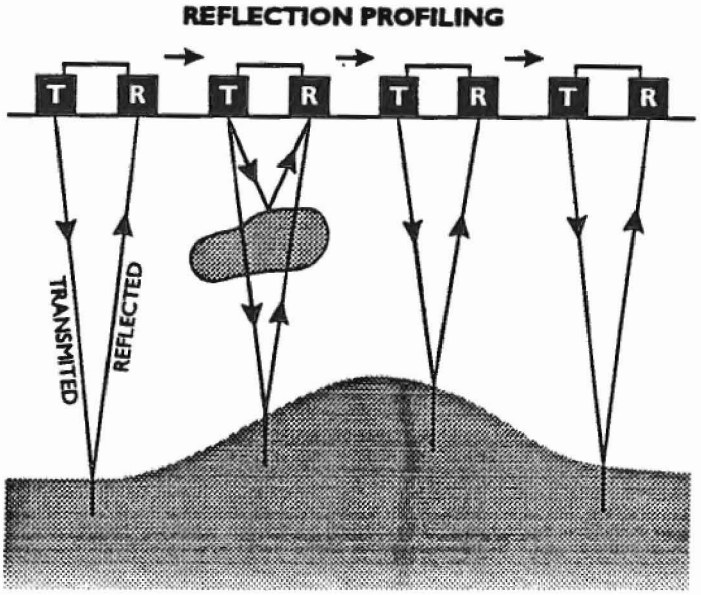

Figure 5.5 *Reflection profiling, in which a trace is collected at a survey station prior to moving both antennas a set distance in the same direction. Separation between transmitter (T) and receiver (R) is also maintained at a set distance. This type of surveying results in a profile such as that in Figure 5.2.*

Common Mid-Point (CMP) velocity surveying

The most common method of calculating velocity is Common Mid-Point (CMP) surveying. CMP sounding is used for obtaining estimates of the radar signal velocity versus depth in the ground by varying antenna separation about a fixed point, and measuring the difference in two-way return time compared to the difference in travel distance. In this manner, GPR CMP surveying is analogous to CMP surveying in the seismic reflection technique (see Chapter 3).

Starting at a fixed mid-point on the surface, each antenna is moved an equal distance in opposite directions from the fixed point, collecting a survey trace at each station before the antennas are moved again (Fig. 5.6). Continue until a suitable number of traces has been collected (usually about 20). The antenna separation at the end of a CMP survey should be 1 to 2 times the target reflector depth. Thus, if the reflector depth is very shallow, the antenna step size should be less than if reflector depth is deep. As the distance from the mid-point is successively increased, reflections from that mid-point will arrive at a later time. With the known increase in distance, and the measured change in two-way travel time, the wave velocity for the material overlying the fixed-point reflector can be calculated. The calculation of velocity is explained in the section on data processing.

It is best to conduct several CMP surveys during the course of a GPR programme, at least one on each survey line and any time a material change is suspected. CMPs should be conducted in areas with flat-lying subsurface features, and should be well away from any potential sources of background "noise" (e.g. transmission wires, buildings). As the antenna separation near the end of a CMP survey is often >10 m, signal response may become weak and the need for a clean signal is paramount.

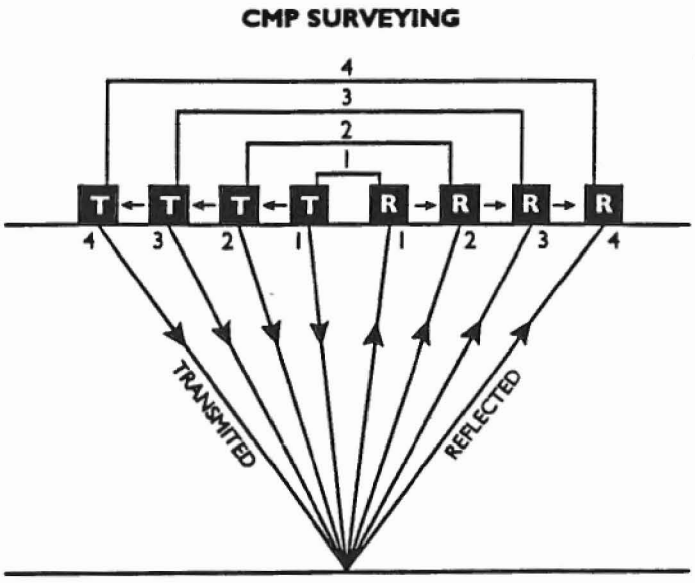

Figure 5.6. *CMP surveying technique, in which the two antennas are moved a set distance in opposite directions between the collection of each trace. This enables the antennas to be centred about a common point, and the velocity can be calculated based on the increase in distance and travel time as the survey progresses.*

Processing GPR data

Remembering that the data as collected only have two-way travel time as a surrogate for actual depth, it is important to calculate velocities from a CMP survey as the first step in data processing. As the radar data produced in a survey is digital, post-survey processing can then be applied to the data to enhance the survey results prior to plotting.

CMP velocity calculation

A simple plot of the CMP profile should be printed out, without any trace-to-trace filters but with some gain applied. The resulting plot has antenna separation (m) on the horizontal axis and two-way travel time (ns) on the vertical axis (Fig. 5.7). The uppermost dipping reflector represents the air wave, and in all cases has a velocity of 0.3 m/ns. The ground wave follows the air wave, but the lower velocity results in a steeper dip. In the case of deeper reflectors, radar geometry causes the waves reflected from the common source to form one limb of a hyperbola (Fig. 5.7a). The basic interpretation for estimating the velocity of the material above the reflector is to plot (travel time)^2 vs. (antenna separation)^2. This yields a straight line relationship with the velocity (in m/ns) being the square root of the rate of change of return time with increasing antenna separation (Fig. 5.7b). Remember that when using a calculated velocity to estimate reflector depth, the antenna-reflector geometry and the fact that plotted times are *two-way travel times* must be taken into account. The measured velocity is then entered into the radar plotting program, which places a depth scale on the printout.

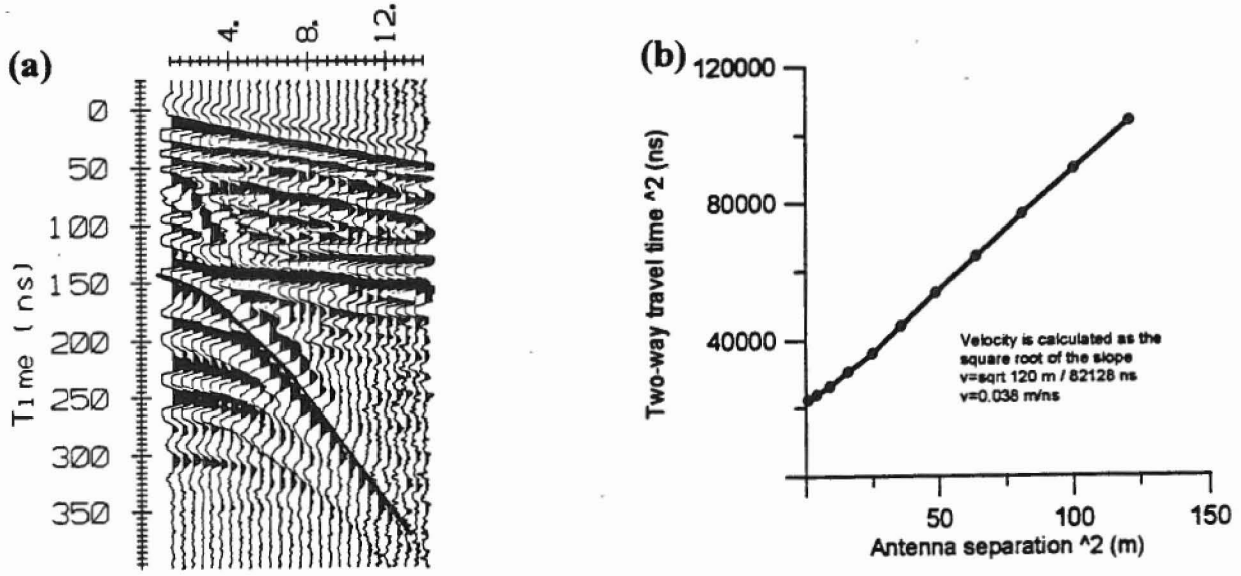

Figure 5.7. *A typical CMP profile (a) from an unfrozen peatland. The velocity can be calculated by plotting antenna separation squared vs. two-way travel time squared (b) for the steeply dipping marked reflector, in this case representing the peat-mineral contact. The velocity is the square root of the rate of change in time with increasing separation, in this case 0.038 m/ns. This value represents an average velocity of all of the peat between the surface and the mineral contact.*

Processing parameters

The most commonly utilized processing parameters are gains, topographic corrections, and spatial and temporal filters. More advanced processing can be obtained in some cases with the radar software, but more often through exporting data to a seismic processing software package.

Gains

Raw GPR data results often show very few deep reflectors until some processing has been applied. In order to account for the rapid attenuation of the signal with depth (or down the trace), the *gain function* can be utilized to increase the amplitude of deeper reflectors (Fig. 5.8). Automatic gain control (AGC) is a commonly used gain function, and is analogous to Time Variable Gain in acoustic data recording (Chapter 6). With AGC function, the objective is to equalize reflector amplitudes all the way down the radar trace. Therefore, the gain is large in sections of the trace with a weak signal and small in areas where the signal is already strong. This and other gain functions are ideal for monitoring the continuity of reflectors, but remember that the original relative relationships between reflector amplitudes is eliminated. Other gain functions are available, including a constant gain (CONST) which maintains reflector amplitudes, and simple exponential function (SEC). The choice and strength of gains to be applied is generally through trial and error, unless the need for maintaining relative reflector amplitudes is paramount.

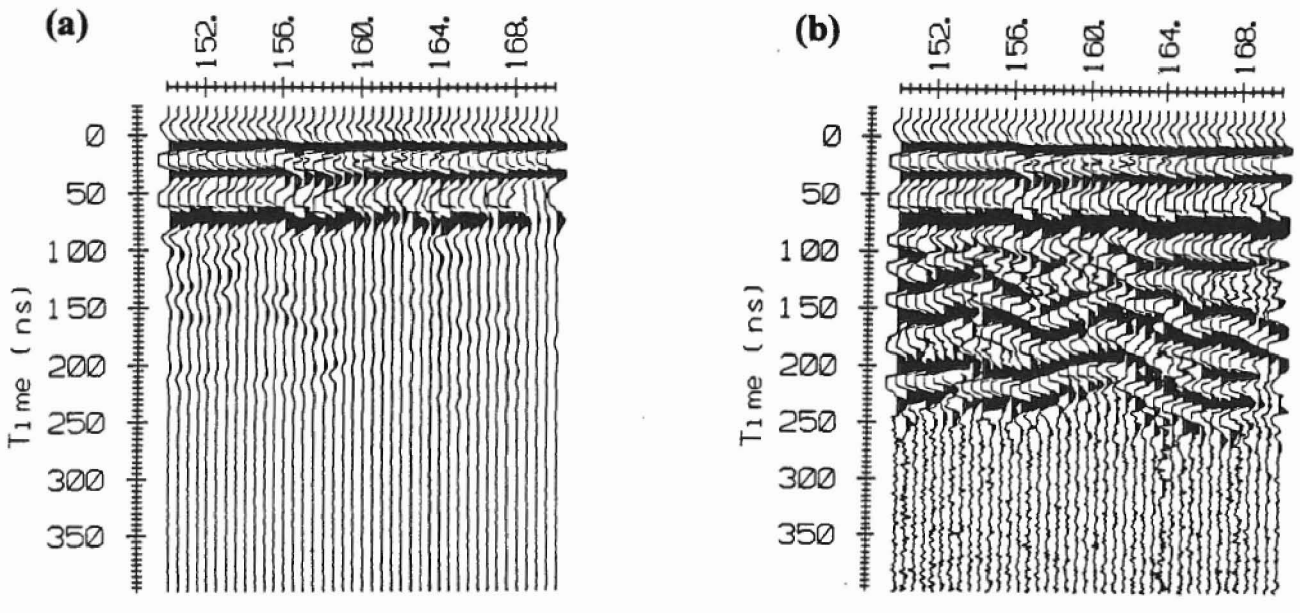

Figure 5.8 *The same raw data file without (a) and with (b) gain functions (AGC).*

Topographic corrections

Small variations in surface topography can distort subsurface reflectors until topographic data are incorporated into the plot. The actual processing of a topographic file is beyond the scope of this paper; however, it is a good idea to take topographic notes in the field for later data entry. In many cases reflector patterns change dramatically once the topography has been added (Fig. 5.9). Several of the case studies presented show the effects of incorporating topography.

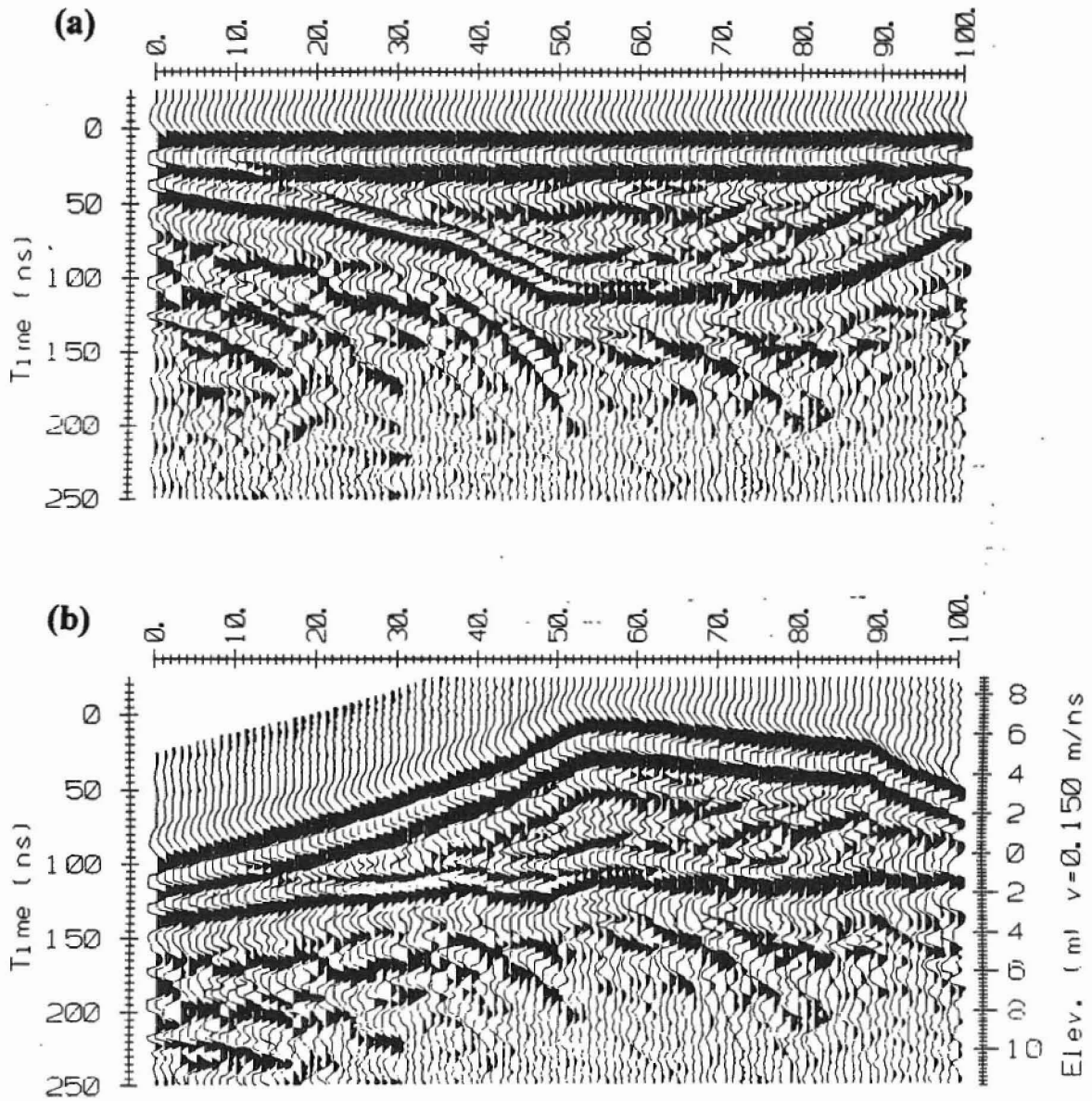

Figure 5.9 *The same data file without (a) and with (b) the application of topography. This example is from a sand dune developed upon glaciolacustine silt and clay, near Fort Simpson, N.W.T. Note that without topography, reflectors that are in fact flat-lying will plot as the inverse of true topography. Source: Robinson and Kettles (unpublished data).*

Spatial and temporal filters

Spatial filters add two or more adjacent traces and average them, resulting in a decrease in random signal noise, and improved continuity of nearly flat-lying reflectors. As this type of filtering tends to enhance flat-lying reflectors, it should not be used in CMP surveys or where the survey objective involves the delineation of dipping or wavy reflectors. *Temporal filters* (also called down-trace averaging) compute a running average of a series of points within the same trace, again resulting in a decrease in random background noise. Care must be taken with these filters not to average too many points as this results in decreased resolution.

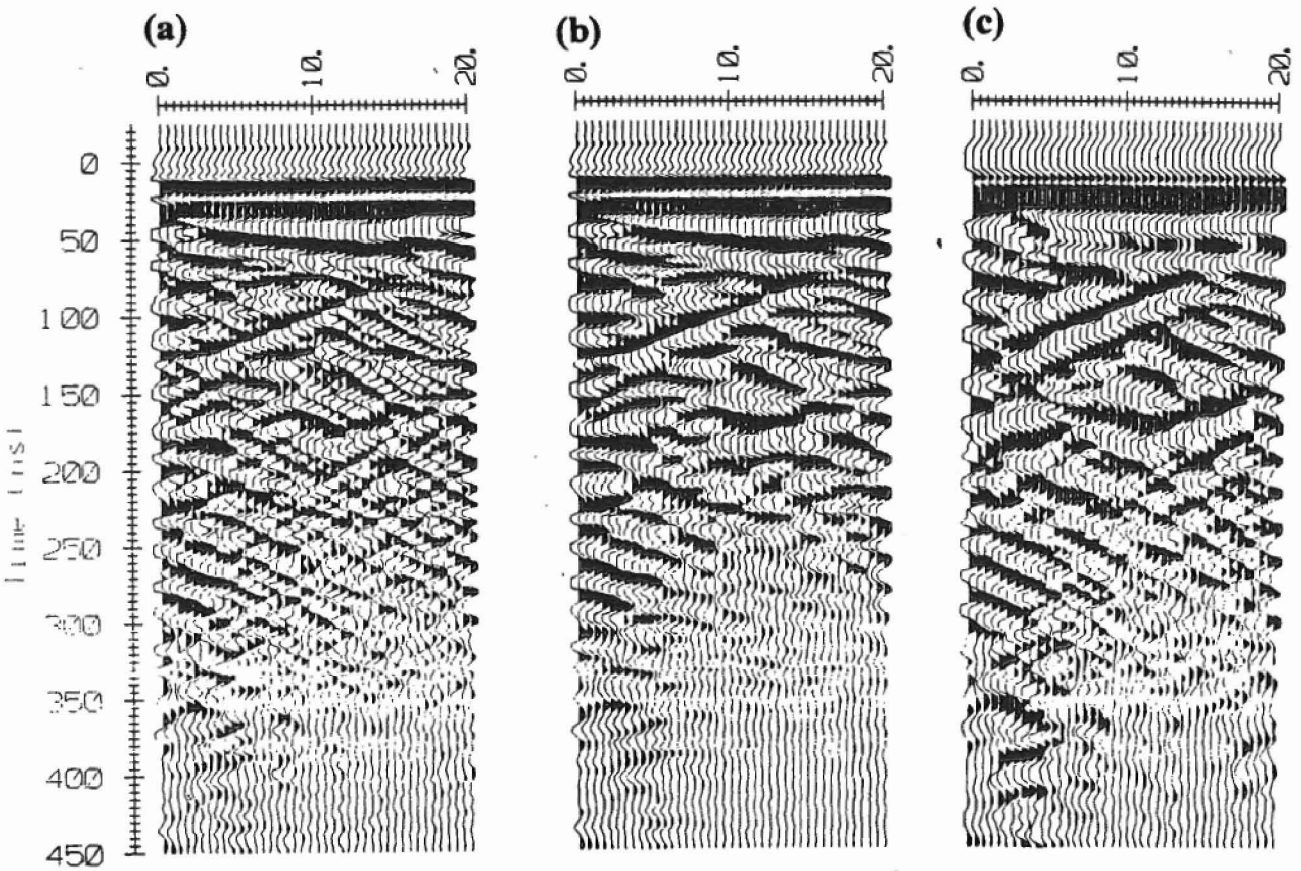

Figure 5.10. *A datafile with only gains applied (a), spatial filtering (b) through the addition and averaging of 4 adjacent traces, and temporal filtering (c) through the averaging of 10 points down the trace.*

Profile plotting

Once all the filters and signal gains have been adequately adjusted and the velocity has been calculated, the profile can be plotted. The plotting software includes numerous parameters for plot size, spacing, axes positions, and other layout features. Plots of different profiles can be merged, or only certain positions or time sections of profiles can be plotted. The finished plot is now ready for interpretation.

GPR data interpretation

The interpretation of radar results is often a very subjective activity in that it depends greatly upon the aims and experience of the individual doing the interpretation. For example, a hydrogeologist may be only interested in delineating the water table, whereas a sedimentologist has a greater interest in the surrounding stratigraphy.

Based upon an understanding of the preceding outline of the principles of GPR, it should be simple to interpret a GPR survey. However, there are several items not covered in the previous discussion that should be elucidated here. Interpretation skills will also be improved through the examination of case studies presented in the following section.

Air and ground wave reflectors

The first two reflectors to appear in a radar trace are the air and ground wave, respectively. The air wave results from energy that passes through the air (V=0.3 m/ns) between the transmitting and receiving antennas. As such it is not a true reflector, but serves as a zero-time marker for the profile. The ground wave results from energy that travels between the transmitter and receiver along the surface of the ground, and at the velocity of the ground. Thus, the ground wave arrives slightly later than the air wave; however, if the ground velocity is high then the two waves may appear as one. Only reflectors that arrive after these two can be considered true reflectors, in that they document changes within the ground.

Hyperbolic reflectors

The energy transmitted from a radar antenna is dispersed in all directions, not just directly downwards. Thus, it is possible for the radar to "see" an object before it passes directly over that object. In these cases, the reflector from a distant object appears in earlier (and later) traces but at greater apparent depths, with the apparent depth decreasing as the object is approached. The two "approach limbs" form a hyperbolic reflector, with the object actually being located at the crest of the hyperbola. This effect is common with strong point-source reflectors such as buried pipes or drums. Linear near-vertical boundaries may also result in hyperbolic reflectors. Note the hyperbolic reflector caused by a buried pipeline in Figure 5.4.

Multiples

The bouncing back-and-forth of energy between reflectors and the ground surface often creates multiple reflectors that are in fact the product of one reflector. These multiples often overwhelm other returns and can be picked out as they should be exact copies of the original reflector, and occur at regular intervals down the trace.

The need for ancillary data

For confident interpretations of radar profiles, ancillary data in the form of borehole logs, soil pits, cut banks, or complementary geophysical data are almost always required. In peatlands, it has been found that simple coring for stratigraphy combined with bulk density and moisture content determinations can aid greatly in determining the source of reflectors. Once the source of the reflectors has been determined from the cores, radar provides a tool for tracing reflectors over larger areas. Much of the work mapping permafrost distribution along the Norman Wells pipeline relied upon borehole logs and ground temperature measurements to provide extremely important backup for the radar interpretations.

Critical aspects of data interpretation

Based upon the outline in Annan (1992), the following are critical aspects of data interpretation:

1. Have a good understanding of the survey objective.
2. Develop a model of the geological setting.
3. Establish an estimate of velocity and attenuation (or depth of penetration).
4. Develop a scenario for the expected radar response (*e.g.* slowly varying continuous events for a geologic horizon, or a spatially limited diffraction hyperbola for a pipe). If possible, process the data to enhance the type of response expected and emphasize the survey objectives.
5. Correlate radar data with geologic control and ground-truth data such as borehole logs.
6. Plot radar anomalies on a plan map to permit the correlation of multiple radar lines.
7. Plan drilling or follow up control work.

Case studies

In the following pages several sample data sets are presented based upon the work of the authors and others (Figs. 5.11-5.21). Profiles contain captions to help explain the interpretations, and in many cases annotated interpretation drawings are included. These examples have been selected to highlight many of the different applications that ground penetrating radar has in geomorphological field work. Many of the examples are also discussed in Table 5.2.

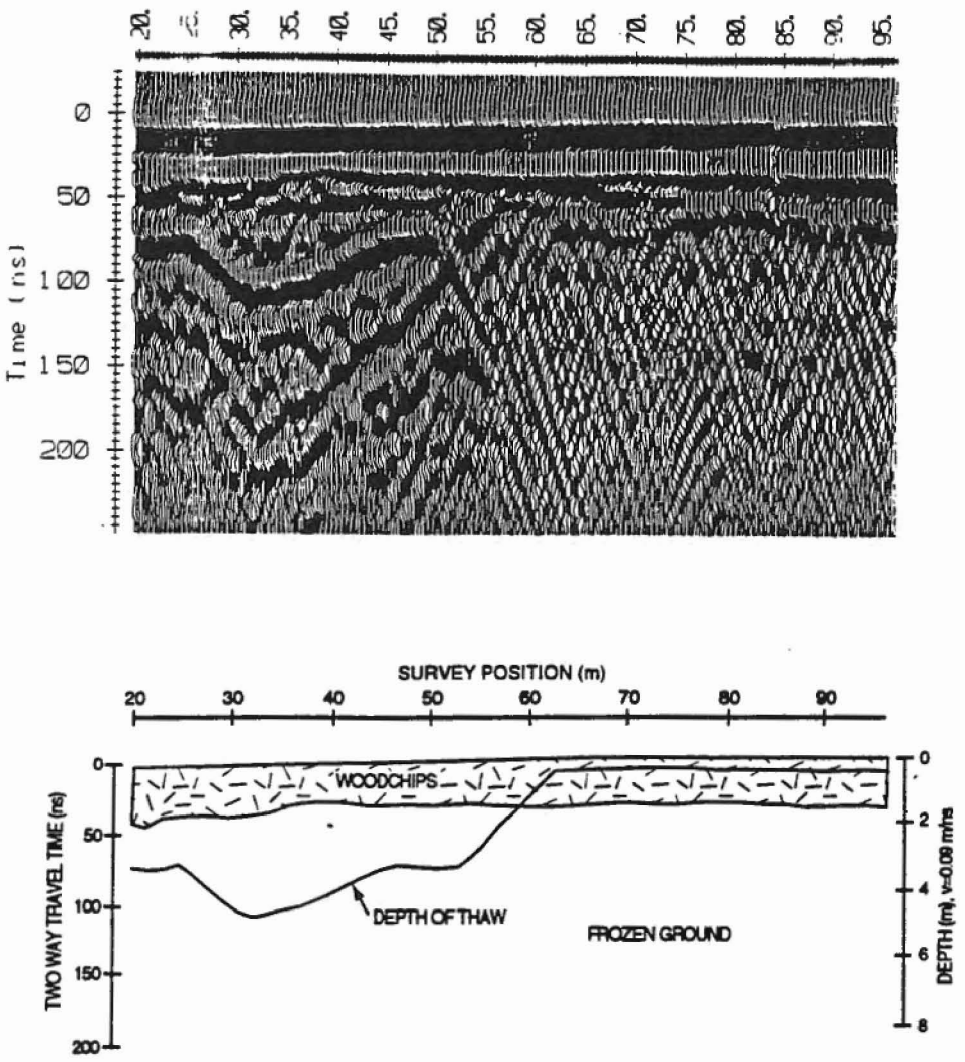

Case study 1

Figure 5.11 *This figure shows a 50 MHz survey down a woodchip insulated slope on the Norman Wells pipeline, N.W.T. During pipeline construction and operation, removal of vegetation and the emplacement of a relatively warm oil-filled pipe required remediation techniques to preserve permafrost on thaw-sensitive slopes. Thus, a 1 to 2 m thick layer of woodchips was placed on the slope as a natural insulator. Although no topographic corrections have been applied to this profile, the profile dips to the right about 8°. Figure 5.11 shows the dramatic difference in radar returns from a section of the slope where thaw has progressed up to depths of 4 m (20 to 55 m) and a section of the woodchip-insulated slope that has maintained permafrost (60 to 96 m). Note that only shallow seasonal active layer development is present in the section with permafrost maintained within the woodchips. The strong cross-hatching pattern found beneath sections of the slope interpreted to be frozen is likely caused by ice lensing in the frozen clay, and has been used as an indicator of the presence of permafrost along the pipeline route. Interpretations were aided by thaw probing, borehole logs and ground temperature measurements in the boreholes. Woodchip thickness is also interpreted. Figure 5.11 source: Burgess et al. (1995) and Robinson and Moorman (1995).*

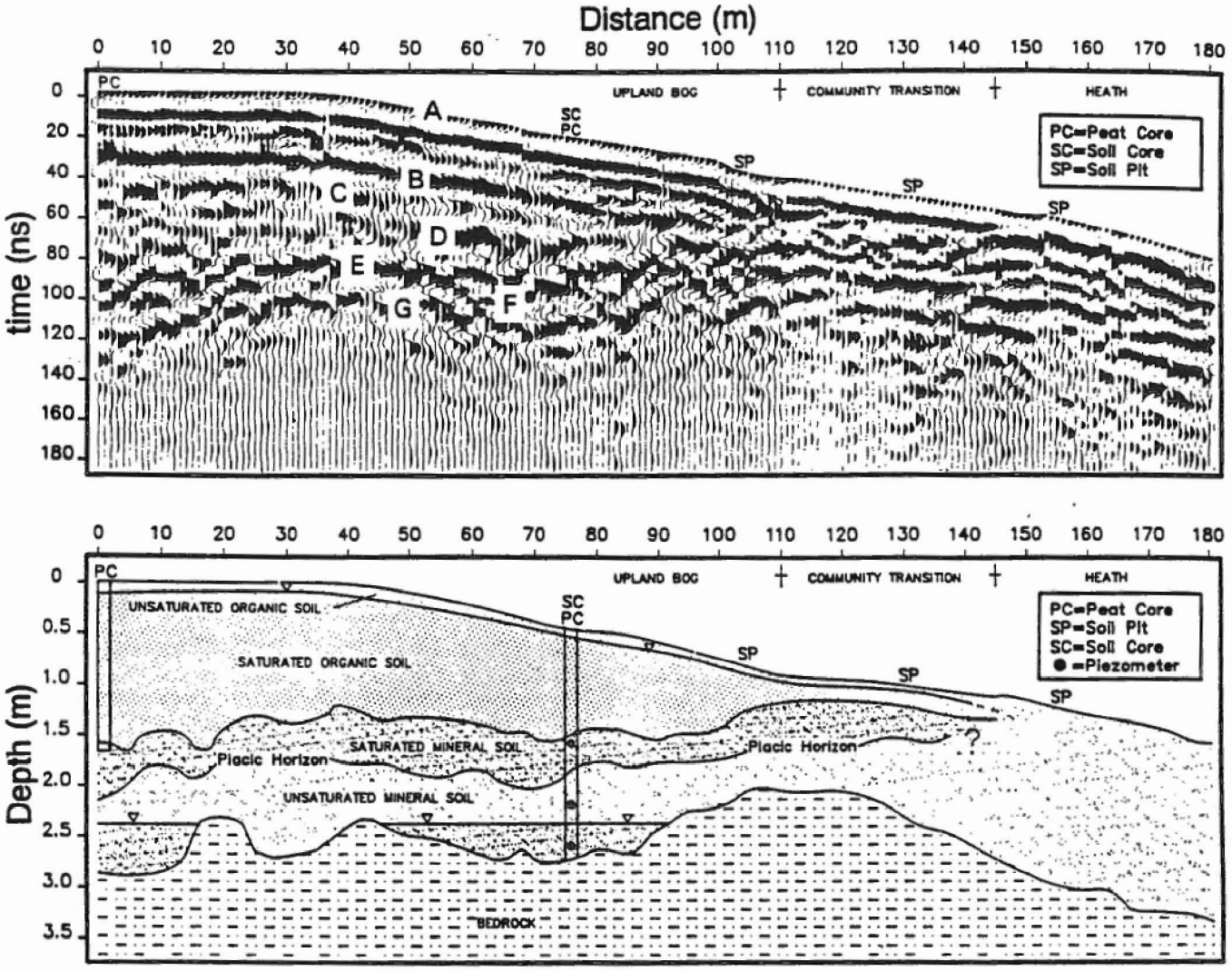

Case study 2

Figure 5.12 *A radar profile and interpretation diagram from a 100 MHz radar survey delineating blanket bog peat and underlying mineral horizons from southeastern Newfoundland. Reflections are interpreted as A = soil surface, B and C = possible water content interfaces in peat, D = organic - mineral soil contact, E = plagic horizon (saturated mineral soil - unsaturated mineral soil contact), F = water table, and G = mineral soil - bedrock contact. Note that interpretations were aided by supplementary information from soil pits, coring, and a piezometer installation. Figure 5.12 source: Lapen et al. (1996).*

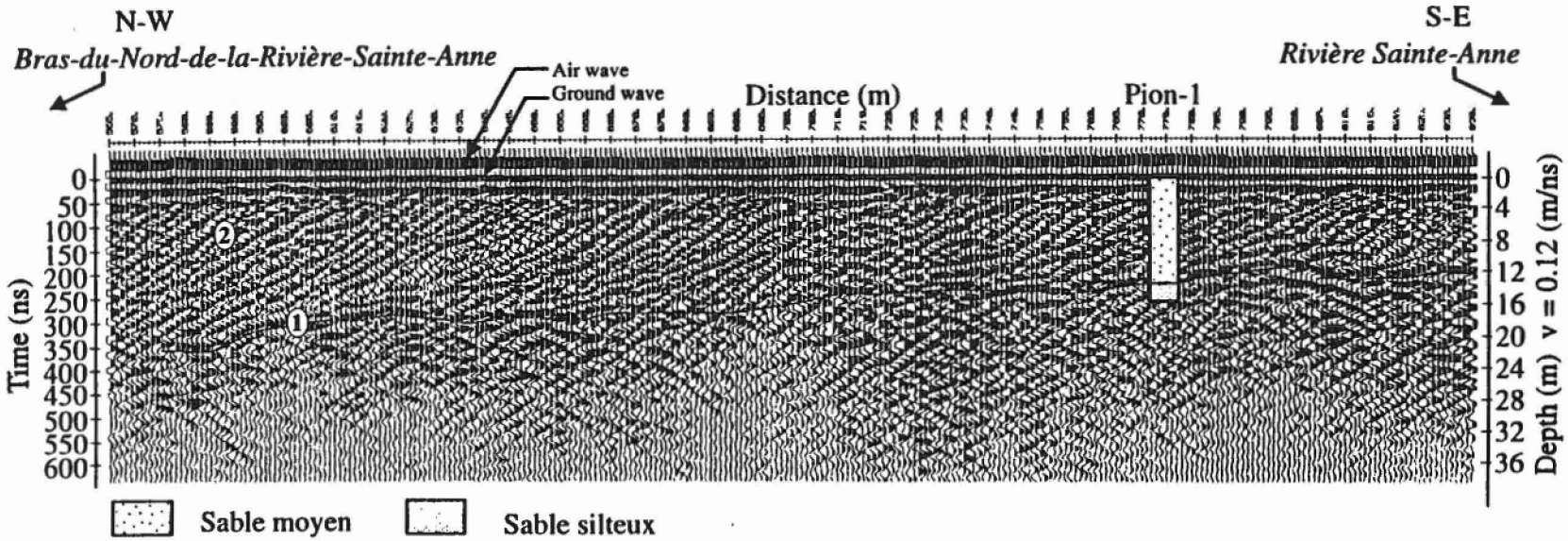

Case study 5

Figure 5.15 *This profile represents a 50 MHz survey in deltaic sand along the Saint-Anne River in Saint Raymond, Québec. Note a stratigraphic contact (reflector 1) and foreset bedding in the upper unit (reflector 2). Figure 5.15 source: Michaud et al. (1997).*

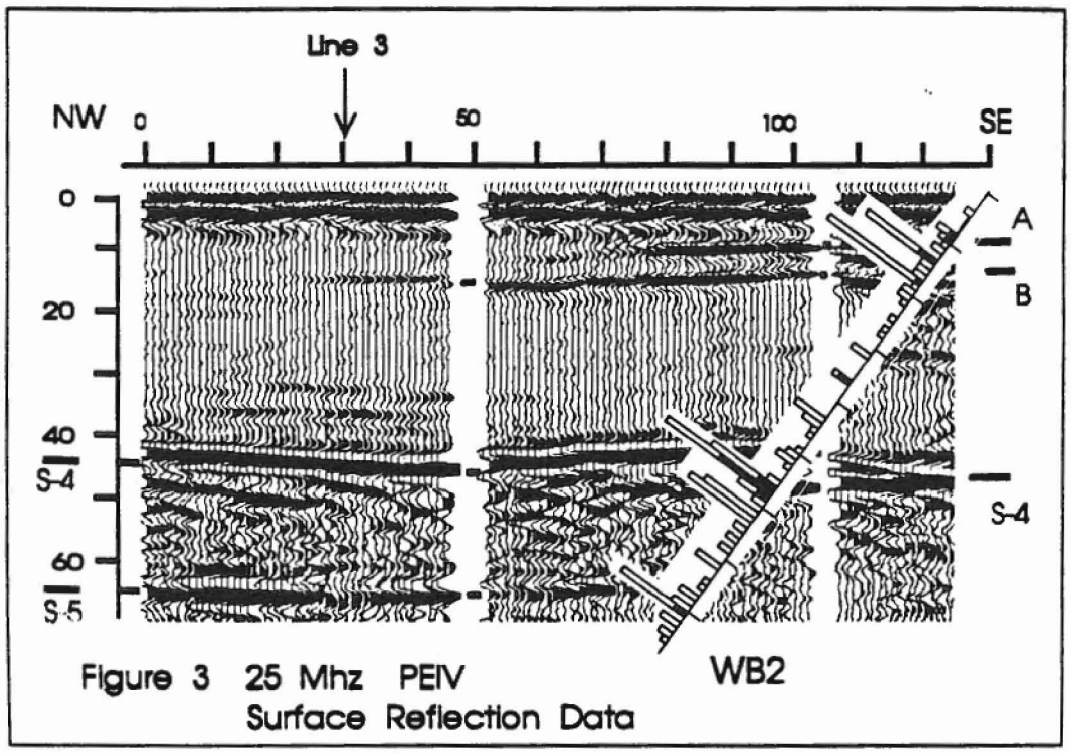

Case study 6

Figure 5.16 *This plot represents a 25 MHz survey conducted to map fractures at depths up to 70 m within granitic bedrock, southeastern Manitoba. The bar graph represents the number of fractures per metre in a borehole (filled bars are open fractures). High velocities (0.12 to 0.125 m/ns) and very low attenuation result in extremely deep signal penetration. Figure 5.16 source: Holloway (1992).*

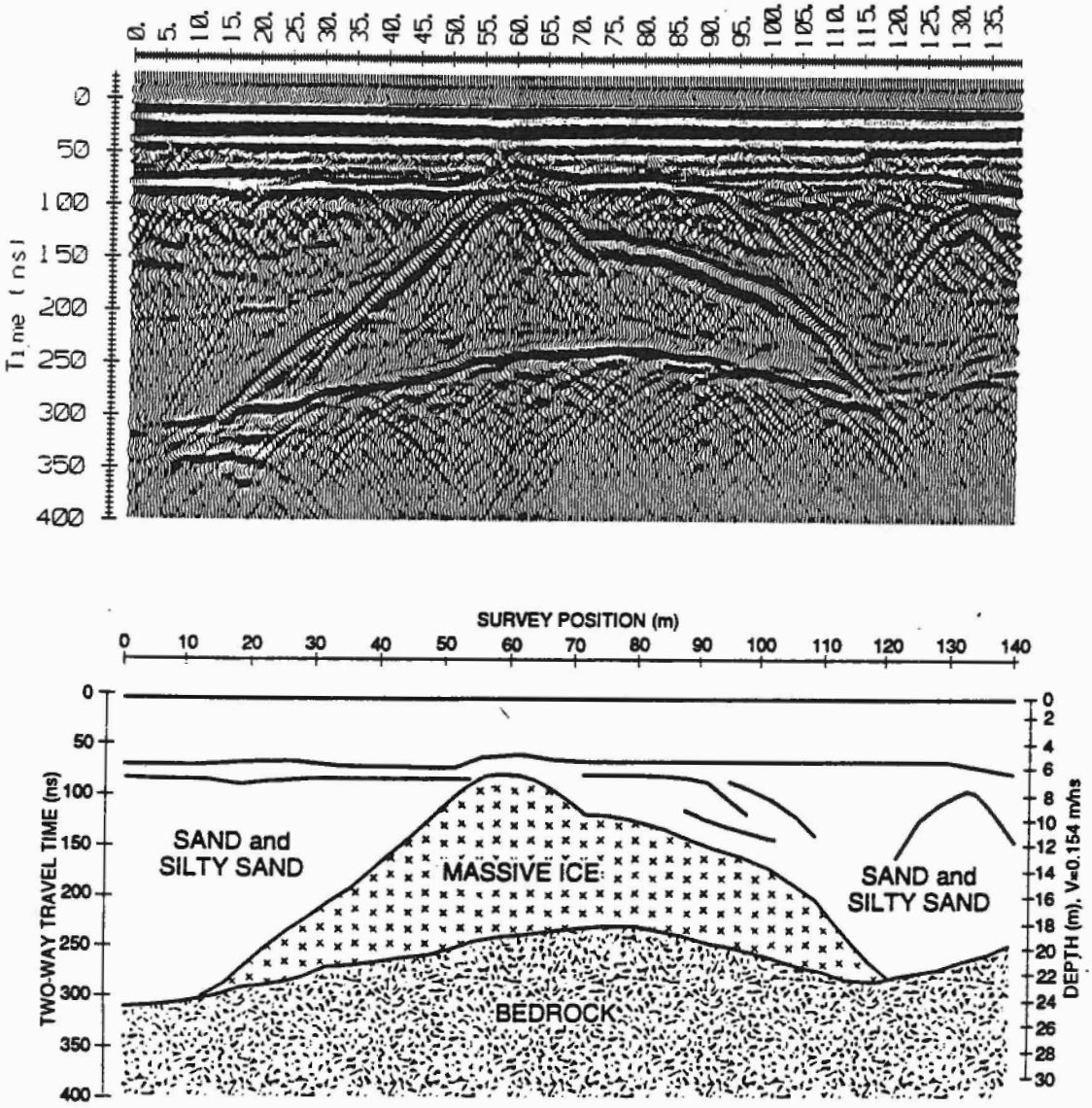

Case study 7

Figure 5.17 *A 50 MHz profile outlining massive ground ice, enclosing frozen sand and silty sand, and underlying bedrock near Contwoyto Lake, Northwest Territories. The presence of a large ice body was confirmed through drilling, however, the increased strength and doming (higher velocity through ice) of the bedrock reflector beneath are also indications that the signal has passed through a material that is of lower attenuation and higher velocity than the surrounding sediments. Note the high average profile velocity (0.154 m/ns) in permafrost. Figure 5.17 source: modified from Wolfe et al. (1997).*

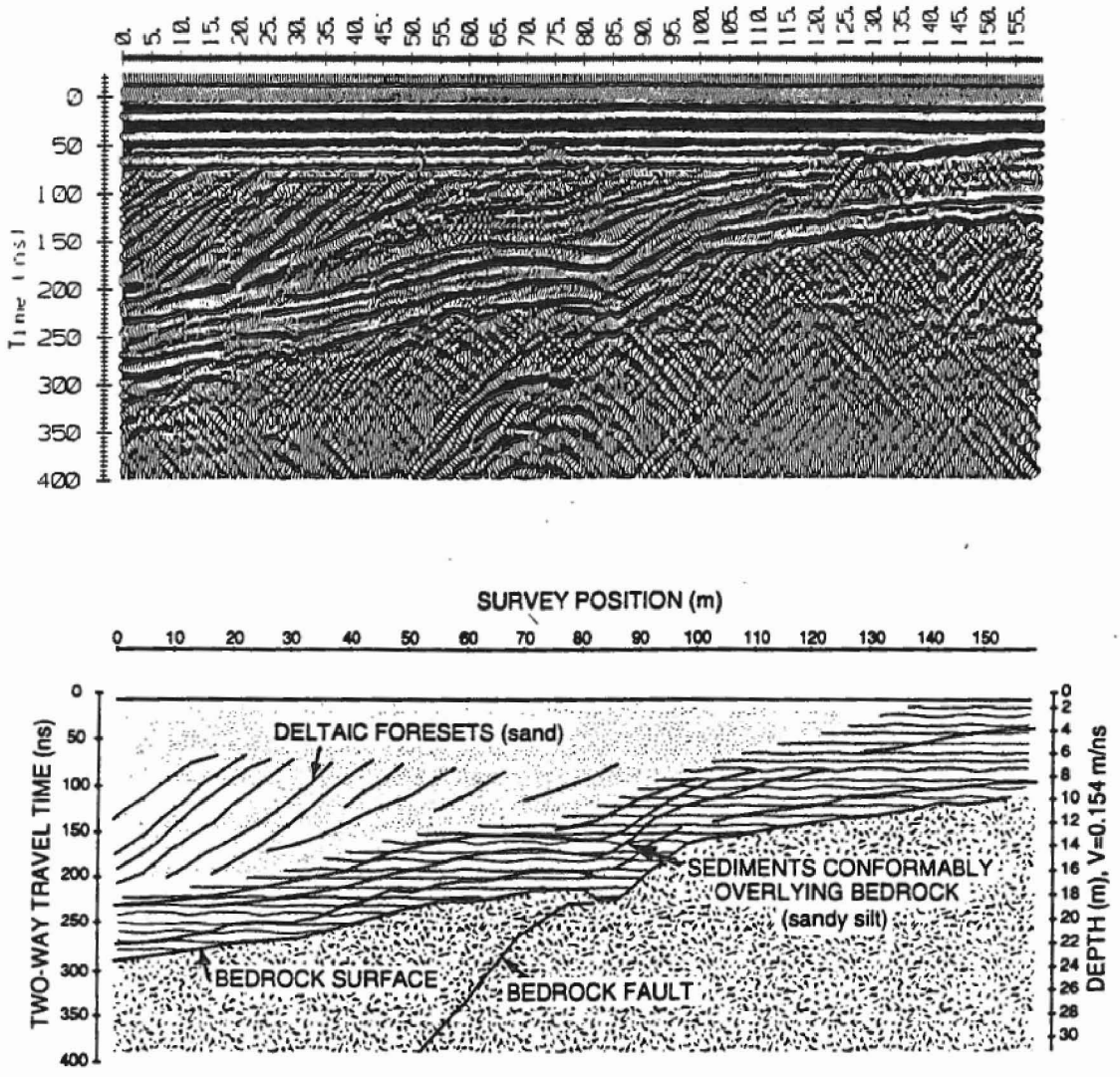

Case study 8

Figure 5.18 *A 50 MHz profile from a frozen esker-outwash complex near Contwoyto Lake, Northwest Territories. Two different sedimentary units are clearly visible in this profile; an upper sandy deltaic unit with prominent foresets, and an underlying sandy silt with bedding conformable with underlying bedrock. Also note the steeply dipping bedrock fault and the hyperbolic reflector caused by a buried boulder at the 129 m position. Figure 5.18 source: modified from Wolfe et al. (1997).*

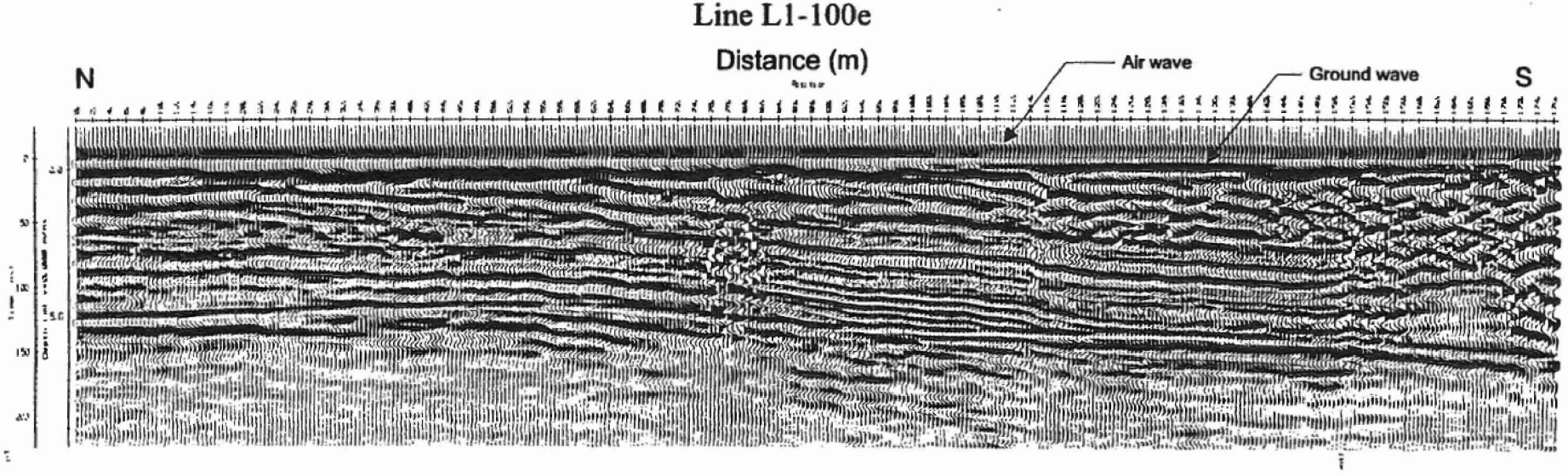

Case study 9

Figure 5.19 *This survey was conducted to determine stratigraphy underlying property owned by an aluminum plant in Québec. The near-surface material consists of fine sand over silt, and all underlain by clay. Note the rapid signal attenuation in clay beneath 5 m, and the presence of a buried concrete pipe at the 78 m position. Figure 5.19 source: Hamel (1997).*

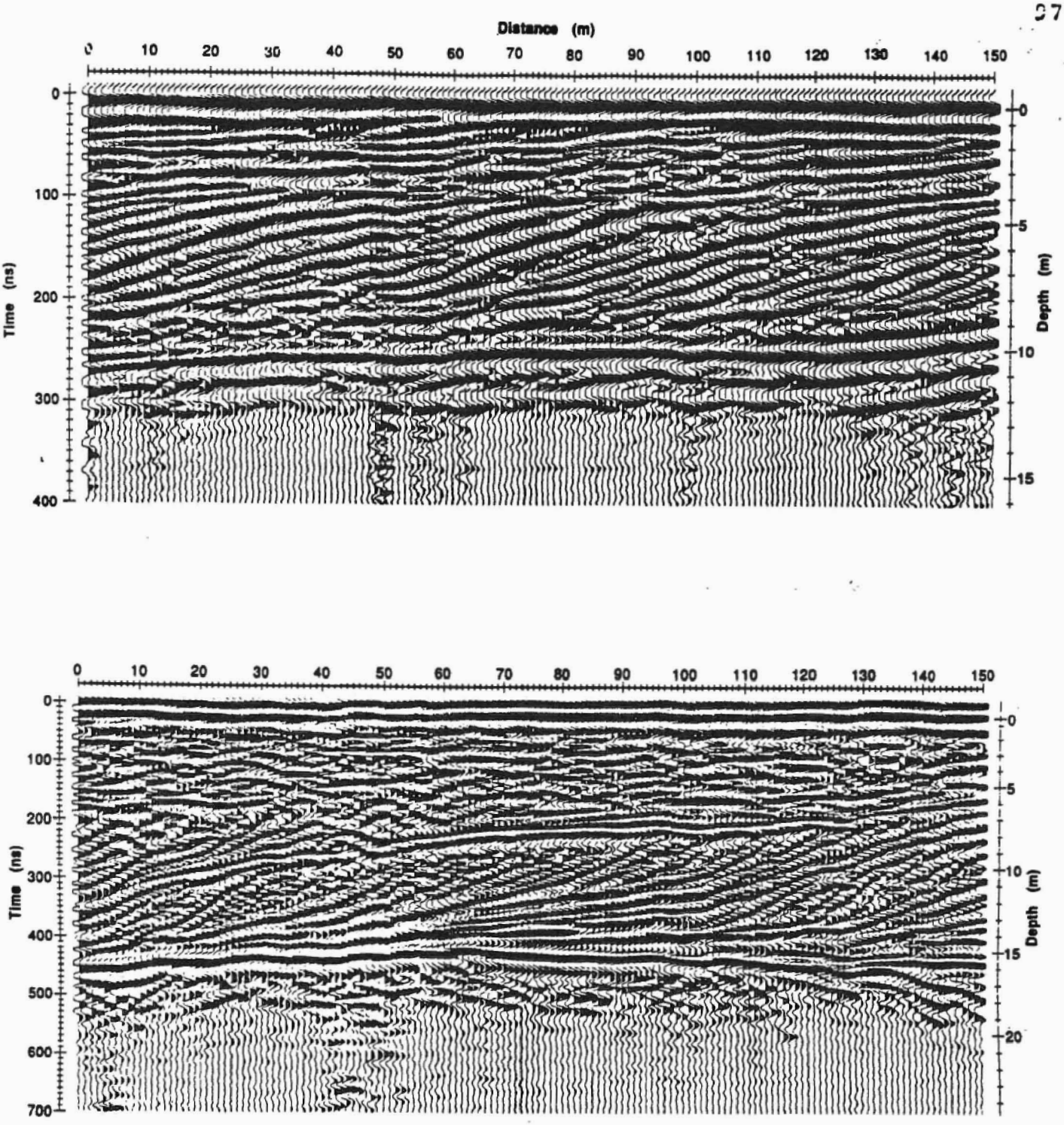

Case study 10

Figure 5.20 *a) GPR profile of the modern Sandy Point spit along the depositional dip, Lake Athabaska, northeastern Alberta. b) 100 MHz profile along the depositional dip of the modern, wave-influenced Williams River delta, Lake Athabaska, northern Saskatchewan. Figure 5.20 source: Jol and Smith (1992).*

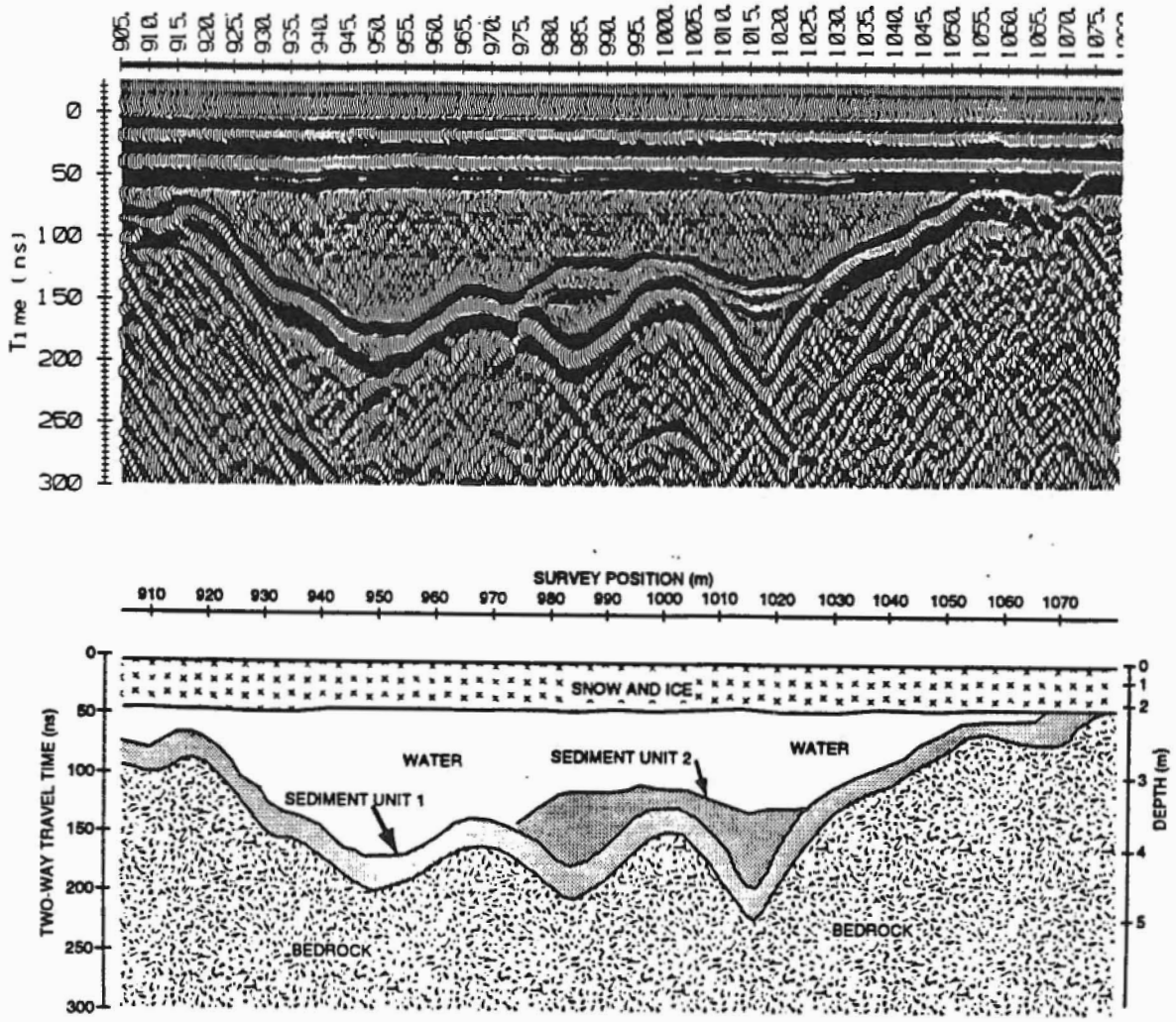

Case study 11

Figure 5.21 *This figure presents a 50 MHz profile and interpretation schematic over a shallow frozen pond near Contwoyto Lake, Northwest Territories. Note the prominent reflectors indicating the base of seasonal ice cover, two distinct sedimentary units and the bedrock surface. Fracturing within the near-surface bedrock causes distinctive hyperbolic reflectors. Also note the variable depth scale, with a velocity of 0.16 m/ns applied for the pond ice and 0.03 m/ns in the water column. Experience suggests that ponds can be profiled with success if the water depth is < 10 m, and the water is of low conductivity and non-turbulent. Figure 5.21 source: Robinson, Burgess, and Wolfe (unpublished data).*

REFERENCES

Annan, A.P.

1992: Ground penetrating radar workshop notes; Sensors and Software Inc., Mississauga, Ontario.

Annan, A.P., and Davis, J.L.

1977: Radar range analysis for geological materials; in Current Research, Part B; Geological Survey of Canada, Paper 77-1B, p. 117-124.

1976: Impulse radar sounding in permafrost; Radio Science, v. 11, p. 383-394.

Arcone, S.A., Lawson, D.E., Delaney, A.J., Strasser, J.C., and Strasser, J.D.

1998: Ground-penetrating radar reflection profiling of groundwater and bedrock in an area of discontinuous permafrost; Geophysics, v. 63, p. 1573-1584.

Behrendt, J.C., Drewry, D., Jankowski, E., and England, A.W.

1979: Aeromagnetic and radar ice sounding indicate substantially greater area for Dufek Intrusion in Antarctica; American Geophysical Union Transactions, v. 60, p. 245.

Bently, C.R., Clough, J.W., Jezek, K.C., and Shabatie, S.

1979: Ice thickness patterns and the dynamics of the Ross Ice Shelf, Antarctica; Journal of Glaciology, v. 24, p. 287-294.

Bridge, J.S., Alexander, J., Collier, R.E.L., Gawthorpe, R.L., and Jarvis, J.

1995: Ground penetrating radar and coring used to study the large-scale structure of point-bar deposits in three dimensions; Sedimentology, v. 42, p. 839-852.

Burgess, M.M., Robinson, S.D., Moorman, B.J., Judge, A.S., and Fridel, T.W.

1995: The application of ground penetrating radar to geotechnical investigations of insulated permafrost slopes along the Norman Wells pipeline; Proceedings, 48th Canadian Geotechnical Conference, Vancouver, B.C., p. 999-1006.

Clasen, M.J.

1989: Application of alternative surface geophysical techniques to hydrogeologic surveys; Unpublished M.Sc. thesis, University of South Florida, Tampa.

Collins, M.E. and Doolittle, J.A.

1987: Using ground-penetrating radar to study soil microvariability; Soil Science Society of America Journal, v. 50, p. 408-412.

Dallimore, S.R. and Davis, J.L.

1992: Ground penetrating radar investigations of massive ground ice; in Ground Penetrating Radar, (ed.) J. Pilon; Geological Survey of Canada, Paper 90-4, p. 41-48.

Daniels, J.J., Gunton, D.J., and Scott, H.F.

1988: Introduction to subsurface radar; Proceedings, Institute of Electrical and Electronics Engineers, v. 135 (#F4), p. 277-320.

Davis, J.L. and Annan, A.P.

1992: Applications of ground penetrating radar to mining, groundwater, and geotechnical projects: selected case histories; in Ground Penetrating Radar, (ed.) J. Pilon; Geological Survey of Canada, Paper 90-4, p. 49-55.

1989: Ground penetrating radar for high-resolution mapping of soil and rock stratigraphy; Geophysical Prospecting, v. 37, p. 531-551.

Dominic, D.F., Egan, K., Carney, C., Wolfe, P., and Boardman, M.R.

1995: Delineation of shallow stratigraphy using ground penetrating radar; Journal of Applied Geophysics, v. 33, p. 167-175.

Doolittle, J.A.

1982: Characterizing soil map units with the ground-penetrating radar; Soil Survey Horizons, v. 23, p. 3-10.

Evans, S.

1963: Radio techniques for the measurement of ice thickness; Polar Record, v. 11, p. 406-410.

Fisher, T.G., Jol., H.M., and Smith, D.G.

1995: Ground-penetrating radar used to assess aggregate in catastrophic flood deposits, northeast Alberta, Canada; Canadian Geotechnical Journal, v. 32, p. 871-879.

Hamel, P.-A.

1997: Caracterisation de la stratigraphie sur le territoire de l'aluminerie Lauralco, Deschambault, MRC de Portneuf; Memoire de baccalaureat., Université Laval, Departement de Geographie, Québec.

Hanninen, P.

1992: Application of ground penetrating radar and radio wave moisture probe techniques to peatland investigations; Geological Survey of Finland Bulletin, v. 1, 71 p.

Holloway, A.L.

1992: Fracture mapping in granite rock using ground probing radar; in Ground Penetrating Radar, (ed.) J. Pilon; Geological Survey of Canada, Paper 90-4, p. 85-100.

Horvath, C.L.

1998: An evaluation of ground penetrating radar for investigation of palsa evolution, Macmillan Pass, Northwest Territories; M.Sc. thesis, University of Alberta, Edmonton, Alberta.

Jol, H.M.

1995: Ground penetrating radar antennae frequencies and transmitter powers compared for penetration depth, resolution, and reflection continuity; Geophysical Prospecting, v. 43, p. 693-709.

Jol, H.M. and Smith, D.G.

1995: Ground penetrating radar surveys of peatlands for oil field pipelines in Canada; Journal of Applied Geophysics, v. 34, p. 109-123.

1991: Ground penetrating radar of northern lacustrine deltas; Canadian Journal of Earth Sciences, v. 28, p. 1939-1947.

Kettles, I.M. and Robinson, S.D.

1996: A ground penetrating radar study of peat landforms in the discontinuous permafrost zone near Fort Simpson, Northwest Territories, Canada; in Northern Forested Wetlands: Ecology and Management, (ed.) C. Trettin; CRC Press, Boca Raton, Florida, p. 147-159.

Lapen, D.R., Moorman, B.J., and Price, J.S.

1996: Using ground penetrating radar to delineate subsurface features along a wetland catena; Soil Science Society of America Journal, v. 60, p. 923-931.

Lawson, D.E., Arcone, S.A., and Collins, C.M.

1991: Geophysical investigations of an anomalous unfrozen zone, Caribou Peak, Alaska; U.S. Army Corps of Engineers, Cold Regions Research and Engineering Laboratory, Report 91-17.

Lowe, D.J.

1985: Application of impulse radar to continuous profiling of tephra-bearing lake sediments and peats: an initial evaluation; New Zealand Journal of Geology and Geophysics, v. 28, p. 667-674.

McCann, D.M., Jackson, P.D., and Flemming, P.J.

1988: Comparison of the seismic and ground probing radar methods in geological surveying; Institute of Electrical and Electronics Engineers, Proceedings F, Communications, Radar and Signal Processing, v. 135, p. 380-390.

Michaud, Y., Allard, M., Parent, M., Paradis, S.J., Menard, E., Fortin, M, and Begin, C.

1994. Cartographie preliminaire des zones pergelisolees dens le secteur du detroit de Manitounuk et de la Petite riviere de la Baleine, Hudsonie. Commission geologique du Canada, Dossier public 2845.

Michaud, Y, Fortier, R., Parent, M., and Pilon, J.

1997: L'utilisation du géoradar et des méthodes électriques pour la cartographie des formations aquifères du piémont laurentien, Québec; in Current Research, 1997-E, Geological Survey of Canada, Paper 97-1E, p. 73-82.

Moorman, B.J. and Michel, F.A.

1997: Bathymetric mapping and subbottom profiling through lake ice using ground penetrating radar; Journal of Paleolimnology, v. 18, p. 61-73.

Olsen, H. and Andreason, F.

1995: Sedimentology and ground-penetrating radar characteristics of a Pleistocene sandur deposit; Sedimentary Geology, v. 99, p. 1-15.

Parent, M. and Michaud, Y.

1996: Dynamique littorale de la presqu'ile de Penouille, Parc National Forillon; Rapport a l'intention de Parcs Canada, Québec.

Peters, L., Daniels, J.J., and Young, J.D.

1994: Ground penetrating radar as a subsurface environmental sensing tool; Proceedings, Institute of Electrical and Electronics Engineers, v. 82, p. 1802-1821.

Robinson, S.D.

1994: Geophysical studies of massive ground ice, Fosheim Peninsula, Ellesmere Island, N.W.T.; in Current Research, 1994-B, Geological Survey of Canada, Paper 94-1B, p. 11-18.

1993: Geophysical and geomorphological investigations of massive ground ice, Fosheim Peninsula, Ellesmere Island, Northwest Territories; unpublished M.Sc. thesis, Queen's University, Kingston, Ontario.

Robinson, S.D. and Moorman, B.J.

1995: Six years of ground penetrating radar surveys along woodchip insulated slopes, Norman Wells pipeline; Geological Survey of Canada, Open File Report 3094.

Smith, D.G. and Jol, H.M.

1992: Ground penetrating radar investigations of a Lake Bonneville delta, Provo level, Brigham City, Utah; Geology, v. 20, p. 1083-1086.

Stevens, K.M., Lodha, G.S., Holloway, A.L., and Soonwalla, N.M.

1995: The application of ground penetrating radar for mapping fractures in plutonic rock within the Whiteshell research area, Pinawa, Manitoba, Canada; Journal of Applied Geophysics, v. 33, p. 125-141.

Tarussov, A., Bonn, F., and Judge, A.

1994: Soil survey from light aircraft using a ground-penetrating radar; Proceedings, First International Airborne Remote Sensing Conference and Exhibition, Applications, Technology and Science, Strasbourg, France, v.3, p. 460-470.

Theimer, B.D., Nobes, D.C., and Warner, B.G.

1994: A study of the geoelectrical properties of peatlands and their influence on ground-penetrating radar surveying; Geophysical Prospecting, v. 42, p. 179-209.

van Overmeeren, R.A.

1998: Radar facies of unconsolidated sediments in The Netherlands: A radar stratigraphy interpretation method for hydrogeology; Journal of Applied Geophysics, v. 40, p. 1-18.

Warner, B.G., Nobes, D.C., and Theimer, B.D.

1990: An application of ground penetrating radar to peat stratigraphy of Ellice Swamp, southwestern Ontario; Canadian Journal of Earth Sciences, v. 27, p. 932-938.

Wolfe, S.A., Burgess, M.M., Douma, M., Hyde, C., and Robinson, S.D.

1997: Geological and geophysical investigations of ground ice in glaciofluvial deposits, Slave Province, District of Mackenzie, Northwest Territories; in Current Research, 1997-B, Geological Survey of Canada, Paper 97-1B, p. 39-50 (also published as Geological Survey of Canada Open File Report 3442).

CHAPTER 6 Subaquatic acoustic techniques

Robert Gilbert

Introduction

The purpose of this chapter is to provide an indication of the technology available to geomorphologists for acoustic survey of lakes and the sea, and of the applications possible. Persons interested in an in-depth discussion of acoustic theory and instrumentation should consult the numerous technical references available, including McQuillin and Ardus (1977), Stoll (1989), and Geyer (1983).

Because light is absorbed by water in relatively short distances of a few metres at the red (long wave) end of the spectrum to a few tens of metres at the blue, it cannot be used for remote sensing of water bodies except in specialized applications. Sound, on the other hand, is transmitted long distances with relatively little attenuation, and so is used to create pictures in sound of the lake or sea and its sediments. Like light, sound in its range of frequencies, behaves differently and can be sensed by different receivers to provide a range of information. As well, sediment is also partially transparent to sound, so with the right equipment one can look deeply into the material on the lake or sea floor. Also like light, remote sensing by sound can be either passive (in which ambient sound is detected to sense the environment) or active (in which the sound is provided as part of the sensing procedure). Of the active systems, in some applications a sound beam is transmitted continuously; this equipment has, for example, naval and military application to detect moving objects by measuring the doppler shift of the reflected sound. The equipment that is used most in the academic study of water and sediment is an active *pulse system* that repeatedly triggers short bursts of sound energy, then records the pattern of the reflected sound that returns to the sensor.

Techniques of acoustic sensing

Table 6.1 summarizes the techniques of acoustic sensing of lakes and the sea. Each is briefly discussed below, along with some of the principles on which they are based and their applications. Acoustic reflection profiling of both the water column and the sediment beneath depends on the reflectivity of a surface or interface which results from a change in *acoustic impedance* (AI) at the interface. AI is a function of the compressional (sound) wave velocity in the medium, which in turn is a function of the compressibility, the shear modulus or rigidity, and the bulk density of the medium.

Thus, in acoustic profiling of the water column, any factor that provides a change in any of these characteristics provides an interface from which reflection may occur. This includes temperature, dissolved salts, suspended sediment, and biological matter (especially phyto- and zooplankton). The difference in AI between water and water-saturated sediment is normally great enough that the lake or sea floor provides a good surface for reflection. However, in extremely underconsolidated sediment such as gyttja, the reflectivity of the upper surface may

be so poor (the difference in AI so slight) that normal acoustic equipment may not detect it and so the "bottom" is falsely recorded at some depth down in the sediment where AI is greater. This change in AI in a normal water column and the sediment beneath can be detected and plotted by a variety of acoustic profiling devices. Most are configured as shown in Figure 6.1.

Table 6.1. Summary of acoustic survey techniques for lakes and the sea.

Acoustic techniques:
Acoustic profiling of the water column
Acoustic profiling of the bottom and sediment by sound reflection
High frequency, low energy sources (echo sounding)
- single transducer sounding
- Remotely operated vehicles
- Swath sounding
Mid frequency, mid energy (subbottom profiling)
Low frequency, high energy (continuous seismic profiling)
- sparker
- boomer
- air gun
Seismic refraction survey
Side scan technology
- conventional
- "smart" technology

Of the techniques that are available for recording output, those based on a hard copy on paper are still in common use. The recorder and display consist of electro- or thermo-sensitive paper which is burned by the electrical signals transmitted through a rotating stylus as they are generated by the outgoing pulse and the returning processed signal. The paper is drawn past the stylus creating a profile through time. Since the device is moving in a boat across the water body, the profile through time is also a profile through space.

As the stylus begins its path across the page, an electrical pulse triggers a transmitter to send a short electrical pulse to a transducer in the water. The transducer, a normally a piezoelectrical device, converts the electrical signal to a sound signal which is propagated into the water. Reflections from various depths in the water and sediment column are returned to a transducer (which may be the same as the transmitting transducer or may be separate hydrophones) in a period of time that depends on the characteristics of the medium (see below) and the distance travelled. The signal is reconverted to an electrical signal, amplified and etched on the recording paper as the stylus moves across the page.

Increasingly, the paper recorder is being replaced or supplemented by data logging technology which allows play-back in the laboratory with various filtering and amplification strategies to best enhance and display the record. For example, colour may be used to

distinguish differing characteristics of the returning signal, and thus to map the character of the lake or sea floor and its sediments. Hard copies are then printed though conventional computer-based software. Commonly in the field, especially in small boat operations where space and power are limited, only a display on a computer monitor is available to the operator in real time, the data disappearing into the black box of the logger for later analysis.

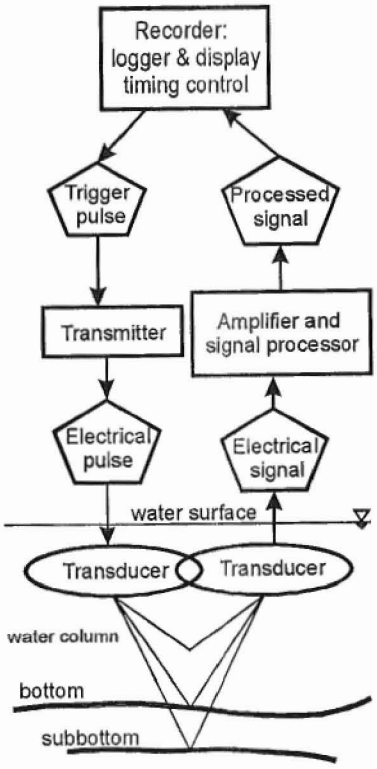

Figure 6.1. *Schematic sketch of the components of an acoustic profiler. The transmitting and receiving transducers may be separate hardware or the same unit.*

Acoustical profiling

Acoustical profiling of the water column has a wide range of applications in physical and biological limnology and oceanography. Figure 6.2 illustrates the record of a highly unstable interface created by flow of less saline surface water over the sill in Knight Inlet. Figure 6.3 illustrates the occurrence of kolks, slowly rotating vortices that rise from the stoss side of fluvial dunes, and which transport significant quantities of sediment upward in the flow. They are commonly observed as "boils" on the water surface. Figure 6.4 shows an acoustical image of a lacustrine phenomenon yet poorly understood. In glacial lakes turbidity currents commonly transport water and sediment along the lake floor. It is proposed that the patterns shown in Figure 6.4 represent rising plumes of river water originally made dense by its suspended sediment load. As the sediment settles from suspension the underflow becomes less dense because its temperature is greater than that of the hypolimnion of the lake, and therefore becomes buoyant as the sediment settles from suspension (cf. Gilbert, 1975). Other studies have

used acoustic profiling to map sediment transport and the daily migration of phytoplankton up and down in the water column in response to changing light.

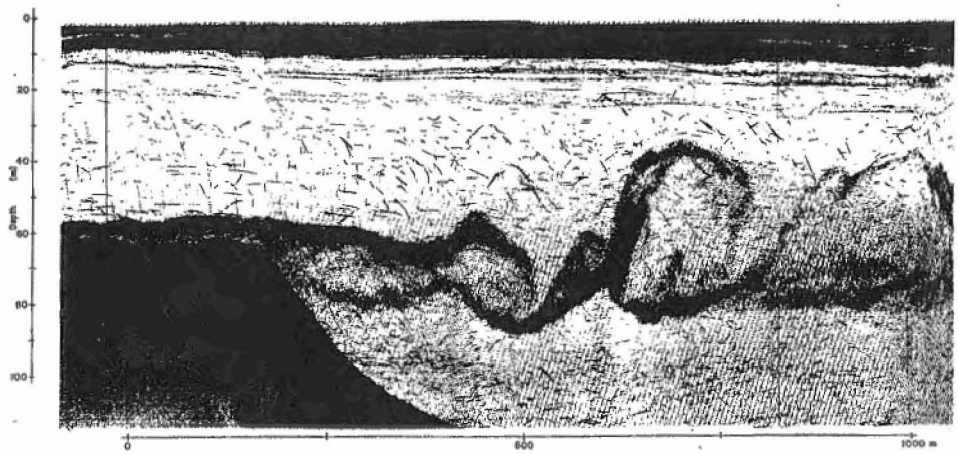

Figure 6.2. Acoustic profile of internal waves at the sill of Knight Inlet, British Columbia (Farmer and Smith, 1980).

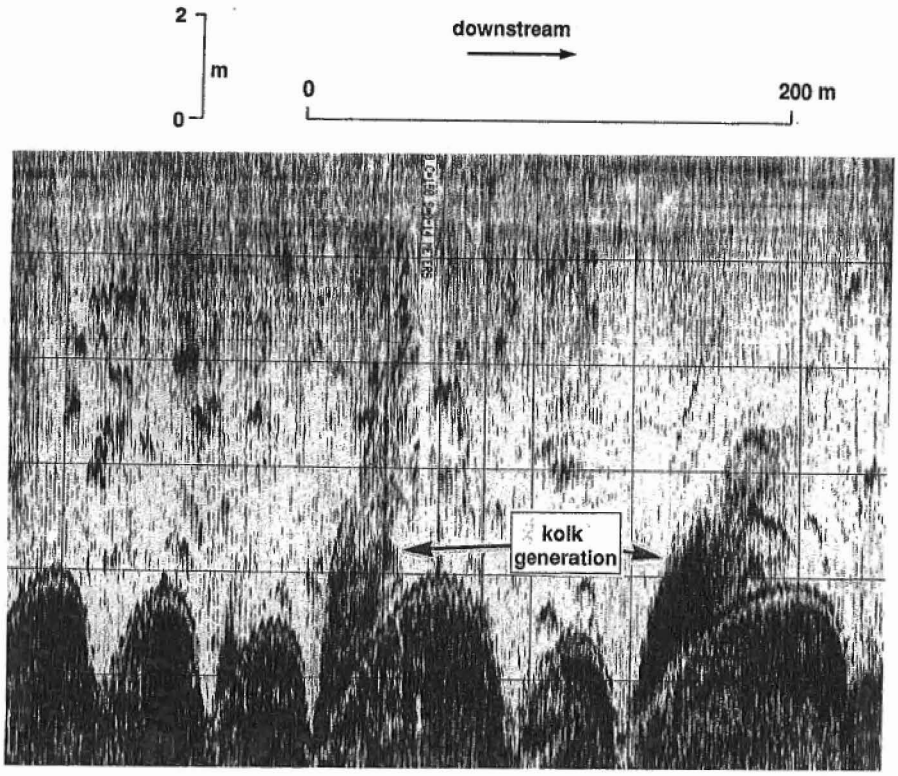

Figure 6.3. Acoustical record from a Data-sonics DFS-2100 system of kolks from a dune field in the lower Fraser River, British Columbia. The spiky surface of the dunes is due to movement of the survey vessel in waves (Kostaschuk and Church, 1993).

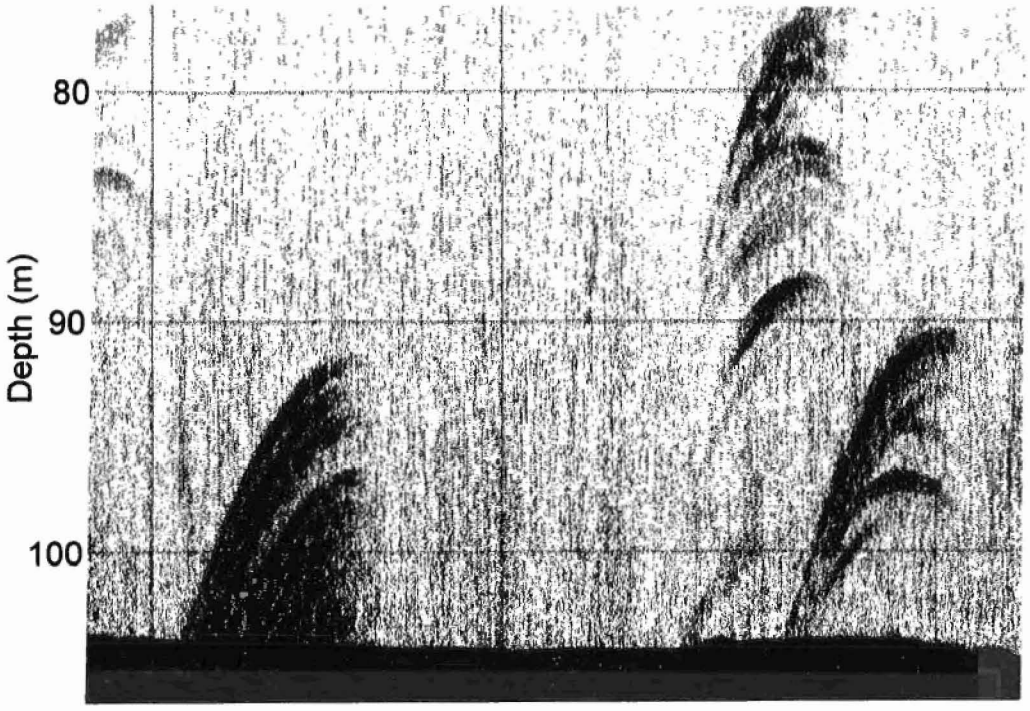

Figure 6.4. *Acoustical record using the same equipment as Figure 6.3 illustrating proposed upwellings from residual turbidity current flow on the bottomset beds of Lillooet River delta in Lillooet Lake (Gilbert and Church, unpublished data).*

Echo sounding

Echo sounding is the simplest form of acoustic profiling of the lake floor and depends on the large value of reflectivity of the sediment/water interface. Thus, a high frequency (50 kHz to 200 kHz), low energy source and relatively simple signal processing is adequate for the purpose of bathymetric mapping. However, to interpret echo profiles requires some knowledge of the way in which sound behaves in the water and at the sediment interface. First, depth as measured by the time the sound pulse takes from the transducer to the bottom and back to the transducer depends on the velocity of sound in water. This varies over a significant range depending on temperature and salinity (Table 6.2)

Table 6.2 Velocity of sound in water

Temperature	Velocity (m/s)	
	Fresh water	Salt water (35 ‰)
0°C	1405	1453
10°C	1450	1492
20°C	1483	1521

Source: Bark et al. (1964).

Depth (pressure) also affects sound velocity; at 100 m the velocity is about 2 m/s greater than at the surface; at 1000 m the velocity is about 16 m/s greater. Details of these and other factors affecting sound velocity are provided by Smith (1974). Conventional echo sounders are normally calibrated for a sound velocity of 1460 m/s. Precise survey sounders allow the operator to set the sound velocity calibration in the field based on temperature and salinity, although both may vary through the water column.

A second significant problem is that a sloping or curved lake floor induces a distortion in the echo-sounding trace that is related to the geometry of sounding. When a sound pulse leaves the transducer it radiates out and is reflected from the point on the bottom normal to the sound propagation. As shown in Figure 6.5, if the bottom is sloped or curving, this point is not beneath the transducer. Simple trigonometry dictates that

$$\sin\theta = \tan\phi$$
$$z = r(1-\tan^2\phi)^{1/2} = r\cos\theta, \text{ and}$$
$$D = r\tan\phi = r\sin\theta$$

where θ is the true bottom slope at A, ϕ is the recorded bottom slope, z is the true depth at A, r is the recorded depth, and D is the distance from the transducer to the point directly above A. Note that for $\theta > 0$, the recorded angle is less than the true angle, the recorded depth is greater than the true depth, and the transducer is not at the position where the sounding is taken.

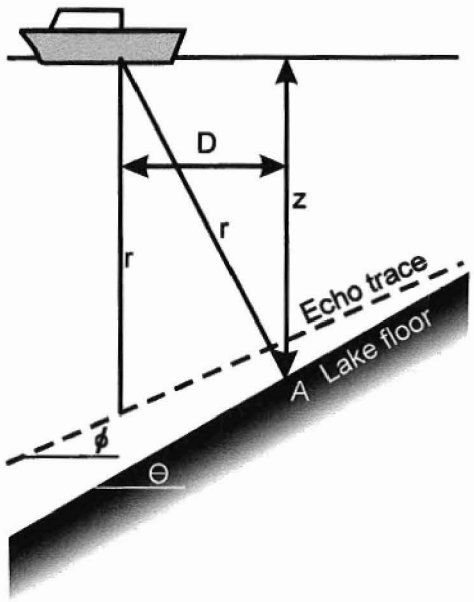

Figure 6.5. *Sketch of the geometry of an echo sounding on the sloping floor of a lake. See text for definitions of the terms (after Krause 1964).*

Over a complex bottom the recorded pattern may bear little apparent relation to the bottom shape. For example, in Figure 6.6a the sides of a depression cross, while the bottom plots in inverted shape below. Thus, a hummocky bottom plots as a series of overlapping parabolas (Fig. 6.6b), analogous to diffraction patterns with light and which may be misinterpreted as subbottom reflections (see below). A point source (such as a fish above the lake floor - Fig. 6c) plots as a convex-upward parabola, and at an edge such as the line of

contact between a side-slope and the flat floor of a lake overlaps and as intersecting half parabolas (Fig. 6.6d). With the equations above, these errors can be corrected and replotted, but as most acoustic profiling is based on interpretation of the graphically recorded image, this is not commonly done.

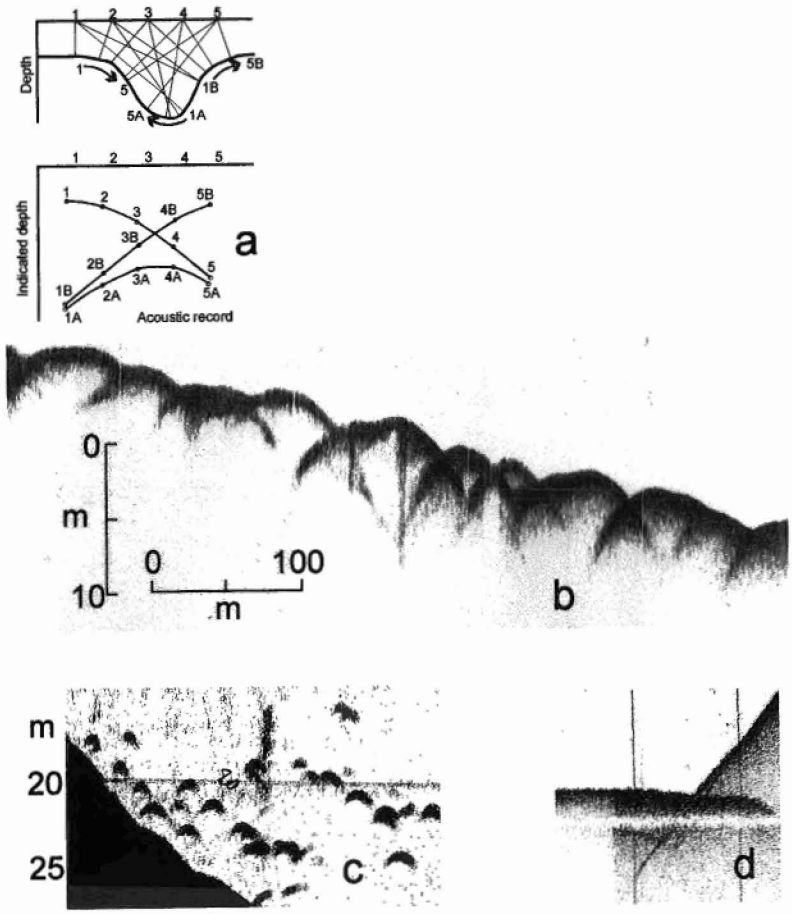

Figure 6.6. *(a) Sounding pattern and displayed reflection pattern over a depression in the bottom (modified from McQuillin and Ardus, 1977). (b) Parabolic returns from the hummocky floor of Lillooet Lake, British Columbia showing overlapping parabolas. (c) Parabolic reflectors from a point source: fish in Lillooet Lake. (d) Apparent overlap along the edge between the side and floor of Lillooet Lake. Source: Gilbert and Church (unpublished data).*

A third problem with acoustic profiles is that they are two-dimensional records of a three dimensional surface, the latter arising because the sound propagates outward in all directions in the water. Thus, so-called side echoes may also be plotted on the profile, confusing the location of the actual bottom, and again giving the impression of a subbottom record (Fig. 6.7).

Fortunately, conventional echo sounding signals can be partially shaped so that a cone of sound is propagated to the lake floor and only signals within that cone are reflected and recorded. Conventional, inexpensive sounders have a propagation cone with an apex angle of about 30°. Survey sounders, where the expense of shaping is justified, may have propagation

angles as low as 5°, significantly eliminating the distortion due to an irregular bottom. However, subbottom and seismic profiling equipment described below cannot have the sound shaped without excessive energy loss and so are allowed to propagate their sound through nearly 180° beneath the water surface.

Normally, echo sounders are mounted singly in a vessel that makes repeated, closely spaced transects of the lake to map its bathymetry. Accurately determined positions are very important in these applications (see a brief history by Loncarevic et al., 1992). The usual standard today is a global positioning system (GPS) linked to a shore-based, fixed receiver and so determining position to within a few metres; this may be linked directly to the sounder and both are recorded or logged in electronic storage (often along with electronic maps) so that a map based on the sensed image (for example, of bathymetry) can be produced with the aid of GIS mapping software (Wells et al., 1992). Nevertheless, air photographs, detailed shoreline maps, and hydrographic charts are still part of surveys of especially small lakes and the nearshore sea, both for plotting positions and planning surveys.

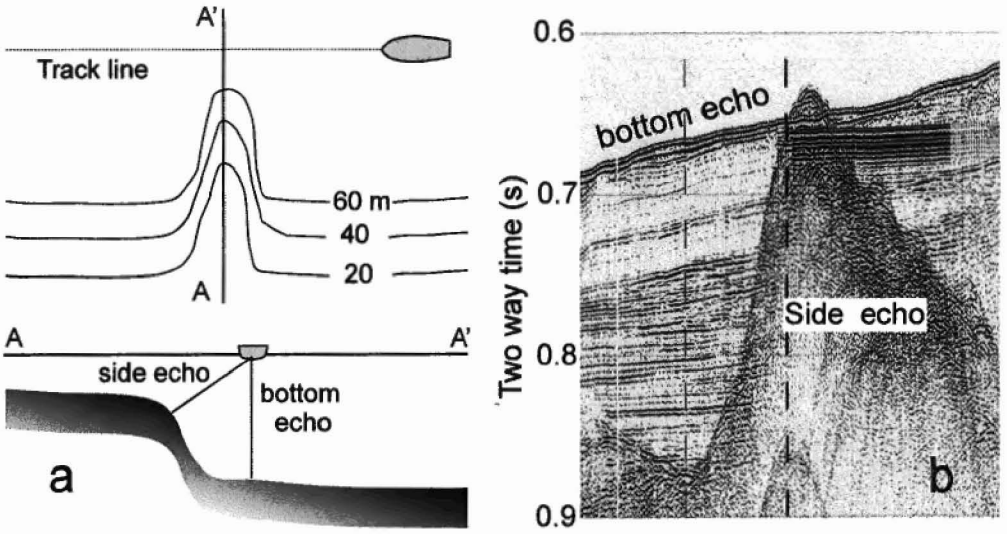

Figure 6.7. *Appearance of a side echo in an acoustic record: (a) Schematic diagram in plan and section; (b) Air gun record from Cambridge Fiord, Baffin Island. The side echo can be recognised because the subbottom echos continue "through" it, except where it masks the subbottom record. Source: Gilbert (unpublished data).*

However, there are variations on this theme of a single sounder mounted in the survey vessel. Small, remotely operated vessels (ROVs), radio controlled from a mother ship, have been used to expand a survey from a large vessel. An advantage is that the ROV can be positioned several metres down in the water (below greatest wave agitation) with a periscope to the surface for engine exhaust and air supply, to provide a stable sounding platform. Alternately, up to 20 transducers can be mounted in a fan-shaped array across the path of the survey vessel, each recording a profile beneath or to the right or left of the vessel track, and each corrected for the angle at which it is mounted. This "swath" mapping provides greater detail of the floor as the lines are much more closely spaced than is normally possible by single-

pass sounding (Matula, 1992). As well, there is virtually no error in the relative positioning of profiles in the array.

Because the lake or sea floor cannot be completely recorded by sounding in the sense that an air photograph records all features in the image to the limit of resolution of the camera and film, it is important to consider the accuracy of the bathymetric map produced by sounding traverses. Ideally, the soundings would be so closely spaced that all features on the lake floor would be recorded and so could be mapped. Except in the preparation of navigational charts this is normally not possible; isobaths are interpolated between sounding lines as the bathymetric map is prepared by hand or by computer. Håkanson (1981) presents an analysis of the accuracy of bathymetric mapping and the consequences of errors in morphometric analysis.

In addition to the obvious and important application of bathymetric mapping, echo sounding has been used for many years to classify the characteristics of the lake or sea bed. The relief of the floor, the hardness of the bottom (as measured in the strength of the reflected signal), and the character of the subbottom return (Gilbert and Shaw, 1992) can all be mapped to illustrate the different environments of the lake or sea bottom (Fig. 6.8).

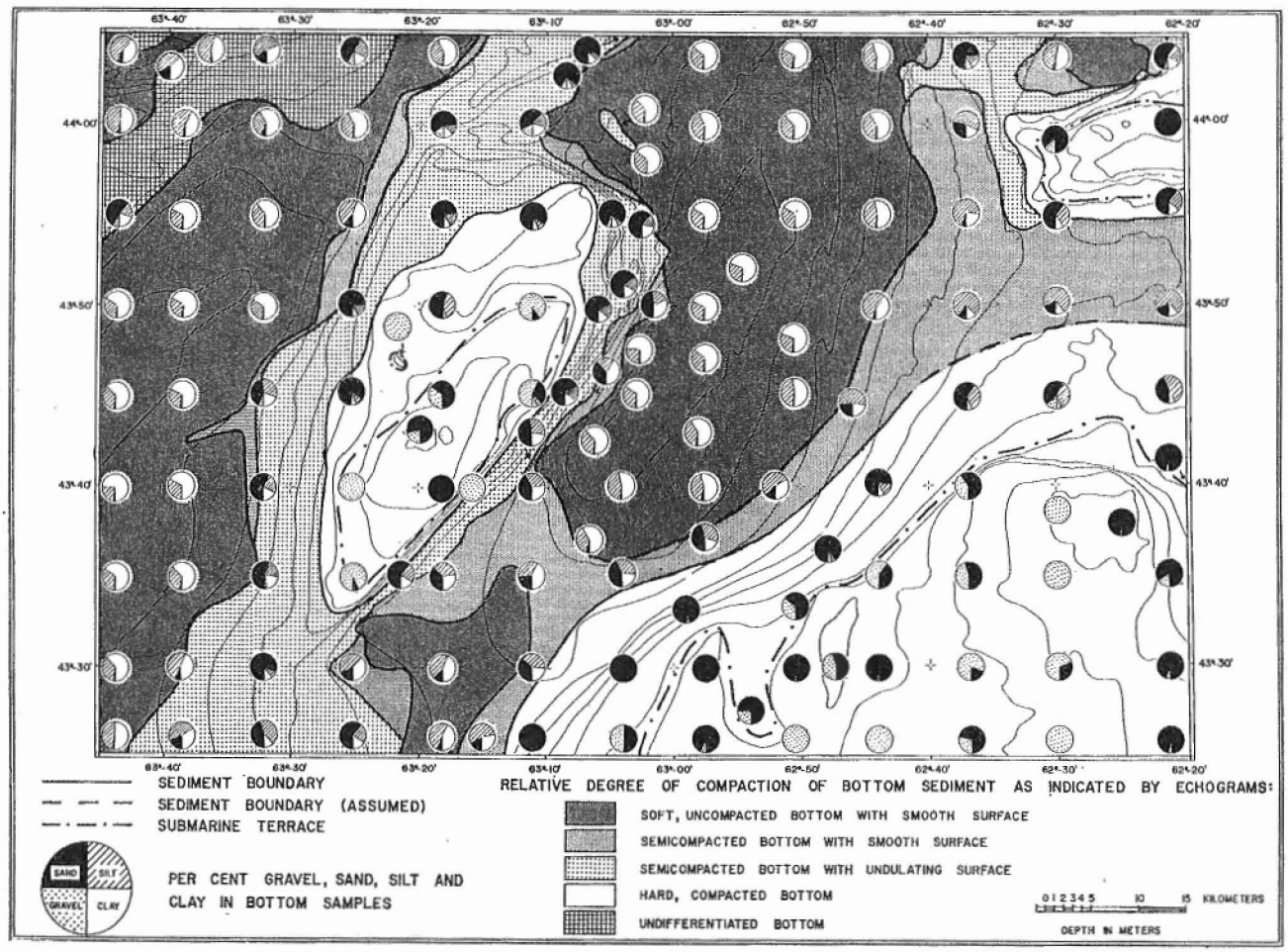

Figure 6.8. *Relation of the texture of surficial sediment on the Scotian Self to acoustic classification of the sea floor from echograms. Source: King (1967).*

Subbottom profiling using tuned transducer systems

As the frequency is lowered and the energy output from the transducers is raised, the ability of the sound to penetrate media with higher acoustic impedance is increased, and reflections from sediment surfaces beneath the lake floor can be detected. These subbottom profiles are used to map the thickness and characteristics of the sediment from which the processes of deposition can be inferred.

A major problem in subbottom profiling is that the velocity of sound is much more variable in sediment than it is in water. An error of 50 m/s for water of the temperature range commonly experienced in a lake (Table 6.2) represents an error of about 3% in depth calculation. But the sound velocity in sediment varies from about 1450 m/s to in excess of 3000 m/s, with values in rock from about 3500 - 7000 m/s, as a function of the compressibility (bulk modulus), rigidity (shear modulus) and the bulk density of the medium. Some examples of sound velocity in sediments are the following:

Gyttja	1400 - 1500 m/s
Silt and clay	1500 - 1800 m/s
Glacilacustrine and glacimarine sediment	1600 - 2000 m/s
Glacial moraine and till	1600 - 2700 m/s

The most important factors controlling sound velocity in sediment are the texture (grain size) and composition (including organic content) of the sediment, the water content as a function of the porosity, and the secondary cementation of the sediment. Commonly, sound velocity increases with the depth of burial of the sediment (a rule of thumb is that the rate of increase is about 1 m/s per metre depth but the relation is very approximate). The only certain way of determining the velocity of sound (and thus the sediment thicknesses recorded) is to measure the sound velocity directly by refraction (see below) or in sediment samples (cores), or by identification of acoustic reflectors in the sedimentary stratigraphy of cores or excavations.

Thus, when a subbottom profile is recorded, the velocity in the sediment is unknown. When it is plotted for display, it is common to plot the depth scale as calculated for the sound velocity in water (about 1460 m/s) even though it is known that this results in an underestimate of the sediment thickness. The axis or the figure caption may indicate "Depth assuming sound velocity as in water". Alternately, (and standard practice for higher energy seismic profiling where the depth of penetration is to sediments and rocks with much higher velocity) depth is plotted as "two-way travel time of the sound in seconds" (Fig. 6.7b). In water a two-way travel time of 0.1 s corresponds to about 74 m depth; in sediment about 80 - 150 m.

Subbottom profiling involves achieving a balance between depth of penetration and return of sound (the thickness of sediment that can be determined) and the resolution possible within the sediment. As well, more powerful equipment requires a larger energy source, and is generally larger, heavier and more bulky (to say nothing of more expensive) and so may not be suited to small-boat operations in small and moderate-sized lakes. Figure 6.9 shows that high frequency sound is attenuated much more rapidly than low frequency sound. Thus, subbottom profiling equipment that achieves its sound from electronic transducers which commonly operate

at frequencies greater than 2 kHz is limited to penetration of less than a few tens of metres, although in very soft, water-laden sediment penetration to 100 m or more is possible. Figure 6.9 also shows that increasing the energy has very little effect on increasing the depth of penetration.

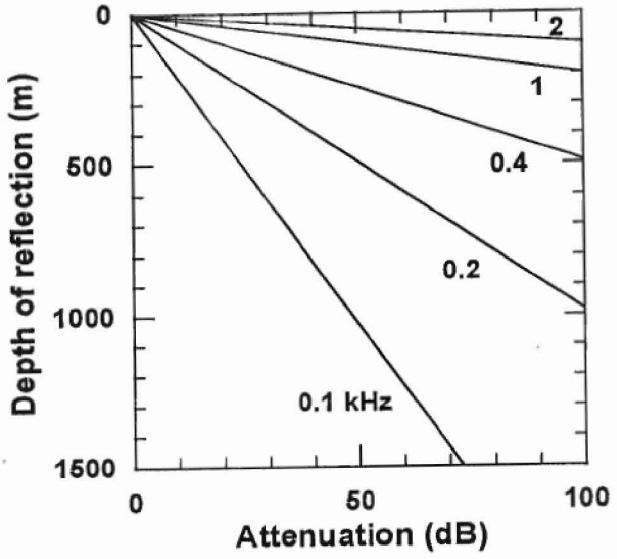

Figure 6.9. *Attenuation of sound in sediment. Because the decibel scale is logarithmic, an attenuation of each 20 db represents a sound loss of 10 times the original value. (modified from McQuillin and Ardus, 1977)*

Because sound is attenuated in water and sediment, acoustic instruments are equipped with a time variable gain (TVG) or amplification of the returning signal. In echo sounders which are not concerned with variable attenuation in sediment the gain rate is normally set internally. It is triggered by the outgoing signal and increases or "ramps up" until the returning sound is detected and plotted. Thus the strength of both shallow and deep returns appears about the same, even though the deep return has a much reduced amplitude. In subbottom profiling equipment, there is normally an option for the operator to set the TVG manually to account for differing rates of attenuation in the sediment. The objective is that the reflections from near the sediment surface should appear on the record about as strong and those from deep within the sediment. Further, this additional TVG for the sediment is not triggered by the outgoing pulse (or it would be ramped up in the water) but normally by the bottom reflection (the first returned) so that it ramps only in the sediment.

The other side of the balance is the ability of subbottom acoustic equipment to resolve closely spaced reflectors in the sediment column, for example, so that bedding patterns may be identified. This is a function of the wave-length of the sound (Fig. 6.10) in a manner analogous to the limitation of a light microscope to resolve objects that are close in size to the wave-length of light. It is also a function of the length of the pulse of sound energy that is transmitted to the sediment. Short pulses are only possible from higher frequency sound sources. 3.5 kHz subbottom profiling equipment (the most common frequency of this type of equipment) is theoretically capable of resolving reflectors as closely spaced as 0.1 - 0.2 m.

Although different sediments transmit sound differently, most lacustrine and marine deposits will allow some resolution of their subbottom reflectors with subbottom profiling equipment. Important exceptions involve freshwater marls (calcium carbonate) and sands

(beaches and deltas for example) which are almost impervious to sound transmission because their high acoustic impedance provides an extremely strong reflector at the sediment-water interface and virtually no transmission of energy to the subbottom. Gas may be trapped in sediment as a result of natural gas from reservoirs in rock beneath the lake or gasification of gas hydrates, or as a result of anaerobic or aerobic decay of organic matter in the sediment. These gassy zones reflect virtually all of the incident sound (again because of the change in acoustic impedance -- the velocity of sound in air is 330 m/s), preventing penetration to greater depth.

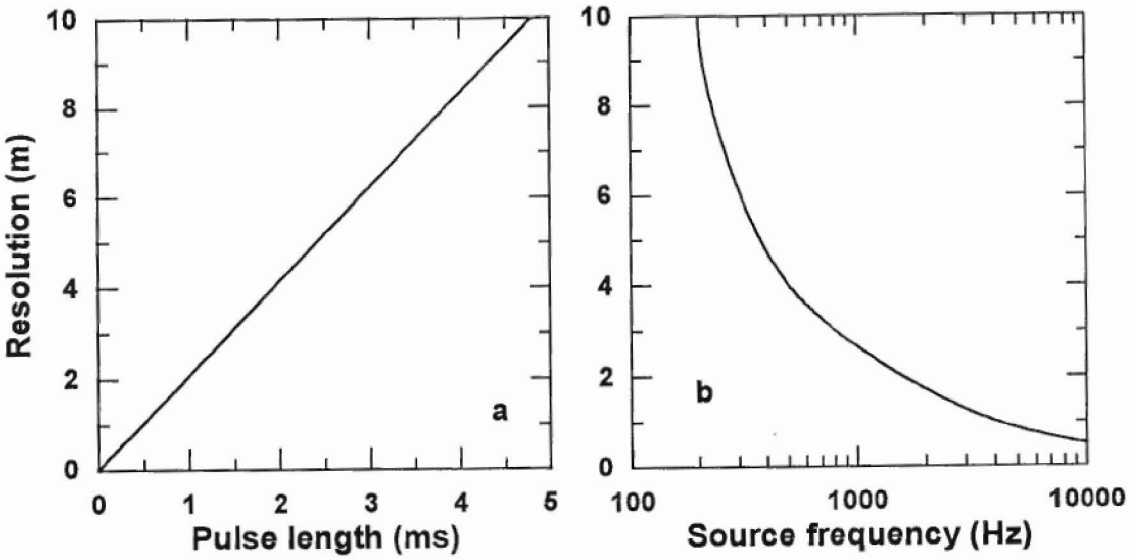

Figure 6.10. *The relation of pulse length (a) and frequency (b) to resolution (minimum spacing between reflectors) in a subbottom profile.*

Examples of 3.5 kHz subbottom profiles are shown in Figure 6.11. Each illustrates the application of the technology to study of limnology and lacustrine sedimentology. Figure 6.12 illustrates that even a conventional echo-sounder can produce an acceptable subbottom image in some circumstances (see also Gilbert and Shaw, 1992).

Subbottom profiling at 3.5 kHz or similar frequency is the most commonly used technique in lacustrine and marine surveys. Of the different instruments available, most offer portability so that they can be transported to remote sites and operated from small boats, that can themselves be transported by vehicle or small aircraft. Power is commonly provided by a 0.5 - 1 kW portable generator, although storage battery power inverted to AC may be used in some circumstances. The transducer or transducer array is attached to the hull of the boat or is towed behind as required. A complete survey of a area (say, less than 100 km^2) can be done in a few days.

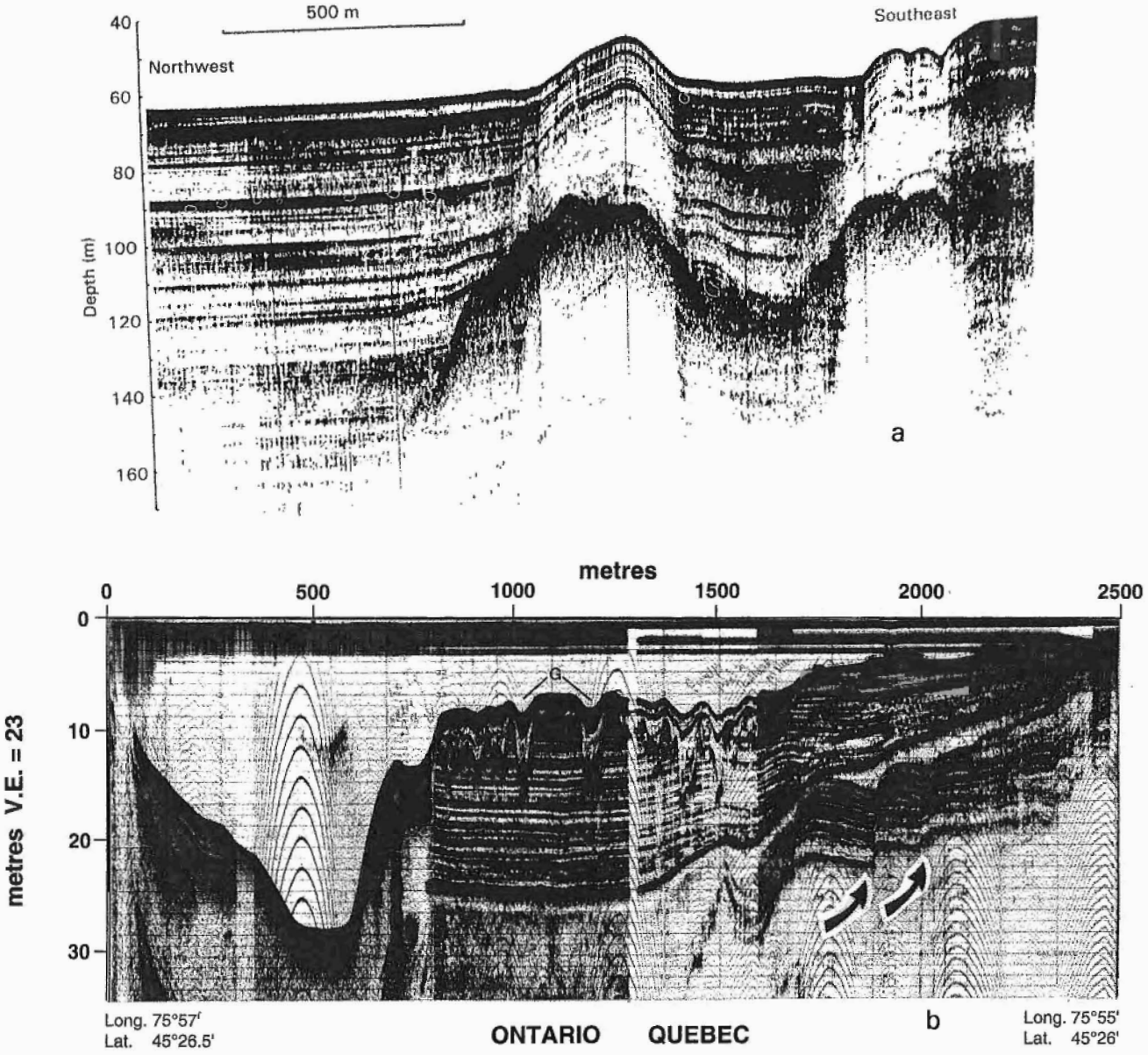

Figure 6.11. *3.5 kHz subbottom acoustic profiles. (a) Datasonics SBP system Bowser Lake, British Columbia illustrating thick glacilacustrine sediment deposited over bedrock or moraines. Note that below about 125 m depth, multiple reflections of the near surface overprint the deep reflectors, especially on the left (Gilbert et al., 1997), (b) Raytheon RTT system on Lac Deschênes on the Ottawa River showing Pleistocene glacilacustrine deposition in several phases, subsequently eroded in a lower lake phase (Shilts, 1994).*

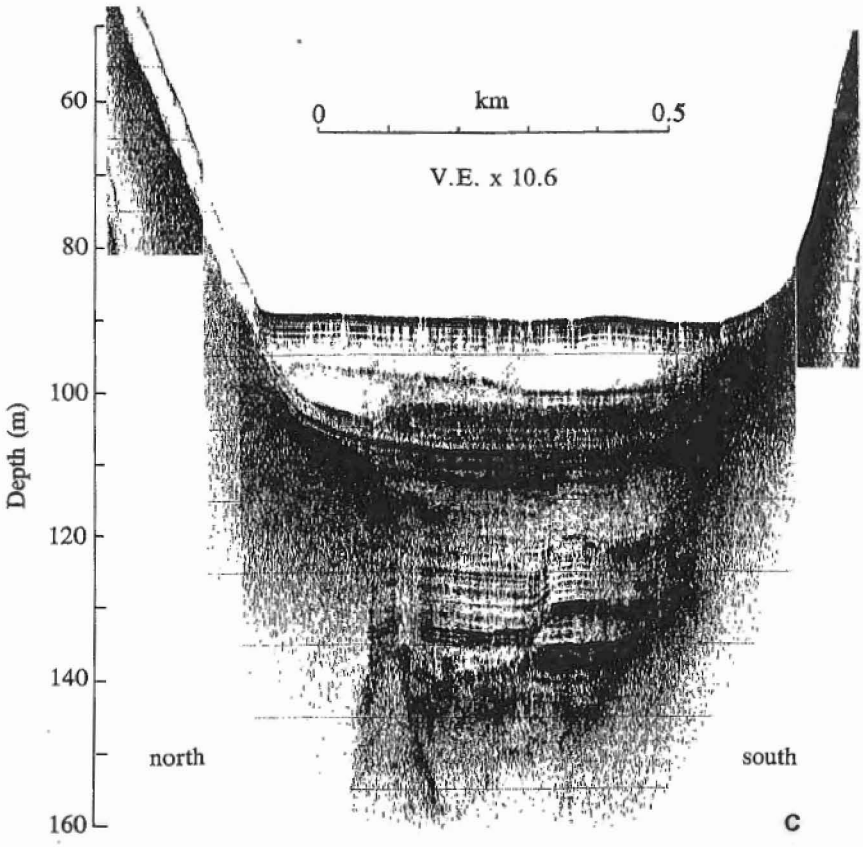

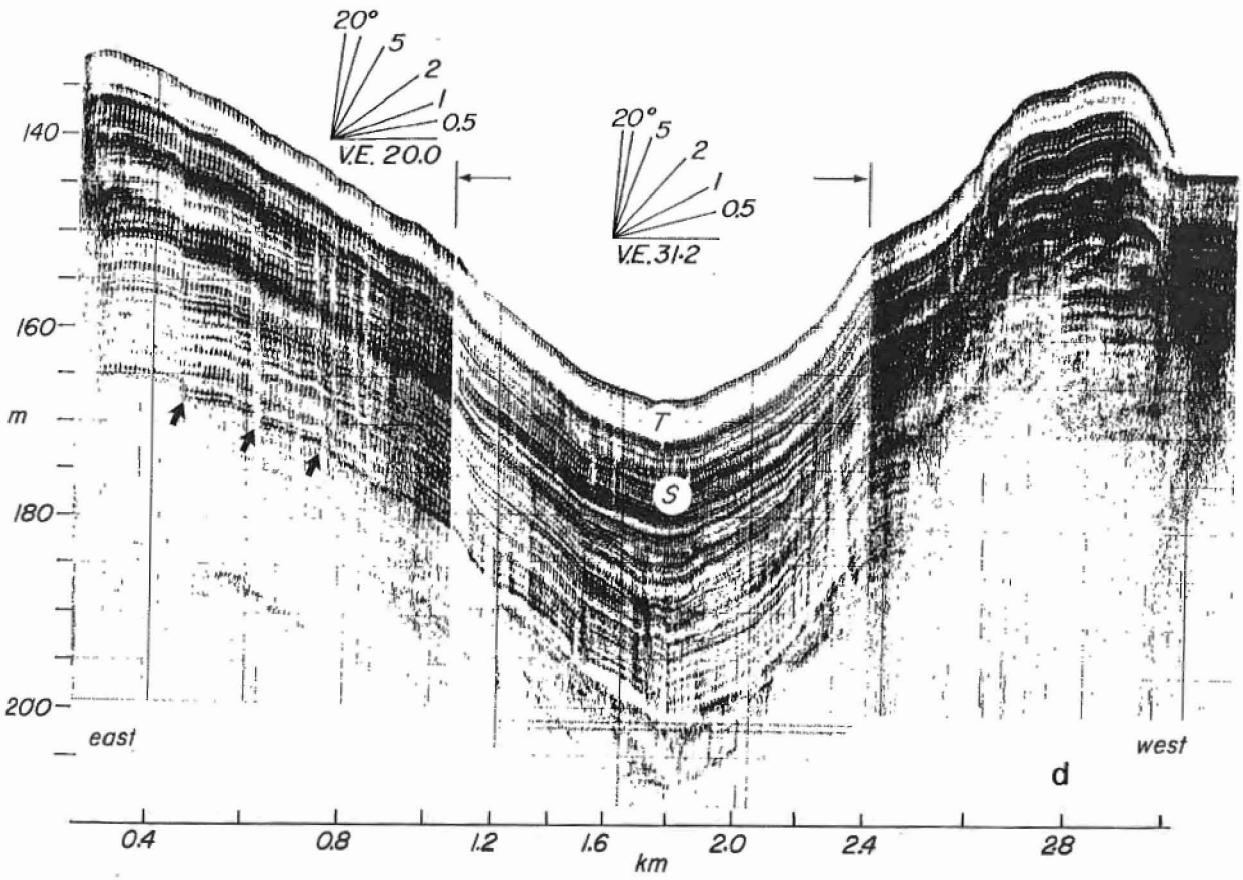

Figure 6.11 (continued). *(c) Subbottom profile from Moose Lake British Columbia showing glacilacustrine fill of the lake basin disturbed by melt-out of buried ice in the bottom, and acoustically transparent Holocene sediment at the top deposited in a lower energy regime (Desloges and Gilbert, 1995). (d) SBP from Harrison Lake British Columbia showing (S) stratified late Pleistocene glacial sediment and (T) lower energy, acoustically transparent Holocene sediment (Desloges and Gilbert, 1991).*

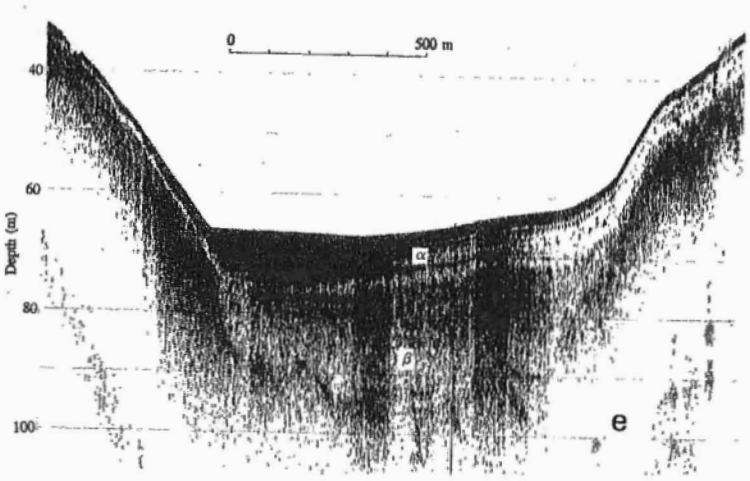

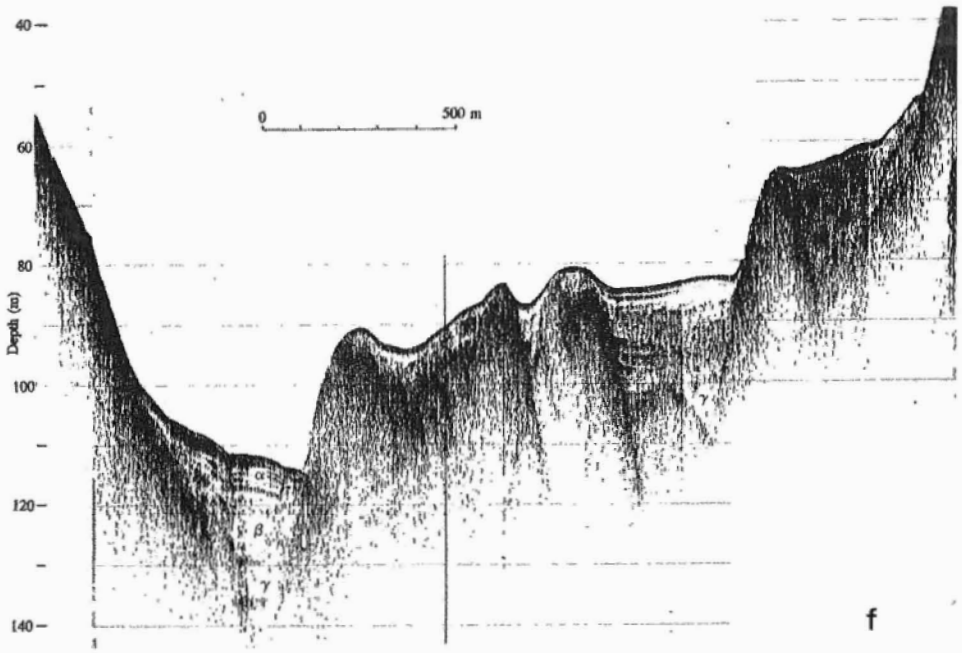

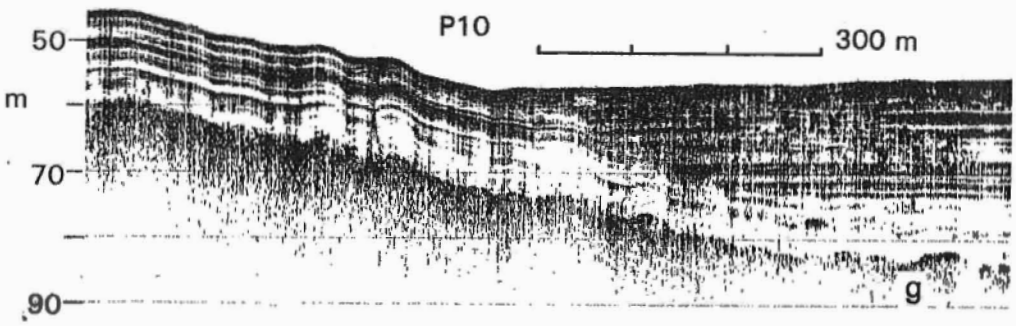

Figure 6.11 (continued). *Subbottom profiles from Kangerluk (Disko Fjord), West Greenland showing differences in patterns of sediment accumulation between the region near the head of the fiord (e) and closer to the mouth (f) where sediment accumulates in pockets on the sea floor (Gilbert et al., 1998). (g) Pattern of basin fill in Expedition Fiord, Axel Heiberg Island showing sediments deposited conformably by rain-out from the water column, and as basin fill from turbidity currents (Gilbert et al., 1993)*

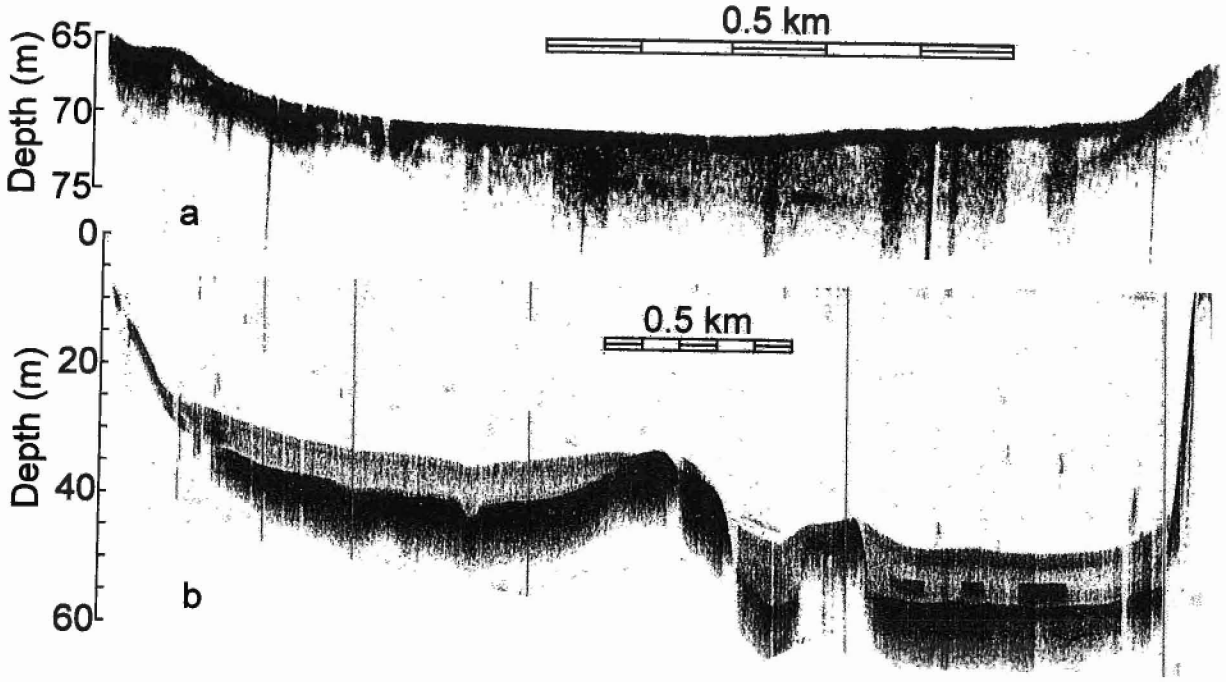

Figure 6.12. *Conventional 50 kHz sounding record (a) from glacier-dammed Ape Lake, British Columbia showing the ponding of glacilacustrine sediment at the end opposite to inflow at left due to damming of turbidity currents (Gilbert and Desloges, 1987) and (b) from Knowlton Lake southeastern Ontario, showing the accumulation of Holocene gyttja over the Pleistocene glacial surface (Gilbert, unpublished data).*

High energy, low frequency continuous seismic reflection survey

This survey is less commonly performed in lakes than at sea, but in some circumstances does provide important information where the sediment column is thick or penetration by lower energy subbottom profiling is limited. In these devices, the tuned piezoelectric transducer that serves as both sound source and receiver is replaced by a sound source that is essentially mechanical. For example, the "boomer" operates on the principle that when a pulse of high voltage is applied to a coil, a nearby plate is magnetically repelled violently a short distance down into the water, creating a powerful sound pulse in the water. After the pulse the plate is recoiled by springs to await the next pulse. In the "sparker" a high voltage pulse vaporizes water between electrodes and creates the pulse of energy. Because the water must be an effective electrolyte, the sparker can only be used in saline lakes or at sea. In both these instruments the electricity is stored in large capacitor banks and released by the trigger pulse from the recorder (Fig. 6.1). Depth of penetration is commonly double to triple that of the subbottom profiler, while resolution is up to an order of magnitude less.

The most powerful of the continuous seismic profilers in common use is the air gun. In this case a chamber with a volume of between 1 and 40 in^3 (16 - 650 mL) and filled with high-

pressure air is opened to the water on the trigger signal from the recorder, creating an explosive burst that serves as the sound source. This equipment provides penetration of up to 1 km or more of sediment with a typical resolution of 10 - 25 m (Fig. 6.13). However, its use is normally restricted to a ship, as a large compressor is required to provide the air supply, although in limited applications, bottled air can be used.

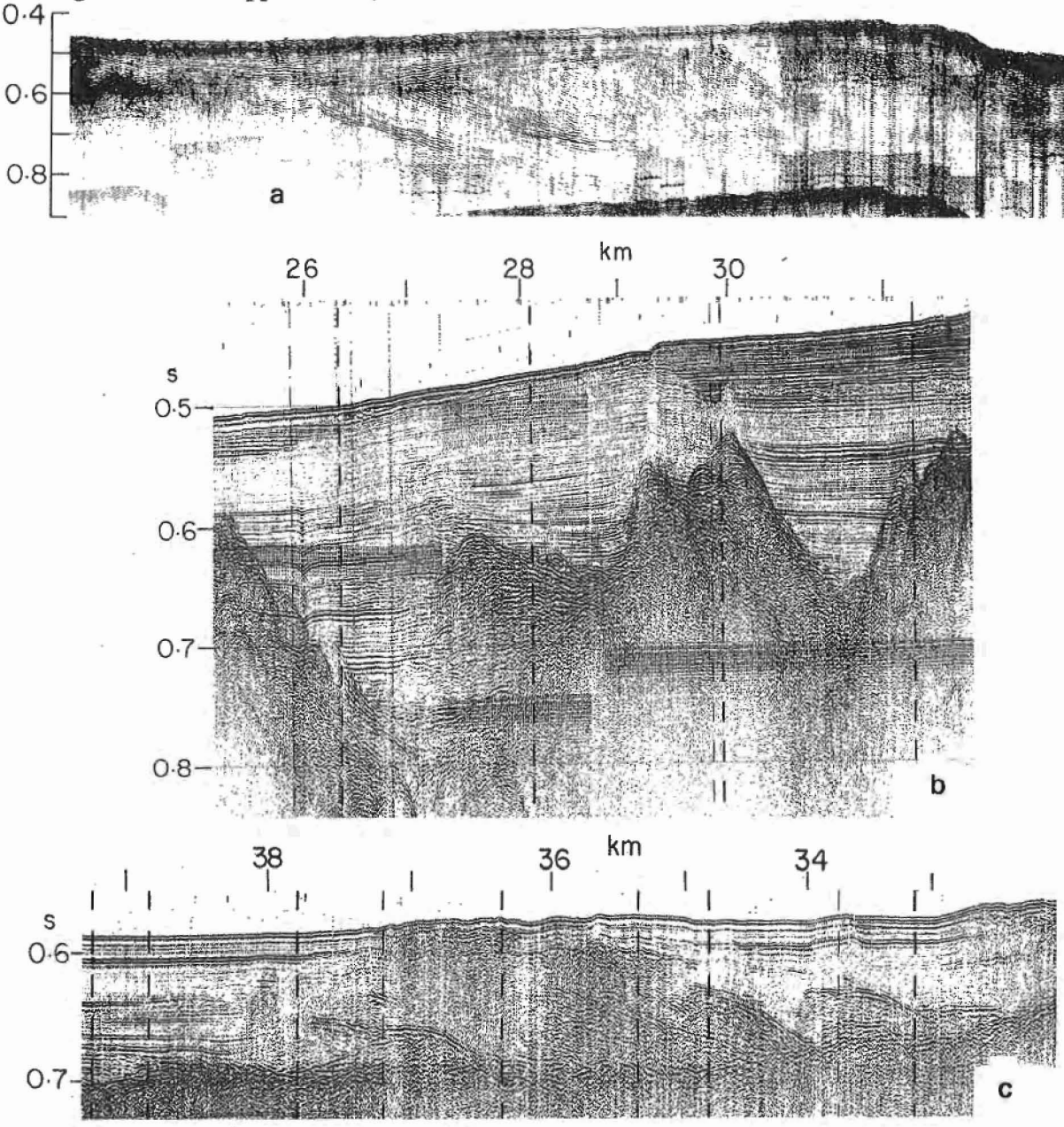

Figure 6.13. *40 in³ (655 mL) air gun surveys of (a) the outer edge of the continental shelf of Baffin Island at the Broughton Trough illustrating a glacimarine delta progressively deposited near the maximum extent of Pleistocene glaciation (Gilbert, 1982), (b) glacimarine fill in Cambridge Fiord, Baffin Island (Gilbert and MacLean, 1983), and (c) glacimarine fill in Itirbilung Fiord, Baffin Island overridden and deformed by subsequent glaciation (Gilbert, 1985). In (a) the field of view is 18 km; in (b) and (c) distances are from the fiord heads. Vertical scale is the two-way time in seconds (0.1 s ≈ 75 m water depth).*

The sound receiver for these systems consists of an array of hydrophones normally towed behind the survey vessel and arranged in a water- or oil-filled flexible tube (referred to as an eel) up to 20 m long to minimize noise created by turbulence as it is pulled through the water.

All the acoustic techniques described above are similar to terrestrial seismic reflection survey (Chapter 3). Subbottom profiling uses a single source-reciever pair (in some cases, a single transducer). The water allows good coupling between source and medium, and a far more rapid survey rate is possible over water than land.

Seismic refraction survey

This technique is a valuable tool for obtaining data at greater depths and lower cost than are possible by reflection survey (although in less detail), and for obtaining velocity data necessary to determine depth, especially in deep reflection survey (see above). The principle of operation is exactly as light refraction: as sound passes into media at different velocities it is refracted (its direction of propagation is changed) according to Snell's Law. As the survey vessel transmits sound (either from the type of sources described above or from more powerful sources including explosives) at locations S1 - S10 from a fixed source of a sonobuoy (Fig. 6.14), the refracted waves are detected and transmitted back to the shipboard recorder by radio (virtually instantaneously compared to sound transmission) allowing determination from a time-distance graph of both layer thickness and velocity.

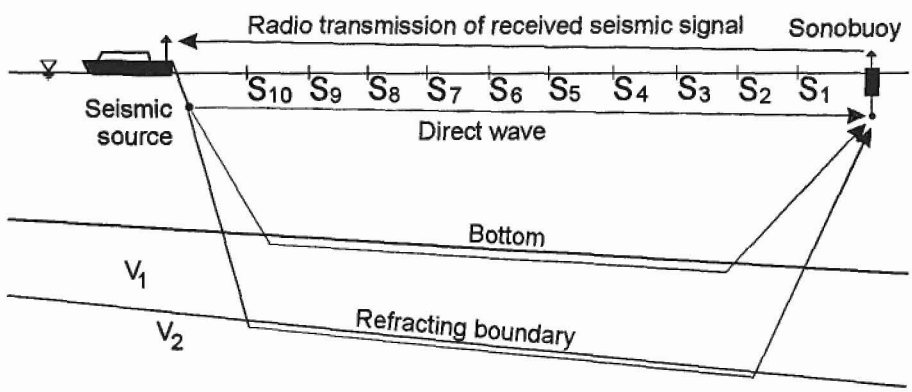

Figure 6.14. *Schematic diagram of seismic refraction survey.*

Side-scan sonar

All the techniques described above provide a two-dimensional slice (or in the case of swath sounding a number of slices) through a lake or sea and its sediments. In side-scan sonar survey, the transducers are located not at the surface but are towed in a streamlined housing (the "fish") near the floor. In addition, they are configured so that one transducer or array of transducers is aimed to the right of the track-line and one to the left (Fig. 6.15). Reflections are returned not from the flat lake floor but from irregularities on it. These might include small disturbances to the floor such as ice scour (Fig. 6.16), objects on the sea floor, or evidence of mass movement and erosional features (Fig. 6.17).

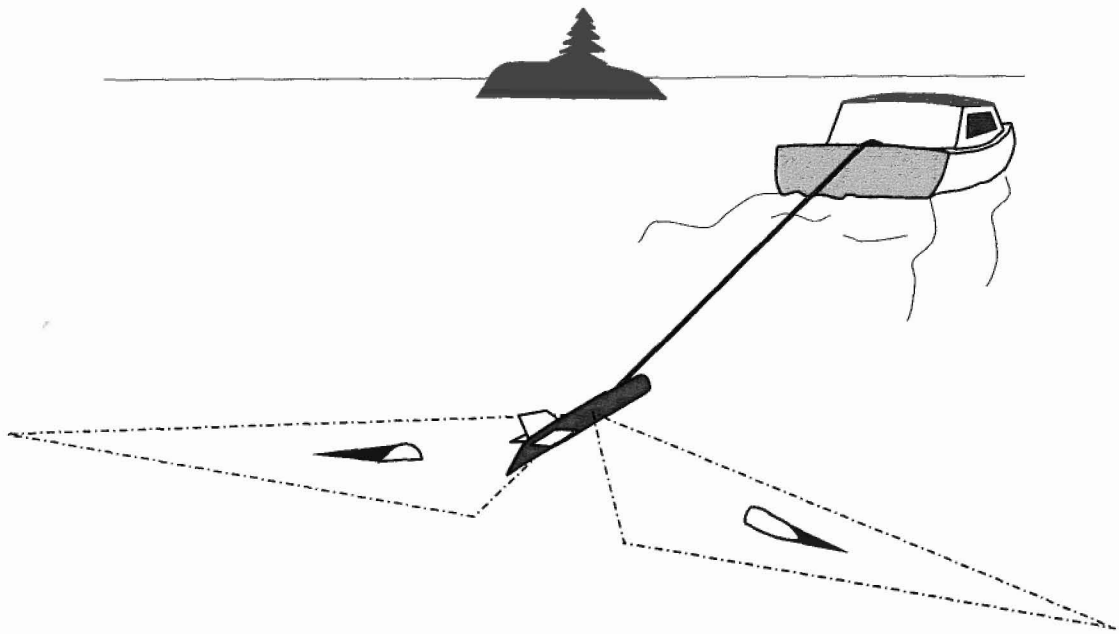

Figure 6.15. *Operation of side-scan sonar from a small vessel.*

The graphic recorder commonly used for side scan sonar survey has two tracks linked mechanically or electronically so that both the left- and right-hand images are plotted simultaneously to build up a sound picture on both sides of the survey vessel as it moves along its track. Side-by-side tracks allow a picture of large areas of the lake or sea floor to be created. As a general rule, the closer the fish is to the floor the better the resolution of the image and the less of a gap there is along the track line between the left- and right-hand sides of the image.

In conventional side-scan sonar the depth of the fish is determined by fixed fins on its housing or on the cable connecting it to the survey vessel, and by the amount of tow-line reeled out and speed of the survey vessel that streams the fish and its tow-line behind. As a result, it is normally not possible to "fly" the fish very close to the floor, especially where the bottom is irregular without risk of it contacting the floor and being damaged or lost. In advanced technology, a "smart" fish is able to sound its distance to the lake floor and adjust its fins to fly up or down as the depth changes to keep a nearly constant height above the bottom. As well,

in advanced systems, the side scan picture or image that is produced may be rectified so that the along-track and cross-track scales are the same, and so that parallax errors created by the sounding geometry are corrected. The image may also be rectified so that the "sound shadows" all appear to be cast in the same direction, rather than in opposite directions from the right- and left-looking transducers. As a result a map, analogous to a shaded relief map on land, may be produced of the lake floor, although the height of the relief features cannot be determined precisely, except along the paths of the transects (Fig. 6.16). Many side-scan sonar instruments are sufficiently portable that they can be deployed from a small boat and so are a potentially valuable tool in lacustrine investigations.

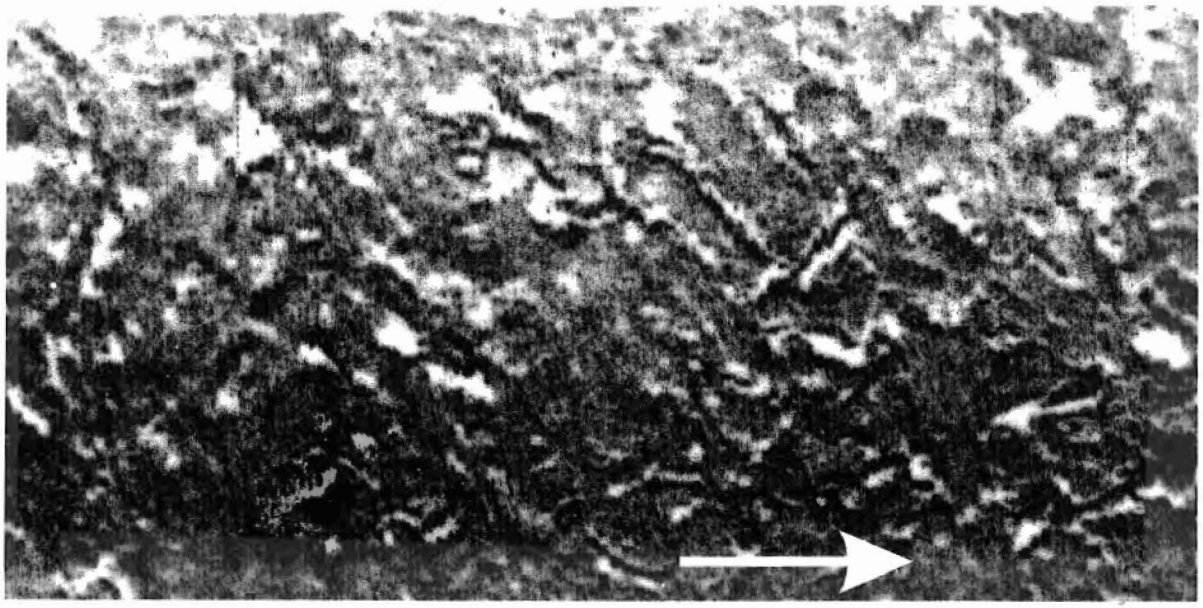

Figure 6.16. *One channel of the AGC side-scan sonar image of the sea floor on the continental shelf of Baffin Island showing iceberg tracks in the Baffin Current, and craters representing wallowing by icebergs under the influence of tides and waves. Field of view is 750 m latterally and about 1.2 km along the ships track (arrow). (Gilbert, unpublished data).*

Conclusions

The physical characteristics of the sedimentary record of lakes and the sea provide important information about the processes by which the sediment was created, transported to and deposited in the aquatic environment. Acoustic surveys provide assessment of regional patterns of sediment distribution and deposition, and the extent of erosion, redistribution and sediment focusing in the basin. When combined with carefully reconstructed stratigraphy and the measurement of textural and bulk properties of sediments in cores, we have a powerful tool for understanding geomorphic processes, the landscapes that result, and environmental change throughout the history of the water body.

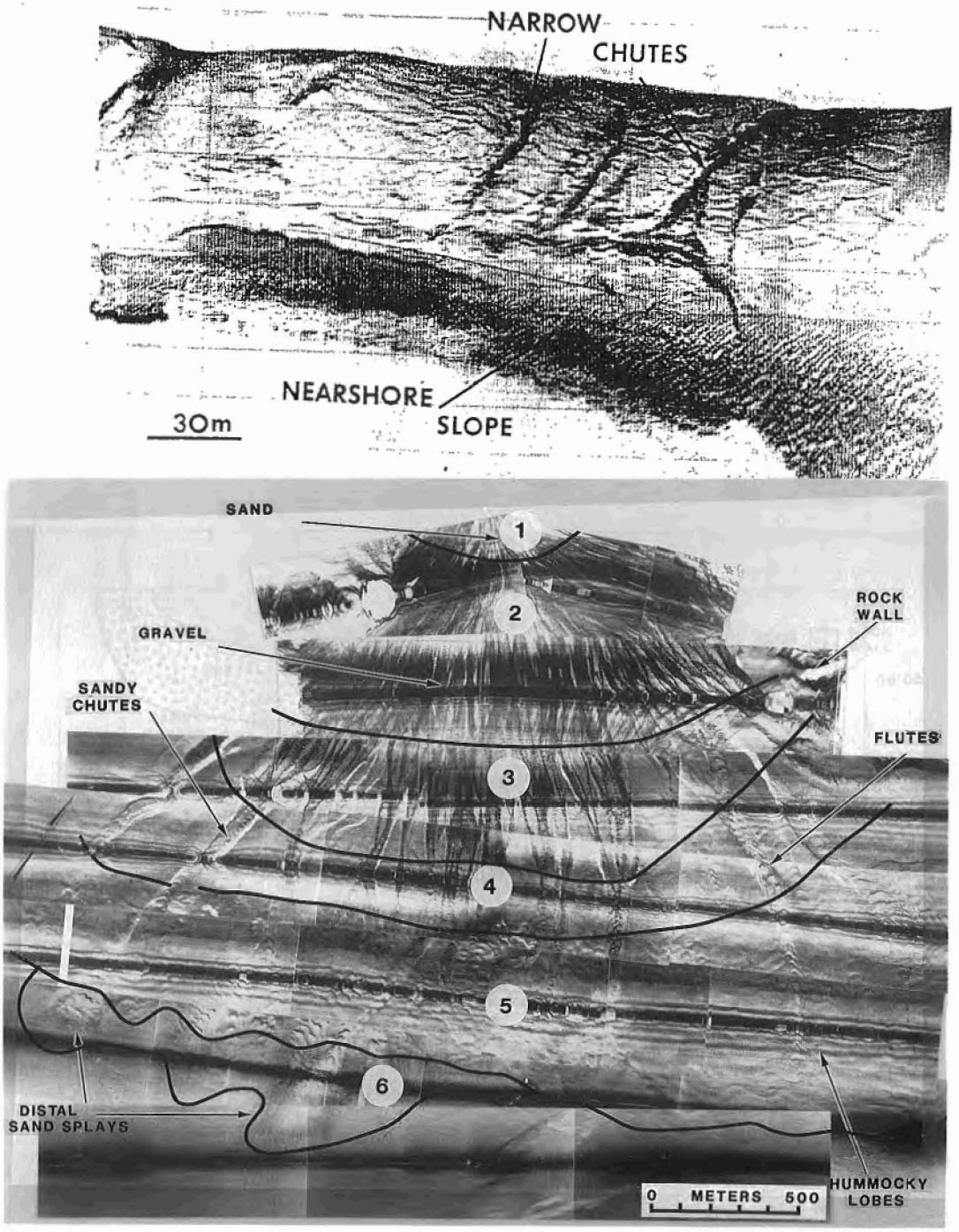

Figure 6.17. *(a) Side-scan sonar image across the slope of the fan-delta on the north side of Howe Sound British Columbia illustrating mass movement scarps parallel to the slope and chutes eroded down the slope (Prior et al., 1981). (b) Side-scan mosaic of the Bear Creek Fan-delta in Bute Inlet, British Columbia illustrating (1) the fan apex, (2) the upper fan, (3) a transition zone, (4) the middle fan, (5) the lower fan, and (6) the distal fan (Prior and Bornhold, 1989).*

References

Bark, L. S., Gunson, P. P., and Meister, N. A.
1964: Tables of the velocity of sound in sea water; Pergamon Press, New York.
Desloges, J. R. and Gilbert, R.
1991: Sedimentary record of Harrison Lake: Implications for deglaciation in southwestern British Columbia; Canadian Journal of Earth Sciences, v. 28, p. 800-815.
1995: The sedimentary record of Moose Lake: implications for glacier activity in the Mount Robson area, British Columbia; Canadian Journal of Earth Sciences, v. 32, p. 65-78.
Farmer, D. M., and Smith, J. D.
1980: Generation of lee waves over the sill in Knight Inlet, in Fjord Oceanography, (ed.) H.J. Freeland, D.M. Farmer, and C.D. Levings; Plenum Press, New York. p. 259-269.
Geyer, R. A.
1983: CRC handbook of geophysical exploration at sea. CRC Press Inc., Boca Raton, Florida.
Gilbert, R.
1975: Sedimentation in Lillooet Lake, British Columbia; Canadian Journal of Earth Sciences, v. 12, p. 1697-1711.
1982: The Broughton Trough on the continental shelf of eastern Baffin Island, Northwest Territories; Canadian Journal of Earth Sciences, v. 19 p. 1599-1607.
1985: Quaternary glaciomarine sedimentation interpreted from seismic surveys of fiords on Baffin Island, N.W.T; Arctic, v. 38, p. 271-280.
Gilbert, R. and Desloges, J. R.
1987: Sediments of ice-dammed, self-draining Ape Lake, British Columbia; Canadian Journal of Earth Sciences, v. 24, p. 1735-1747.
Gilbert, R. and MacLean, B.
1983: Geophysical studies based on conventional shallow and Huntec high resolution seismic surveys of fiords on Baffin Island; in Sedimentology of Arctic Fiords Experiment HU 82-031 Vol. 1, (eds.) J.P.M. Syvitski and C.P. Blakeney; Canada Department of Fisheries and Oceans, Canadian Data Report of Hydrography and Ocean Sciences No. 12, p. 15-1 - 15-92.
Gilbert, R. and Shaw, J.
1992: Glacial and early postglacial lacustrine environment of a portion of northeastern Lake Ontario, Canadian Journal of Earth Sciences, v. 29, p. 63-75.
Gilbert, R., Aitken, A. E., and Lemmen, D. S.
1993: The glacimarine sedimentary environment of Expedition Fiord, Canadian High Arctic; Marine Geology, v. 110, p. 257-273.
Gilbert, R., Desloges, J. R., and Clague, J. J.
1997: The glacilacustrine sedimentary environment of Bowser Lake in the northern Coast Mountains of British Columbia, Canada; Journal of Paleolimnology, v. 17, p. 331-346.
Gilbert, R., Nielsen, N., Desloges, J. R., and Rasch, M.
1998: Contrasting glacimarine sedimentary environments of two arctic fiords on Disko, West Greenland; Marine Geology, v. 147, p. 63-83.
Håkanson, L.
1981: A manual of lake morphometry: Springer-Verlag, Berlin.

King, L. H.
1967: Use of conventional echo-sounder and textural analysis in delineating sedimentary facies: Scotian Shelf; Canadian Journal of Earth Sciences, v. 4, p. 691-708.
Kostaschuk, R. A., and Church, M. A.
1993: Macroturbulence generated by dunes: Fraser River, Canada; Sedimentary Geology, v. 85, p. 25-37.
Krause, D. C.
1964: Interpretation of echo sounding profiles; International Hydrographic Review, v. 39, p. 65-123.
Loncarevic, B. D., Piper, D. J. W., and Fader, G. B. J.
1992: Application of high-quality bathymetry to geological interpretation on the Scotian Shelf; Geoscience Canada, v. 19, p. 5-12.
Matula, S.
1992: Bridging the gap - creating nearshore bathymetric maps from multibeam swath sonar systems and conventional hydrographic data; U.S. Geological Survey, Circular 1092, p. 118-126.
McQuillin, R., and Ardus, D. A.
1977: Exploring the geology of shelf seas; Graham & Trotman Ltd., London.
Prior, D. B. and Bornhold, B. D.
1989: Submarine sedimentation on a developing Holocene fan delta; Sedimentology, v. 36, p. 1053-1076.
Prior, D. B., Wiseman, W. J., and Gilbert, R.
1981: Submarine slope processes on a fan delta, Howe Sound, British Columbia; Geo-Marine Letters, v. 1, p. 85-90.
Shilts, W. W.
1994: Lac Dechênes acoustic profiles and cores; in A Field Guide to the Glacial and Postglacial Landscape of Southeastern Ontario and Part of Quebec, (ed.) R. Gilbert; Geological Survey of Canada, Bulletin 453, p. 58-62.
Smith, E. G. W.
1974: Handbook of marine science. CRC Press; Cleveland, Ohio.
Stoll, R. D.
1989: Sediment acoustics; Springer-Verlag, Berlin.
Wells, D., Mayer, L., and Hughes-Clarke, J. E.
1992: Ocean mapping: from where? to what?; Canadian Institute of Surveying and Mapping Journal, v. 45, p. 505-518.